1521-0081/74/3/825–875$35.00
PHARMACOLOGICAL REVIEWS
dx.doi.org/10.1124/pharmrev.121.000564
Pharmacol Rev 74:825–875, July 2022

ASSOCIATE EDITOR: QIANG MA

Carbon Monoxide Signaling: Examining Its Engagement with Various Molecular Targets in the Context of Binding Affinity, Concentration, and Biologic Response[S]

Zhengnan Yuan,[1] Ladie Kimberly De La Cruz,[1] Xiaoxiao Yang, and Binghe Wang

Department of Chemistry and Center for Diagnostics and Therapeutics, Georgia State University, Atlanta, Georgia

Address correspondence to: Xiaoxiao Yang, Department of Chemistry, Georgia State University, 145 Piedmont Avenue Southeast, Atlanta, GA 30303. E-mail: xyang20@gsu.edu; or Binghe Wang, Department of Chemistry, Georgia State University, 145 Piedmont Avenue Southeast, Atlanta, GA 30303. E-mail: wang@gsu.edu

This work was supported by National Institutes of Health National Institute of Diabetes and Digestive and Kidney Diseases [Grant R01-DK119202] (B.W.), the Georgia Research Alliance Eminent Scholar fund, and internal resources at Georgia State University.

There are no conflicts to declare.

[1]Z.Y. and L.K.D.L.C. contributed equally to this work.

dx.doi.org/10.1124/pharmrev.121.000564.

[S] This article has supplemental material available at pharmrev.aspetjournals.org.

***Abstract*——Carbon monoxide (CO) has been firmly established as an endogenous signaling molecule with a variety of pathophysiological and pharmacological functions, including immunomodulation, organ protection, and circadian clock regulation, among many others. In terms of its molecular mechanism(s) of action, CO is known to bind to a large number of hemoproteins with at least 25 identified targets, including hemoglobin, myoglobin, neuroglobin, cytochrome c oxidase, cytochrome P450, soluble guanylyl cyclase, myeloperoxidase, and some ion channels with dissociation constant values spanning the range of sub-nM to high μM. Although CO's binding affinity with a large number of targets has been extensively studied and firmly established, there is a pressing need to incorporate such binding information into the analysis of CO's biologic response in the context of affinity and dosage. Especially important is to understand the reservoir role of hemoglobin in CO storage, transport, distribution, and transfer. We critically review the literature and inject a sense of quantitative assessment into our analyses of the various relationships among binding affinity, CO concentration, target occupancy level, and anticipated pharmacological actions. We hope that this review presents a picture of the overall landscape of CO's engagement with various targets, stimulates additional research, and helps to move the CO field in the direction of examining individual targets in the context of all of the targets and the concentration of available CO. We believe that such work will help the further understanding of the relationship of CO concentration and its pathophysiological functions and the eventual development of CO-based therapeutics.**

***Significance Statement*——The further development of carbon monoxide (CO) as a therapeutic agent will significantly rely on the understanding of CO's engagement with therapeutically relevant targets of varying affinity. This review critically examines the literature by quantitatively analyzing the intricate relationships among targets, target affinity for CO, CO level, and the affinity state of carboxyhemoglobin and provide a holistic approach to examining the molecular mechanism(s) of action for CO.**

I. Introduction

Carbon monoxide (CO) is widely known to the general public as a poisonous gas. However, research in the last few decades has firmly established CO as an endogenous signaling molecule (Ingi and Ronnett, 1995; Friebe et al., 1996; Siow et al., 1999; Boehning and Snyder, 2002; Morse et al., 2002; Ryter et al., 2002; Bilban et al., 2008; Piantadosi, 2008; Olson and Donald, 2009; Wang et al., 2009; Farrugia and Szurszewski, 2014; Choi et al., 2016; Wood, 2016; Kim et al., 2017; Klemz et al., 2017; Correa-Costa et al., 2018; Joe et al., 2018; Minegishi et al., 2018; Chen et al., 2019a; Rahman et al., 2019; Stucki et al., 2020b; Park et al., 2021) produced largely from heme oxygenase (HO)-mediated degradation of heme with biliverdin/bilirubin and Fe^{2+} as accompanying products in stoichiometric ratios (Wang, 2001; Wang and Otterbein, 2022). There are two isoforms for HO, HO-1 and -2, with HO-1 being inducible and HO-2 being constitutive. Further, results from a large number of studies have clearly demonstrated a range of physiologic roles for CO with importance on par with that of nitric oxide (NO) and hydrogen sulfide (H_2S) (Wang and Otterbein, 2022). Incidentally, CO, NO, and H_2S are collectively referred to as gasotransmitters because they are gaseous molecules at room temperature, although they largely exist in dissolved and/or bound forms in vivo. It is also widely recognized that CO is a very promising molecule for developing therapeutics with a range of therapeutic indications, including anti-inflammation, cytoprotection, analgesia, organ protection, anticancer, and organ preservation

ABBREVIATIONS: AdoMet, adenosylmethionine; Akt, protein kinase B; Bcl-2, B-cell lymphoma 2; BK_{Ca}, large-conductance calcium-activated potassium; BMAL1, brain and muscle Arnt-like protein 1; CBS, cystathionine β-synthase; CD, cluster of differentiation; CLOCK, circadian locomotor output cycles kaput; CNS, central nervous system; CO, carbon monoxide; COHb, carboxyhemoglobin; CORM, CO-releasing molecule; CO-T, target CO saturation; COX, cytochrome c oxidase; Cry, cryptochrome; CSE, cystathionine gamma-lyase; CYP450 or P450, cytochrome P450; cyt c, cytochrome c; 2/3/4-D, two/three/four-dimensional; DEPC, diethyl pyrocarbonate; DOX, doxorubicin; EPO, erythropoietin; GCL, glutamate cysteine ligase; GS, GSH synthetase; GSH, glutathione; GSSG, oxidized glutathione; Hb, hemoglobin; HBD, heme-binding domain; HBM, heme-binding motif; HBP, heme-binding peptide; HEK, human embryonic kidney; HIF-1, hypoxia-inducible factor 1; H-NOX, heme nitric oxide/oxygen binding; HO, heme oxygenase; H_2S, hydrogen sulfide; iCORM, inactivated CORM; IDO, indoleamine-pyrrole dioxygenase; IRI, ischemia reperfusion injury; K_{ATP}, ATP-sensitive K^+; K_d, dissociation constant; Keap1, Kelch-like ECH-associated protein 1; K_i, inhibition constant; k_{off}, dissociation rate constant; k_{on}, association rate constant; Kv, voltage-gated potassium; Kyn, kynurenine; LDL, low-density lipoprotein; L-NAME, N(G)-nitro-L-arginine methyl ester; LPS, lipopolysaccharide; MAPK, mitogen-activated protein kinase; Mb, myoglobin; MbO_2, oxymyoglobin; MetHb, methemoglobin; MetMb, metmyoglobin; NF-κB, nuclear factor-kappaB; Ngb, neuroglobin; NO, nitric oxide; NOS, NO synthase; NPAS2, neuronal PAS domain protein 2; Nrf2, nuclear factor erythroid-related factor 2; PAS, Per-Arnt-Sim; PBD, Protein Data Bank; PDE, phosphodiesterase; PEG-SOD, polyethylene glycol-superoxide dismutase; Per, period; PFKFB3, phosphofructokinase/fructose bisphosphatase type 3; PKA, protein kinase A; PKG, cGMP-dependent protein kinase; PLP, pyridoxal phosphate; pO_2, partial pressure of oxygen; PPP, pentose phosphate pathway; R state, high-affinity relaxed state; RBC, red blood cell; redox, oxidation-reduction; ROS, reactive oxygen species; SAH, subarachnoid hemorrhage; sGC, soluble guanylyl cyclase; SUR2A, sulfonylurea receptor 2A; T state, low-affinity taut (tense) state; TGF, tubuloglomerular feedback; TLC, thin-layer chromatography; TNF-α, tumor necrosis factor alpha; WT, wild-type; YC-1, lificiguat.

(Motterlini and Otterbein, 2010; Chen et al., 2019b; Yang et al., 2020c, 2021a; Wang and Otterbein, 2022). Specifically, CO has been shown to have pharmacological efficacy in animal models of kidney injury (Faleo et al., 2008; Nakao et al., 2008; Goebel et al., 2010; Abe et al., 2017; Correa-Costa et al., 2018; Taguchi et al., 2020; Yang et al., 2020b; De La Cruz et al., 2021), heart ischemia-reperfusion injury (Fujisaki et al., 2016; Wollborn et al., 2020; Dugbartey et al., 2021), liver injury (Kaizu et al., 2005; Ikeda et al., 2009; Zheng et al., 2018; Chen et al., 2019b; Murokawa et al., 2020), lung injury (Kohmoto et al., 2006; Kohmoto et al., 2008; Sahara et al., 2010; Tripathi et al., 2021), chemically induced gastric injury (Bakalarz et al., 2021), colitis (Hegazi et al., 2005; Naito et al., 2012; Joe et al., 2014; Ji et al., 2016; Nagao et al., 2016; Steiger et al., 2016; Takagi et al., 2018), and chemotherapy-induced cardiotoxicity (Suliman et al., 2007), among many other examples. The signaling mechanisms at the pathway level have been extensively studied and well established in the context of various pharmacological functions (Wang, 2001; Wang and Otterbein, 2022).

For examples, in cell culture, ~5%–10% CO gas has been shown to suppress the activation and DNA binding of hypoxia-inducible factor 1 (HIF-1) (Liu et al., 1998b; Huang et al., 1999). However, under normoxic conditions, 0.1% CO gas induced accumulation of HIF-1α in rats brains, presumably due to CO-induced anoxia (Bani Hashemi et al., 2008). In mouse hepatic ischemia/reperfusion injury models, inhalation of 250 ppm CO gas was found to induce phosphorylation of protein kinase B (Akt) in liver cells, thus inhibition of glycogen synthase kinase β (GSK3β) through phosphorylation to offer cytoprotective effect (Kim et al., 2013). Along the same line, CO treatment was shown to protect against apoptosis by upregulating the p38 mitogen-activated protein kinase (MAPK) and phosphoinositide 3-kinase (PI3K)/Akt-dependent signal transducer and activator of transcription 3 (STAT3) pathways in an in vitro anoxia/reoxygenation cell culture model using rat pulmonary endothelial cells (Zhang et al., 2005). Along the MAPK pathway, inhalation of 550 ppm CO in an isogeneic rat lung ischemic injury model suppressed extracellular signal-regulated kinase (ERK) activation, early growth response 1 (Egr-1) expression and Egr-1/DNA binding, thus interrupting proinflammatory and prothrombotic mediators (Mishra et al., 2006). In human monocytic THP-1 cells, the activation of p38 MAPK, ERK1/2, and Akt pathway caused transitory delay in lipopolysaccharide (LPS)-induced c-Jun N-terminal kinase (JNK) activation. Phosphorylation and degradation of IκBα induced by LPS treatment was also blocked by CO, thereby inhibiting nuclear factor-kappaB (NF-κB) signal transduction. It was shown that about 81% of the genes that can be suppressed by CO have promoters with putative NF-κB binding sites, demonstrating a broad inflammatory response suppression activity of CO (Chhikara et al., 2009). In the autophagy pathway, inhalation of 250 ppm CO gas for 2 hours in a mouse liver injury model was found to induce expression of the E3 ligase Parkin in hepatocytes via the protein kinase RNA-like ER kinase/eukaryotic translation initiation factor 2α (PERK/eIF2α) pathway. Parkin could target damaged mitochondria to proteosome degradation (mitophagy), leading to liver protective effects (Chen et al., 2019b). Inhibition of inflammatory cytokines has been widely established as one of CO's immunomodulatory roles (Sahara et al., 2010). A book comprehensively covers the pharmacological roles of CO in various areas (Wang and Otterbein, 2022). Along this line, there have been some excellent studies that have firmly established the relationship between molecular targets and events at the pathway level. These studies are discussed in pertinent sections.

As indicated by its manifold therapeutic functions, CO can bind with multiple targets. This contrasts with the functions of most traditional drugs or signaling molecules, which often tend to act on a single or a small number of targets with high selectivity. Together with the pleiotropic effects of CO come some unique therapeutic properties, including those that seem to offer bidirectional controls of certain activities, graded regulation of signaling processes, balanced moderation of therapeutic effects, and "synthetic pharmacology" or "synthetic lethality." For example, Otterbein reported CO's effect in enhancing the host's ability to fight off infection while simultaneously offering anti-inflammation effects (Wegiel et al., 2014). CO's demonstrated effects in treating experimental sepsis is similar in that it is anti-inflammatory without the negative effect on the host's ability to fight off infection (Nakahira and Choi, 2015). In cancer chemotherapy, it has been reported that CO is able to sensitize cancer cells toward chemotherapy through an anti-Warburg effect while simultaneously offering protection of normal cells and host organs (Suliman et al., 2007; Wegiel et al., 2013). Very few known drugs or biologically active agents, if any, have this diverse and divergent type of activities that are sometimes seemingly bidirectional. Such properties are very interesting, intriguing, and important from the perspective of developing therapeutics and understanding CO's physiologic roles.

All of these unique properties of CO beg the question of the underlying molecular mechanism(s). A key in discussing the molecular mechanism(s) of action of CO is the recognition of its ability to bind certain transition metals with high affinity. It is well known that there is a large number of heme-containing proteins (i.e., hemoproteins) in mammals, including enzymes (Poulos, 2014), proteins for transport and storage (Gell, 2018), iron-regulatory proteins (Nishitani et al., 2019), sensors (Gilles-Gonzalez and Gonzalez, 2005), transcription

factors (Mense and Zhang, 2006), ion channels (Wang, 2017; Kapetanaki et al., 2018), and others (Smith et al., 2010; Li et al., 2011; Hada et al., 2014). Over the years, many hemoprotein targets for CO have been identified and extensively studied by a long list of remarkable researchers (Yang et al., 2021a). At this time, there are no fewer than 25 confirmed molecular targets for CO (Table 1). At this time, there has not been a nonhemoprotein identified as the direct molecular target of CO in mammals, though nonhemoprotein targets may exist in bacteria (Hopper et al., 2020). With so many known targets come the question: how does CO engage with 25 or more targets in the body and achieve its therapeutic effects while at the same time avoid significant side effects and toxicity at a given dosage? Does CO engage with all of the targets at the same time? If so, is there a network-like effect? If not, what are the factors that allow CO to select among a large number of targets? Such questions are not always as clearly defined in conducting cellular or biochemical experiments when not all of the target(s) exist in a particular model and/or when CO is supplied in ample quantity to allow for engagement of even some low-affinity target(s). Further, the effect against any individual target needs to be considered in the context of all of the other targets when the experiments are done in vivo.

Fortunately, there has been tremendous and heroic work in identifying and studying the various molecular targets for this promiscuous CO molecule, including determining the binding constants and on-off rates for CO against these targets. In this review, we discuss the various molecular targets that have been reasonably established and provide a simplified but quasi-quantitative perspective of the biochemical landscape of CO target engagement. In Fig. 1, we show the general landscape of the binding affinities of CO with various identified targets and the two affinity states of hemoglobin (Hb), which is the carrier of CO for its distribution to various parts of the body in the form of carboxyhemoglobin (COHb), in addition to the dissolved form (Levitt and Levitt, 2015; Wang et al., 2020; Yang et al., 2021b). In understanding CO's pharmacokinetic behaviors and its availability, Hb plays a reservoir role through binding with CO, similar to albumin to small-molecule drugs. Therefore, we feel that it is critical to keep in mind the relative CO affinity for Hb and various targets in analyzing target engagement and their relative CO occupancy levels. It is our central view that only transferring CO from a low-affinity complex to a high-affinity target is an energetic favorable and thus pathophysiologically meaningful process. All of these are intuitive descriptions of thermodynamic laws governing binding processes, which dictate that transferring CO from COHb to a target is an energetically favorable process only when the target has a lower dissociation constant (K_d) (higher affinity) for CO than COHb. Before detailed discussions of target engagement in subsequent sections, we briefly layout the landscape in terms of binding affinity. The affinity of Hb for CO ranges from 0.7 nM to 4.5 μM in terms of K_d, depending on the location, oxygen saturation level, pH, and sometimes presence of other ligands. The affinity of CO for various targets has a much wider range: from 0.2 nM for neuroglobin (Ngb), 29 nM for myoglobin (Mb), 1.4–10 μM for cytochrome P450 (CYP450 or simply P450), to 240 μM for the soluble guanylyl cyclase (sGC) (Fig. 1).

In the following sections, we aim to examine the various identified targets by considering their molecular nature, physiologic, and pharmacological implications of binding with CO and established affinity for CO. As such, targets are not considered in isolation. Whenever possible, target engagements are evaluated in the context of CO levels, binding affinity, and the possible effects of patho/physiologic conditions, when relevant. We hope that these types of analyses will allow us to understand target engagement both individually and in the context of possible involvements of other targets.

II. General Considerations in Examining the Molecular Targets of CO

In examining the molecular targets of CO, there are a few very important general factors to consider. First is the chemical nature of the molecular targets. As one of the smallest organic molecules, CO seems to be too small to occupy a "binding pocket" of a protein in a traditional sense; essentially all known targets have a metal-containing moiety that allows for CO binding. This is also the general expectation for future identification of additional targets. Known targets in mammals are largely, if not exclusively, Fe^{2+}-based. There have been extensive studies of CO's affinity for iron (Collman et al., 1976, 1979; Calderazzo, 2006). Therefore, such discussions are not duplicated here. Though binding of CO to a target is largely driven by its affinity to Fe^{2+}, the native ligand that is attached to the iron center makes a significant difference in terms of the binding affinity for CO. Among the large number of iron-containing proteins, hemoproteins occupy a very special place because of their large number and diverse functions (Reedy et al., 2008; Lin, 2015), including oxygen transport (e.g., hemoglobin or Hb) (Berg et al., 2002; Gell, 2018), electron transfer (Sarewicz and Osyczka, 2015; Chong et al., 2018), chemical catalysis (Guengerich et al., 2016; Manikandan and Nagini, 2018; Tornio and Backman, 2018; Borisov and Siletsky, 2019), circadian clock control (Carter et al., 2017; Klemz et al., 2017; Minegishi et al., 2018), protein degradation (Ishikawa et al., 2005a; Zenke-Kawasaki et al., 2007; Elton et al., 2015; Carter et al., 2016; Nishitani et al., 2019), signaling and regulation of transcriptional events (Alam

TABLE 1
Binding affinity of CO and other gaseous signaling molecules to various targets

Target	K_d for CO	K_d for NO	K_d for H_2S	K_d for O_2	K_i for CO	Comments
Hb alpha (T)	1.8 μM (Vandegriff et al., 1991; Unzai et al., 1998)	0.15 nM (Cooper, 1999)		422 μM (Sharma et al., 1978)		
Hb beta (T)	4.5 μM (Vandegriff et al., 1991; Unzai et al., 1998)					
Hb alpha (R)	1.7 nM (Vandegriff et al., 1991; Unzai et al., 1998)	0.9 pM (Cooper, 1999)	17 μM (to MetHb) (Bostelaar et al., 2016)	0.3–1 μM (Brunori et al., 1972)		
Hb beta (R)	0.7 nM (Vandegriff et al., 1991; Unzai et al., 1998)					
Mb	29 nM (Gibson et al., 1986; Moffet et al., 2001)	70 pM (Cooper, 1999)	18.5 μM (to MetMb) (Kraus et al., 1990)	0.8 μM (Gibson et al., 1986; Moffet et al., 2001)		
Ngb	0.2 nM (Dewilde et al., 2001; Azarov et al., 2016)	1 nM (Trashin et al., 2016)	370 μM (Ruetz et al., 2017)	3.2 nM (Dewilde et al., 2001)		
Cyb	0.29 μM (dimer); 68 nM (monomer) (Tsujino et al., 2014; Beckerson et al., 2015)					
sGC	260 μM (human) (Martin et al., 2006); 98 ± 15 μM (bovine) (Stone and Marletta, 1998)	4.2 pM (Martin et al., 2006)	1 pM (Cooper, 1999)			H_2S stabilizes the NO responsive form.
sGC (in presence of YC-1)	94 ± 14 μM (bovine) similar activation effects to NO (100 μM) (Stone and Marletta, 1998).K_d decreases about 20- to 50-fold in mouse-derived sGC.	YC-1 potentiates the effect of NO on sGC by 27%. (Friebe and Koesling, 1998)	NR	NR	NR	Change in K_d of CO in presence of YC-1 varies among different species.YC-1 binds sGC: K_d of $9-21$ μM and $0.6-1.1$ μM (CO); BAY 41-2272 binds sGC: K_d = $30-90$ nM in the presence of CO (Purohit et al., 2014).
CBS	1.5 ± 0.1 μM (Puranik et al., 2006); 68 ± 14 μM (Puranik et al., 2006) (dimeric binding);45 μM (Vicente et al., 2016)	281 ± 50 μM (Taoka and Banerjee, 2001);<0.23 μM (Vicente et al., 2014)		Oxidation to Fe(III)	5.6 ± 1.9 μM (Taoka et al., 1999);9.5 μM (Vicente et al., 2016)	
CBS (AdoMet)	4.5 μM (Vicente et al., 2016)	NR	NR	NR	0.7 μM (Vicente et al., 2016)	
Reduced form COX	0.3 μM (Gibson and Greenwood, 1963)[a]	0.2 nM (Cooper et al., 2008)	No binding	Low O_2 (5 μM):second-order rate constant: (Gibson and Greenwood, 1963) 3×10^7 to 6×10^7 M^{-1} s^{-1}	0.32 μM (Petersen, 1977);1.44 μM (normoxic, HEK cells) (D'Amico et al., 2006);0.35 μM (hypoxic, HEK cells) (D'Amico et al., 2006)	
NPAS2	1–2 μM, 21 μM (Dioum et al., 2002)			Reacts irreversibly		3 μM impairs DNA binding (Dioum et al., 2002)
CLOCK	0.1 mM (Minegishi et al., 2018)					
K_{ATP} channel (heme-HBD complex)	0.6 ± 0.3 μM (Kapetanaki et al., 2018)[a]					
Kv channel (Kv11.3, heme-HBD complex)	1.03 ± 0.37 μM (Burton et al., 2020)[a]					Between CO-heme complex and HBD: 10.55 ± 1.34 μM (Burton et al., 2020)
	50 nM (Yi et al., 2010)[a] (reduced state)					

(*continued*)

TABLE 1—*Continued*

Target	K_d for CO	K_d for NO	K_d for H_2S	K_d for O_2	K_i for CO	Comments
BK_{Ca} channel (heme-HBD complex)						Redox state of the Cys residues on HBD affects ligand binding affinity.
P450	1.4–10 μM (Debey et al., 1973)					
P450 isoforms					0.35 (DB1), 1.1 (TB), 3.9 μM (NF) (Leemann et al., 1994)	pH-insensitive (PB); (Oertle et al., 1985) effect of other factors on affinity: (Balny and Debey, 1976; Davydov et al., 1980, 1986; Gray, 1982; Tuckey and Kamin, 1983; Mitani et al., 1985; Khanina et al., 1987) 770 nM (rabbit) (Rösen and Stier, 1973)
Cardiolipin-cytochrome c	20 nM (Kapetanaki et al., 2009)					
Eosinophil peroxidase	18 μM (Abu-Soud and Hazen, 2001)[a]	18 μM (Abu-Soud and Hazen, 2001)				
Lactoperoxidase	2.2 μM (Abu-Soud and Hazen, 2001)[a];20.71 μM (Abu-Soud and Hazen, 2001)[a]	46 μM (Abu-Soud and Hazen, 2001)				Two binding forms (Abu-Soud and Hazen, 2001)
Chloroperoxidase (ferrous form, bacterial)	Neutral form: (Campbell et al., 1982);30.5 μM[a]; acidic form: (Campbell et al., 1982) 0.2 M[a]					
β-Lactoglobulin	0.5 μM (heme-CO complex) (Marden et al., 1994)					
Calmodulin	0.5 μM (heme-CO complex) (Leclerc-L'Hostis et al., 1996)					
Myeloperoxidase	1.6 mM (Murphy et al., 2010)[a] (pH 6.3)					
Hemopexin	0.22 μM (Shaklai et al., 1981)[a] (pH 8);2.5 μM (Shaklai et al., 1981)[a] (pH 6)					
NOS (White and Marletta, 1992)	10^{-3} μM and 100 μM in the absence and presence of substrate and cofactor, respectively					(Sato et al., 1998; Bengea et al., 2003, 2004)

[a]Some data are calculated from reported k_{on} and k_{off} values. NR, not reported.

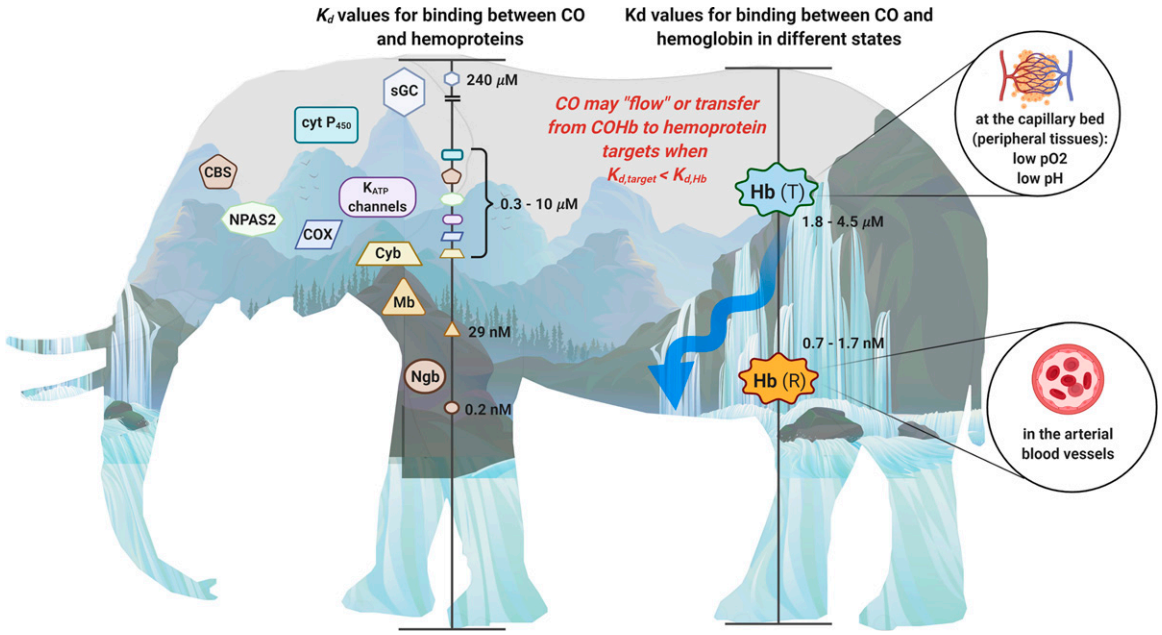

Fig. 1. Elephant in the dark no more: the binding affinities of CO toward various targets in biologic systems. Various hemoproteins with different binding affinities to CO shown as the K_d on the left scale in the elephant figure, and they are also placed on top of the mountains with the height representing their K_d values. The K_d for binding between CO and hemoglobin in the T state and R state, respectively, is marked on the right scale in the figure and overlaid on the waterfalls. As water naturally flows to a lower level than that of the waterfall, CO is more likely to transfer from hemoglobin to a hemoprotein target with a higher binding affinity (lower K_d) on the left side.

et al., 2004; Elton et al., 2015; Zhou et al., 2016; Fleischhacker et al., 2018; Nishitani et al., 2019; Shimizu et al., 2019), protein posttranslational modification (Lin, 2015; 2018), ion channel regulations (Faller et al., 2007; Barr et al., 2012; Weitz et al., 2014; Hines et al., 2016), and microRNA processing (Faller et al., 2007; Barr et al., 2012; Weitz et al., 2014; Hines et al., 2016). Among all of these functions, there are overlaps and crosstalks (i.e., they are clearly not all discrete processes). Though the number of iron-containing molecules is large, the oxidation state of the iron center is important and thus limits the number of targets among iron-containing proteins. For example, most peroxidases cycle between Fe(III) and Fe(IV) (Dunford, 2010), whereas various oxidases involved in mitochondrial oxidation-reduction (redox) reactions, such as cytochrome c oxidase, cycle between Fe(II) and Fe(III) (Michel, 1999; Alonso et al., 2003).

The second question is whether there is discrimination in CO binding to various metal-containing proteins. Even with all of the limitations stated above, the number of potential targets for CO is still large. However, it is very important that we do not view all of the heme- or metal-containing proteins as a simple list of equal molecular targets with which CO would interact. In examining the interplays among the various targets, it is essential that we do so in the context of the relative affinity of these targets for CO. Questions have been raised as to whether CO would interact with all of the hemoproteins indiscriminately upon exposure. The answer is an unequivocal "No." The relative affinity varies by at least six orders of magnitude among all of the identified targets for CO. For example, the K_d in binding with CO is 0.2 nM for Ngb, 0.7 nM for the β-subunit of the high-affinity relaxed state (R state) of Hb, 1.4–10 μM for certain forms of cytochrome P450 and 240 μM for sGC. Therefore, under nonsaturating and physiologic conditions, the high affinity of Hb for CO and its high abundance (mM range) almost certainly mean that very little CO would partition to sGC. Having a good understanding of the relative affinity of the various targets will help to delineate a seemingly complex problem for CO's biologic activity: the availability of a large number of potential targets. There is one section below specifically devoted to this topic. In discussing specific molecular targets for CO in detail in the respective sections, we also relate bioactivity with affinity information whenever applicable. It also needs to be noted that CO binding of the most abundant form of hemoprotein, Hb, is cooperative and is influenced by a large number of factors; there is no single model for describing the binding cooperativity that experts agree upon (Yuan et al., 2015; Gell, 2018). Therefore, the discussion of "CO partitioning" between Hb and other hemoproteins in a quantitative manner will need to take various factors into consideration.

Third, because of the special role of heme in CO-related functions, it is worth some effort to briefly describe heme and hemoproteins. Heme as a prosthetic group consists of a ferrous iron chelated in the center of the porphyrin molecule. The heme complex binds

with molecules with lone pair or unpaired electron such as O_2, CO, NO, and cyanide. A histidine moiety in the heme-binding domain (HBD) that coordinates with the ferrous center of the heme is conserved among all hemoproteins, thus making the ferrous iron five-coordinated. The structural property of distal side of the heme from the coordinated His contributes to the selectivity in small-molecule binding. A hydrophobic apolar environment prevents binding of polar molecules such as H_2O, H_2S, and cyanide and vice versa. Steric hinderance can cast a stringent influence on the binding selectivity of small molecules depending on the shape of their molecular orbitals and consequently binding orientations. Before binding, the five-coordinated heme molecule adopts a "domed" shape owning to the His coordination. Since the porphyrin ring of heme binds with the host protein through other interactions, the conformation is such that favors this "domed" heme. Upon binding with a sixth ligand, the ferrous iron adopts an octahedral geometry that "pushes" the iron back to the porphyrin plane (Fig. 2). This conformational change, though seemingly minor, can trigger further conformational changes of the host protein through amplification via structural variable domains such as a hinge-like structure. These conformational changes induce protein functional changes such as catalysis inhibition/enhancement, phosphorylation/dephosphorylation, dimerization/polymerization, and protein-protein interactions, among others, to pass on to downstream pathways. This efficient biomolecular switch machinery is ubiquitously adopted by living organisms from bacteria to mammals.

The fourth factor to consider is the effect of other signaling molecules on CO binding to its target. For example, steroid is known to affect CO binding to P450 (Tuckey and Kamin, 1983). In discussing mechanistic questions related to CO, it is also very important to examine this in the context of the presence and concentration of two other gaseous signaling molecules: nitric oxide (NO) and H_2S. The promiscuity of CO, NO, and H_2S in binding with hemoprotein targets is arguably among the most complex in terms of direct "crosstalks" of different signaling molecules. Further, binding of NO and sulfide to an iron center can be at a different redox state from that of CO. NO binds to heme at both the ferric and ferrous states; H_2S binds at the ferric state; and CO only binds at the ferrous state of heme. Therefore, these three gasotransmitters sometimes provide synergistic effects, whereas other times they may seem to antagonize each other depending on their relative concentrations, affinities, and magnitude and nature of their pharmacological responses. Mechanistic studies will need to consider all of these factors. In Table 1, we also include the affinity of various targets for the other two gasotransmitters whenever possible to present a picture of the competitions in CO binding.

The fifth important factor to consider in studying CO's mechanism is its source. Ideally, CO gas is the purest form of this molecule without other interference. However, CO gas is difficult to handle, with issues involving the risk of gas leaks, difficulty in controlling dosage, and the need for special apparatus. Therefore, different CO delivery forms have been developed. Initial efforts include those of Motterlini and Mann by using CO-immobilized on a metal center as CO-releasing molecules (CORMs) as well as using Hb as a carrier (Motterlini et al., 2002; Motterlini and Otterbein, 2010; Mann, 2012; García-Gallego and Bernardes, 2014; Heinemann et al., 2014). Later efforts by others expanded to CORMs capable of triggered release of CO by light (Niesel et al., 2008; Jackson et al., 2011; Jimenez et al., 2016; Daniels et al., 2019; Kawahara et al., 2019a) and enzyme (Romanski et al., 2011; Sitnikov et al., 2015); encapsulated or conjugated CORMs to minimize metal exposure (Brückmann et al., 2011; Steiger et al., 2016, 2017; Wollborn et al., 2018); and organic CORMs, which are photo-sensitive (Poloukhtine and Popik, 2006; Antony et al., 2013; Peng et al., 2013; Palao et al., 2016;

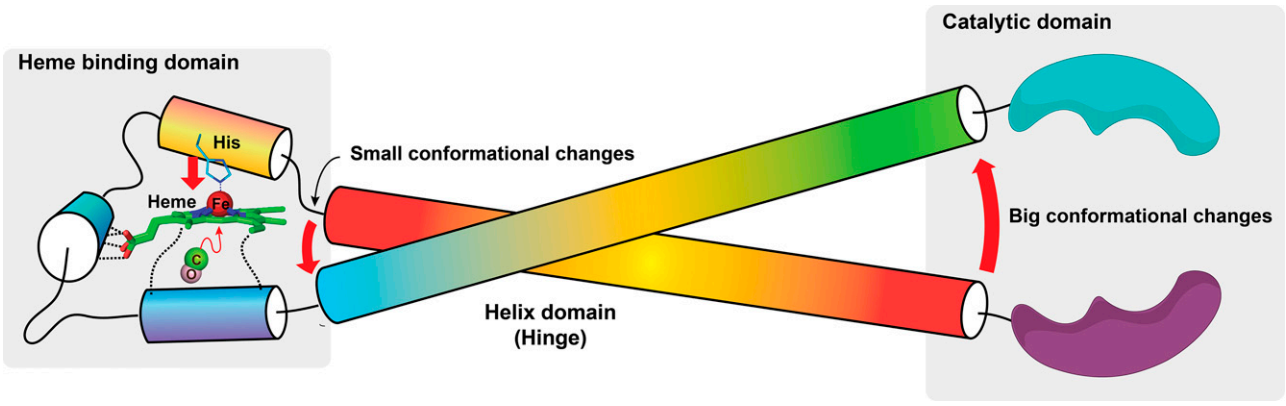

Fig. 2. Schematic demonstration of how small conformational changes to the heme upon binding with CO leverage big changes to the catalytic domain and thus its substrate selectivity and catalytic activity. The transformation of the five-coordinated heme into a six-coordinated heme pulls the histidine imidazole side change toward the heme plane, thus causing conformational changes that can be transduced to larger conformational changes of the functional domain (catalytic domain in this case) of the hemoprotein.

Popova et al., 2018; Soboleva and Berreau, 2019). Recently, we (Wang et al., 2014; Ji and Wang, 2018; De La Cruz et al., 2021; Yang et al., 2021b, 2022b) and others (Kueh et al., 2017) have developed organic prodrugs capable of CO release under physiologic conditions without the need for light and with characteristics of tunable release rate (Ji et al., 2016; Pan et al., 2017), triggered release (pH, reactive oxygen species, and enzyme) (Ji et al., 2017a,b,c; 2019a,b; Pan et al., 2018), delivering two payloads from a single prodrug (De La Cruz et al., 2018; Ji et al., 2019a), and organelle targeting (Zheng et al., 2018). There have been recent reviews on these subjects (Ji and Wang, 2018; Kueh et al., 2020; Yang et al., 2020c). Therefore, the donor chemistry is not discussed in detail here. However, one thing that is worth discussing is the recent findings of the chemical reactivity of some widely used CORMs, including CORM-2 and CORM-3 (Dong et al., 2008; Santos-Silva et al., 2011a,b; Nielsen and Garza, 2014; Wareham et al., 2015; Nobre et al., 2016; Gessner et al., 2017; Southam et al., 2018, 2021; Juszczak et al., 2020; Nielsen, 2020a,b; Nielsen et al., 2020; Rossier et al., 2020; Stucki et al., 2020a; Yuan et al., 2020, 2021a,b) (Fig. 3). Such reactivities cannot be duplicated with the commonly used negative controls: spent CORMs, or inactivated CORMS (iCORMs). Therefore, these CORMs may have activities of their own that have little to do with their ability to deliver CO. Such factors need to be considered in examining the various mechanistic issues, especially at the cell culture and animal model levels.

The sixth factor to consider is the abundance/high concentration of CO often used in cell culture studies, including mechanistic studies. When CO level is much higher than what can be achieved in an in vivo environment, the concept of concentration dependency is lost. Then caution is needed in extrapolating findings from cell culture studies to therapeutic relevance in vivo.

Seventh, endogenous CO production may provide transiently high local concentrations of CO, which allows for engagement of low-affinity targets. This point is especially important when CO production and target binding are faster than diffusion from the production site. This might be the case in parts of the central nervous system (CNS) as discussed in section IV.C (*Neuroglobin and Cytoglobin*).

Eighth, some delivery approaches may leave a substantial amount of CO dissolved in the blood (as "free" CO) for a long enough period of time (min) to allow for engagement of low-affinity targets in various organs and/or peripheral tissues, which would otherwise seem to be hard when analyzed in the context of CO transfer from COHb to the target. Such nonequilibrium conditions may arise due to kinetic barriers to distribution and binding and may allow for direct engagement of a cellular target without the need to transfer CO from COHb. There is one recent publication that examines this issue in detail (Yang et al., 2021b). For the purpose of this review, the analysis is limited to the partition between COHb and a given target under quasi-equilibrium conditions and may only represent a "snapshot" under a given set of conditions.

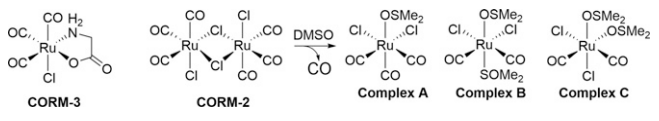

Fig. 3. Structures of CORM-2 and CORM-3. For CORM-2, studies showed that incubation in DMSO leads to iCORM-2, a mixture of three complex species (Seixas et al., 2015). For CORM-3, there is no definitive structure(s) for iCORM-3 after incubation in aqueous solution.

We list all of these factors with the hope of stimulating additional work to fully understand the specific implications of each factor individually and holistically. Below we discuss some major known molecular targets of CO by considering their affinities for CO and biologic functions.

III. A Bird's-Eye View of the CO Target Collection: Its Landscape and Topography

To us, the most fascinating aspect of CO's physiologic roles is its pleiotropic effects and the multiplicity of known molecular targets. As such, CO signaling seems destined to be much more convoluted than those that have a single molecular target. Or is it necessarily the case? A critical issue in examining the pleiotropic effects of CO and its associated molecular targets is the relationship among all of the targets. Would CO engage all of the targets equally and at the same time? If so, that would surely be very complicated in terms of the outcome. If not, then what controls target engagement? In studying the molecular target of a given compound, often a reductionist approach is the first step in gaining critical understandings the mechanism(s) of action in detail. Such information forms the foundation of our understanding of CO's role at the whole organism level. However, often studies of various targets were done independently of each other. Biochemical and cellular studies often supply ample amounts of CO in such a way that the concentration relevance of the study is lost. For going beyond individual molecular targets, it is important to take a holistic approach so that the intertwined relationships among the various targets are at least part of the consideration. Then, it would allow us to see both the individual "trees" as well as the "forest." Here we would like to present the "forest" before we discuss individual "trees." Metaphorically speaking, seeing the "forest" would allow us to begin to unveil the concealed elephant as in the fable of "Elephant in the Dark," which describes the incomplete descriptions of an elephant by those who only touch one part of the elephant in the dark without seeing the subject in its entirety (Rumi and Whinfield, 2004).

Figure 1 shows some major targets arranged in the order of their K_d values in binding with CO. At this point,

it is important to note that, generally speaking, carbon monoxide exists in the form of carbonylhemoglobin, also known as carboxyhemoglobin (COHb), in the blood. Or at least, this is the form that one can use in examining the binding competition between Hb and the target. This is also considered the major form of CO transportation through the systemic circulation. Carbon monoxide dosage and pharmacokinetic studies use concentrations of COHb as the key parameter (Levitt and Levitt, 2015; Wang et al., 2020). Reported COHb levels vary widely depending on study subjects, analytical methods, and whether it is banked or fresh blood. Normally, COHb concentrations are less than 2%. However, smokers can get up to 14% or higher COHb, though this number is typically below 9% (Goldman, 1977; Mitchell, 1979; Hart et al., 2006; Eichhorn et al., 2018; Meuli et al., 2020; Supervía et al., 2021). With such information as the background, target occupancy needs to consider the exchange of CO between a target and Hb. As a result, their relative affinity becomes an important, if not critical, consideration. It goes without saying that transferring CO from COHb to a target with a higher affinity (lower K_d) is an energetically favorable process, at least thermodynamically. In Fig. 1, competition for CO is represented as a "downhill" process. This is the case in transferring CO to neuroglobin, cytoglobin, and cardiolipin-cytochrome c complex. By the same token, transferring CO to a target with a higher K_d (lower affinity) is an energetically uphill process, such as in the case of soluble guanylyl cyclase (sGC). Looking at this thermodynamic equilibrium process in such a way does not automatically imply that the whole organism is in a "homogenous" equilibrium state. This is because of the need to consider the issue of "topography." There are significant factors that may affect the conditions in various locations, leading to "valleys" that vary among different locations in terms of CO concentrations and local conditions that may affect the various K_d values. This point will become clear in subsequent discussions once we bring in factors that affect CO binding to Hb and other targets.

At this moment, one might ask the question: how could COHb transfer CO to a range of targets with widely different K_d values? The answer lies with nature's marvels in "designing" Hb with tunable $K_{d,}$ in the range of 0.7–4.5 μM for CO, depending on other physiologic factors such as O_2 partial pressure, pH, and possibly other small organic molecules such as NO, H_2S, adenosylmethionine, steroids, and 2,3-bisphosphoglyceric acid. NO and H_2S are known to compete for binding to certain targets against CO; adenosylmethionine (AdoMet) is known to affect the affinity of cystathionine β-synthase (CBS) for CO; steroids are known to affect binding of CO to P450; and 2,3-bisphosphoglyceric acid is known to affect the conformation of Hb and its affinity for O_2 and CO. This tunable K_d aspect is discussed in the next section, but for now, this range of K_d values means that CO transfer can happen to a range of targets depending on the specific location and local conditions. The metaphor of having waterfalls at different elevation would allow the engagement of targets with K_d that is within (or close to) the K_d of CO for Hb at a particular location.

For some of the known hemoprotein targets, we would like to provide a visual presentation of published affinity data and their implications in CO occupancy relative to Hb in the form of figures so that readers can readily see how variations in COHb level would affect CO occupancy of a given target. In doing so, we take a binary approach in presenting the partitioning of CO between Hb and a given target based on their respective K_d values. Because Hb exists in high abundance, this binary approach should be a very good approximation. This approach is based on thermodynamics and does not take kinetics into account, which might become a factor, especially if there is rapid local production of CO in response to upregulated HO levels. Without hard data, discussing kinetics in any quantitative term would not be meaningful anyway. The equation to derive these figures is stated as follows (eq. 1) with details of their derivation provided in the Supplemental Appendix 1. In such a way, one can directly model the CO saturation level of a given target (CO-T)% resulting from "extracting" CO from the major CO carrier, COHb. This is essentially an equilibrium consideration in solution.

$$CO-T(\%) = \frac{\mathrm{COHb}\% \times Kd(co-Hb)}{Kd(CO-T) + \mathrm{COHb}\% \times (Kb(CO-Hb)Kd(CO-T))} \times 100\% \quad (1)$$

By plotting this equation based on the known range of K_d of CO for Hb (~0.7–4.5 μM) and the K_d of CO for various hemoproteins (~0.1–10 mM), we present Fig. 4 to show what it means quantitatively in transferring CO from COHb to a target with a defined K_d. This means that molecular targets with K_d values in the same range as COHb all have the chance for "lateral" transfer of CO from Hb. This CO transfer process depends on the location and local conditions and thus the K_d of Hb for CO ($K_{d(CO\text{-}Hb)}$) at that location. In this figure, we present a three-dimensional (3-D) and contour plot by using a fixed concentration of 14% COHb, which is what the US Food and Drug Administration had allowed as an upper limit for human clinical trials (Yang et al., 2020b). Fixing the COHb level allows us to accommodate a number of possible targets without going to 4-D in presenting an overall landscape. In discussing individual targets in the subsequent sections, we fix the K_d of the target protein for CO ($K_{d(CO\text{-}T)}$) and then vary the level of COHb to allow for more detailed analyses of the saturation levels for each target under different conditions. Figure 4A shows the target CO saturation level

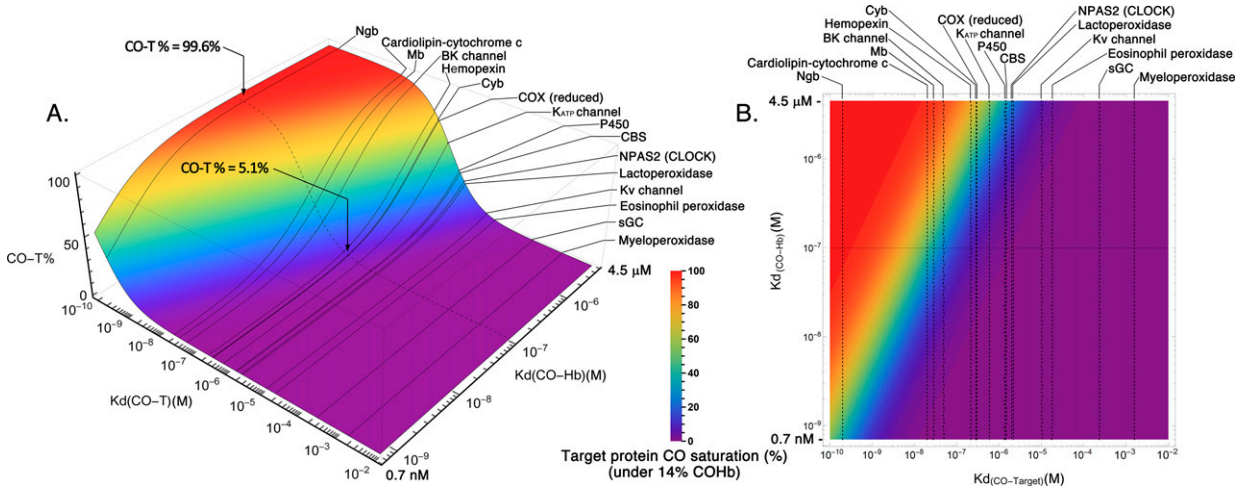

Fig. 4. Overall contour map of CO's binding with various targets under 14% COHb level as the reference point. (A) A 3-D plot of the target CO saturation percentage (CO-T%, *z*-axis) of various hemoproteins with definitive K_d(CO-T) (*x*-axis) at a given K_d(CO-Hb) (*y*-axis); (B) A 2-D contour map of the 3-D plot A. Target protein CO saturation percentage is shown by different colors. In (A) and (B_, the dashed lines in the graphs mark the point of K_d = 0.1 μM CO-hemoglobin binding. It serves as a reference level showing that for a high-affinity target (Ngb), 14% COHb leads to saturation by CO to a level of 99.6%, whereas for a target of moderate CO affinity (COX), 14% COHb only leads to 5.1% CO saturation. The graphs were generated based on eq. 1 by using Mathematica 12 (codes provided in Supplemental Appendix 2).

(CO-T%, *z*-axis) at a given $K_{d(CO\text{-}Hb)}$ (*y*-axis). The various targets are positioned on the *x*-axis based on their known K_d values for CO. For example, neuroglobin (Ngb) has a very high affinity for CO, with the reported K_d being 0.2 nM. Therefore, the transfer of CO from COHb, even at its high-affinity state (K_d 0.7 nM), is an energetically favorable process. At a COHb concentration of 14% in the blood, the net partitioning of CO between Hb and Ngb would allow more than 36% saturation of Ngb, even with high-affinity R state COHb. If the partitioning is between Ngb and Hb at its low-affinity state (K_d 4.5 μM), then Ngb can reach nearly 100% saturation. On the other hand, the competition for CO between Hb and sGC (K_d 240 μM) is such that very little CO is expected to transfer to sGC and the maximum sGC CO saturation is no more than 0.3%, even when COHb is at its low-affinity state (K_d 4.5 μM). There are other targets that are in between. For example, transferring CO from COHb to cytochrome c oxidase (COX) would only happen when COHb is in its low-affinity state, presumably at peripheral tissues, where oxygenation level and pH are low. Figure 4 is meant to provide an overview of the effect of the binding affinity of the various known targets on target engagement. Figure 4B is the 2-D contour map of Fig. 4A that allows estimation of the target protein CO saturation based on color. Detailed analyses for each target are presented in subsequent sections.

IV. Carbon Monoxide Binding to Hemoproteins Involved in Oxygen Transport and Storage

A. Carbon Monoxide Binding to Hemoglobin

Hb is the most abundant hemoprotein and serves as a heme reservoir in the body. Therefore, any discussion of CO's effects needs to start with Hb binding with CO, leading to carbonylhemoglobin, also referred to as carboxyhemoglobin (COHb), formation. The physiologic roles of Hb (Dickerson, 1983; Ahmed et al., 2020) and the implications of CO binding (Hampson, 2018; Yang et al., 2021a) have been discussed in detail elsewhere and are not duplicated here (Hampson, 2018; Yang et al., 2021a). Whichever way CO is administered, COHb is likely the major "carrier" form of CO to the various targets accessible via systemic circulation, allowing for transfer of CO to the final target(s) either directly or more likely through release and diffusion. At this time, it is important to put the issue of diffusion in the context of CO's solubility under various partial pressures. At 1 atmosphere (atm), the solubility of CO is about 1 mM. However, the solubility is much smaller within the normal range of CO exposure that one would experience. For example, at 250 ppm (0.025% of 1 atm), the CO concentration in water is only 200 nM at 37°C based on calculations using Henry's law (Levitt and Levitt, 2015). However, in a human body most of the time, one has to deal with nonequilibrium conditions. Because the K_d of Hb for CO can be as low as 0.7 nM, the water solubility of CO under 250 ppm is sufficient to drive to full saturation of Hb if ample amount of CO is supplied, leading to toxicity. For therapeutic applications, the issue of COHb percentage (saturation level) becomes very important. Therefore, the exposure level of a given target and COHb saturation level are two important considerations. Further, one also needs to consider the interplay of factors such as CO delivery rate, diffusion rate, binding kinetics (especially the on rate) with Hb and possible local targets at the delivery site, and the relative abundance of various targets in designing experiments to minimize toxicity

and maximize intended effects. There is one recent review that specifically focus on CO delivery and toxicity issues (Yang et al., 2021b).

When considering the transfer of CO from COHb to a target, the relative affinity of CO with Hb and a specific target is an important consideration. Because of its essential role in carrying life-supporting oxygen in the circulation, Hb concentration in adult human blood is high at about 1.9–2.8 mM hemoglobin tetramer (Beutler and Waalen, 2006; Lodemann et al., 2010), which is the circulating form with four heme molecules in each Hb. As a result, heme concentration is about 7.5–11.3 mM. CO at high levels is known for its toxicity because of its ability to bind with Hb, resulting in impeded oxygen carrying ability. The overall apparent K_d for CO to Hb is approximately 1.3 nM and is 234 times lower than that of O_2 (Chakraborty et al., 2004). The overall apparent K_d, however, does not tell the whole story and represents the composite results of different forms of Hb with varying K_d values for CO, depending on the level of oxygen saturation, the Hb conformational state, and pH (Zock, 1990). The dynamic equilibrium among different states of Hb is probably what allows CO to be transferred from Hb to other targets with a much lower affinity (higher K_d) than a K_d of 1.3 nM. It is well understood that the four heme molecules, one in each subunit of Hb, work cooperatively in binding with oxygen (and CO). It is generally believed that Hb exists in two conformations, a low-affinity taut (tense) form (T State) and a high-affinity relaxed form (R State), with some complex mechanistic interpretations that are subject to debate and interpretations (Mihailescu and Russu, 2001; Yonetani et al., 2002; Fan et al., 2013; Yuan et al., 2015; Cho et al., 2018). However, for the purpose of this discussion, we can accept the generally agreed observations without getting into the details of each model and the mechanistic questions. Briefly, deoxyHb adopts the T state at low oxygen concentrations due to the allosteric effect from increased CO_2 concentrations, increased acidity in remote tissues (Bohr effect), and a stabilization effect by 2,3-bisphosphoglyceric acid (2,3-BPG or 2,3-DPG). In the well oxygenated pulmonary capillaries, the elevated pH and reduced CO_2 concentration destabilize the T state. Binding of the first oxygen molecule to the T state of Hb has a K_d of 422 μM (Sharma et al., 1978). However, this binding changes the ferrous iron to a six-coordinated state and an octahedral conformation, leading to allosteric changes of the Hb tetramer to the high-affinity R state (Brunori et al., 1972), with a K_d of 0.3–1 μM for O_2. As a result of the conformational changes, binding affinity increases by about 300-fold (Unzai et al., 1998). This cooperative binding phenomenon gives a sigmoidal shape O_2-Hb dissociation curve (Fig. 5A) and empowers Hb to bind fast and tight with oxygen in the lung where the oxygen partial pressure is high while readily allowing unloading of oxygen to the peripheral tissue where the oxygen partial pressure is low. CO binds with Hb in a similar manner as oxygen. Binding of the first CO molecule to the T form of deoxyHb transforms it into the R form, with increased affinity for the successive CO or O_2 molecules. This is a part of CO's toxicity effect. At a low CO concentration, when O_2 can compete against CO binding, the consequence of CO binding is the formation of partially CO-bound Hb forms such as $Hb_4(O_2)_2(CO)_2$ and $Hb_4(O_2)_3CO$ (Sharma et al., 1976), which results in not only a decreased oxygen binding capacity but also a shift of the oxyHb dissociation curve to the left with a decreased ability of Hb to unload oxygen at peripheral tissue where the oxygen partial pressure is low (Hlastala et al., 1976; Andersen and Stark, 2012) (Fig. 5B). At high CO concentration, CO can occupy the entire tetrameric Hb to form $Hb_4(CO)_4$ (Sharma et al., 1976), leading to a complete loss of oxygen carrying ability. The K_d for CO with the T state Hb was determined to be 1.8 μM for the α-subunit and 4.5 μM for the β-subunit. In contrast, in the R state, the K_d of CO binding to Hb was determined to be 1.7 nM for the α-subunit and 0.7 nM for the β-subunit (Vandegriff et al., 1991; Unzai et al., 1998). The difference in affinity between the R and T states is 1000- to 6400-fold, which is far greater than that of oxygen. This means that the difference in affinity between CO and O_2 with Hb is higher (about 600-fold) in the R state than the difference

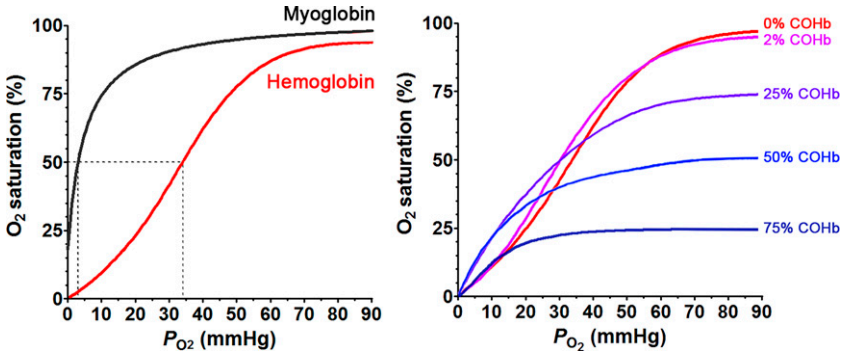

Fig. 5. Oxygen dissociation curves of hemoglobin and myoglobin (left) and O_2 saturation curves at different COHb levels (right); adapted with permission from ASPET (Hlastala et al., 1976).

in the T state (about 230-fold). The higher relative affinity for CO in the R state (lung) than in the T state (peripheral tissue) is one way in the literature to explain why inhaled CO is more prone to causing toxicity than CO administered in other ways, such as infusion of COHb in experimental animal models (Goldbaum et al., 1975; Romão et al., 2012). There are other systematic analyses as to why inhaled CO is more toxic (Yang et al., 2021b).

The influence of CO on the binding affinity of O_2 to Hb and vice versa not only is responsible (at least partially) for CO's toxicity but can also influence the pharmacokinetics of CO. The apparent oxygen binding/dissociation characteristics depend on the Bohr effect, which is the reason for the efficient delivery of O_2 to the remote tissue. The Bohr effect for oxygen is expressed by the Bohr factor: $\Delta\log(P_{50})/\Delta pH$, in which $\Delta\log(P_{50})$ is the change of log value of the partial pressure of O_2 to saturate 50% of hemoglobin (P_{50}) and ΔpH is the change of the pH value. Hlastala et al. (1976) conducted a series of experiments on the influence of CO on the Bohr effect of human Hb. It was found that besides the lower O_2 saturation level and P_{50}, increased COHb levels significantly increase the Bohr factor. At high COHb levels (>25%), a small pH decrease was found to lead to a great decrease of oxygen's binding affinity to Hb, thus facilitating unloading of the remaining oxygen. It seems that this effect offers protection for the host under CO intoxication conditions (Hlastala et al., 1976). It should be noted that the Bohr effect also applies to CO's binding to Hb (Brunori et al., 1972). Sawicki and Gibson (1978) used a flow-laser flash experiment to demonstrate that CO's binding cooperativity is also pH dependent, though less pronounced than that of O_2. At pH 7 in phosphate buffer, Hb is completely switched to the R state after binding three CO molecules. In contrast, at pH 9, significant conformational changes occur after binding with one CO molecule (Sawicki and Gibson, 1978). However, the physiologic relevance of pH 9 is not clear. At a lower physiologic pH, upon CO binding, mammalian Hb still exists as a mixture of the T and R states, due to the high binding affinity of CO and cooperativity in binding of mammalian Hb. On the contrary, fish hemoglobin appears to have an exaggerated Bohr effect under acidic pH, which provides hints for understanding the affinity of T state Hb for CO at acidic pH (Saffran and Gibson, 1978).

All of the discussions of the different conformational states, variations in binding affinities, and pH dependence in binding between CO and Hb mean that CO binding is a dynamic process, which allows unloading and transferring of CO to the targets in various parts of the body (Mao et al., 2021; Yang et al., 2021b, 2022a). Further, the partitioning of CO between Hb and a given target should probably not be directly calculated based on the global average binding affinity without considering local conditions. How exactly the dynamic equilibrium of the various states affects the ability of Hb to bind and unload CO is a question that will require many more experimental studies. Another aspect of CO binding to hemoglobin is its reservoir role as in the case of albumin for small nonvolatile organic molecules. Therefore, hemoglobin helps to keep the free concentration of CO "in check" based on binding affinity and equilibria. The sections below have extensive discussions of this aspect in the context of individual molecular targets. We have also discussed this aspect elsewhere in the context of pharmacokinetics and drug delivery (Yang et al., 2021b, 2022a). Recently, Kitagishi and colleagues used a high-affinity cyclodextrin-encapsulated Fe(II) porphyrin to determine tissue CO concentrations, providing evidence that hemoglobin helps to dampen CO's toxic effects via controlling availability of free CO (Mao et al., 2021).

B. Carbon Monoxide and Myoglobin

Myoglobin (Mb) is the second most abundant heme pool in the human body. Structurally, myoglobin is a homolog of Hb's α- and β-subunits and has a single polypeptide chain with only one oxygen binding site. It has a molecular mass of 16.7 kDa and is mainly located in the muscle tissue, with about 0.9–2.2 g per 100 g of dry muscle depending on the autopsy position (Akeson et al., 1968). On average, the amount of total myoglobin in an adult male with a body weight of 70 kg is about 120–150 g, corresponding to about 6.6–8.4 mmol. As myoglobin has only one heme group, the total heme from myoglobin is calculated to be approximately one-seventh to one-fifth of that from the Hb pool in the body. Mb has a higher affinity for oxygen than Hb does. Therefore, it functions as an oxygen storage pool in the skeleton muscle to preserve oxygen for muscle functions under poorly oxygenated conditions (Garry and Mammen, 2007). However, its binding affinity to CO is less than that to Hb at its R state of the highest affinity, and the difference between CO and O_2 binding affinity for Mb is only about 28-fold. The K_d of human Mb is 0.8 μM for O_2 and 29 nM for CO (Gibson et al., 1986; Moffet et al., 2001). Like Hb, CO binding also results in conformational changes for Mb (Fig. 6). By using nanosecond laser-pulse photolysis to dissociate the bound CO, it was found that myoglobin undergoes conformational relaxation after CO dissociation (Ansari et al., 1994). However, because Mb is a monomer and only has one heme binding site, there is no cooperativity in binding with CO (or O_2). Therefore, its oxygen saturation curve is hyperbolic, whereas for Hb it is a sigmoid curve (Fig. 5A). At this point, it is important to discuss the affinity difference between Hb and Mb for CO in the context of CO transfer from the blood (COHb) to Mb with a K_d of 29 nM. As discussed above, the K_d for

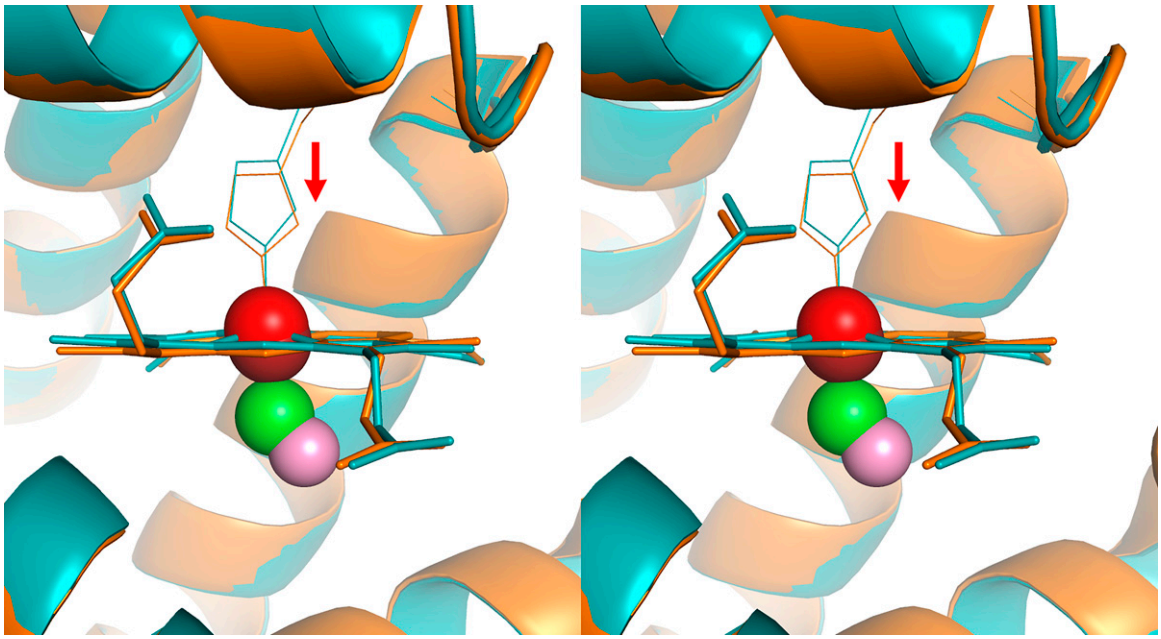

Fig. 6. Conformational changes before and after CO binding with myoglobin (cross-eye stereo, generated from Protein Data Bank (PDB) 1mbc and 1mbd). Cyan coil and cyan stick heme molecules show the conformation before CO binding with the iron center (red sphere) slightly above the heme plane. After CO (green carbon and pink oxygen sphere) binding with the iron center of the heme, it pulls the iron atom (dark red sphere) back to the heme plane and consequently the histidine residue toward the heme plan, leading to conformational changes (orange coil and stick).

CO with Hb in the T state is 1.8 μM for the α-subunit and 4.5 μM for the β-subunit. In contrast, in the R state, the K_d of CO binding to Hb is 1.7 nM for the α-subunit and 0.7 nM for the β-subunit (Vandegriff et al., 1991; Unzai et al., 1998). Presumably, the T state is the predominant form in peripheral tissues and poorly oxygenated sites where the pH is also low, whereas the R state is the dominant form in the artery, the heart, and the lungs. If this is true, CO transfer from the T state of Hb to Mb is a thermodynamically and presumably kinetically favorable process. However, in the lung and heart, it becomes hard to say where the equilibrium lies.

As discussed above, because of the dynamic equilibrium of the various states for Hb and their different binding affinities (Changeux, 2012; Hilser et al., 2012), transferring CO from COHb to Mb is more likely in muscle tissues with reduced oxygen tension and thus with Hb predominantly in the T state. In an experiment to assess myoglobin's oxygen tension (partial pressure of oxygen that binds to myoglobin), a small volume of pure CO was administered to a dog, leading to a COHb level of 12%–23% (Coburn and Mayers, 1971). In the meantime, COMb in hamstring muscle also increased to 9%–24% and the COMb/COHb ratio was calculated to be 1.1 ± 0.12. Such results suggest that at the site of hamstring muscle, the "average" K_d of Hb for CO was probably similar to that of Mb (29 nM) under the specified experimental conditions.

The above experiment is an excellent example in assessing target engagement when CO is "delivered" in the form of COHb. Because the most convenient way of measuring CO exposure is the COHb level, published pharmacokinetic studies of CO all relied on COHb concentrations (Levitt and Levitt, 2015; Wang et al., 2020). Therefore, in studying CO's target engagement, the ratio of the relative CO "saturation level" between Hb and the target is the parameter that will allow quantitative assessment and intuitive expression of the relationship between COHb level and target binding. In doing so, we introduce a 3-D plot and a 2-D contour map to illustrate the theoretical CO saturation level of the target protein in a binary system (Fig. 7). The system only involves the preequilibrated hemoglobin with the COHb % as one variable and the K_d of CO-Hb binding affinity as the other variable. The change of the latter variable is due to the two affinity states of Hb (T and R states) as discussed in the hemoglobin section.

In such a way, one can directly estimate target's CO saturation levels resulting from "extracting" CO from the major CO carrier, COHb. Herein and for all of the targets we discuss in subsequent sections, we select three representative COHb levels to discuss the corresponding target saturation level in the context of being physiologically and therapeutically relevant. The specific COHb levels marked on the 3-D and 2-D contour maps are: 1%, representing a normal physiologic COHb level resulting from endogenous CO generation

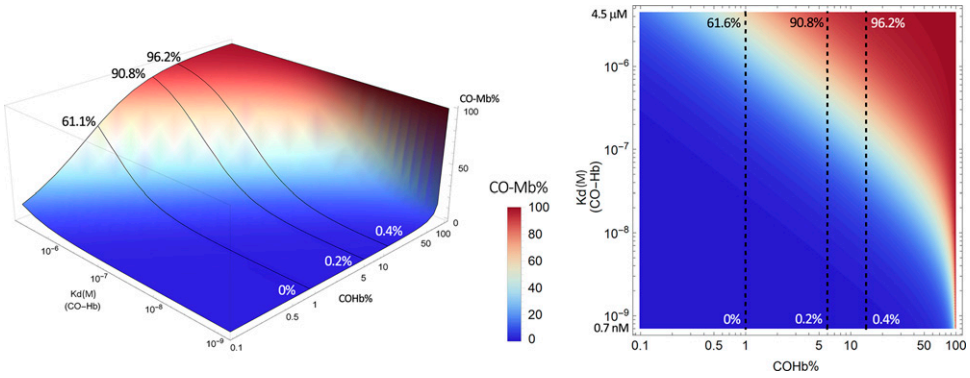

Fig. 7. Estimated CO saturation levels of myoglobin in the presence of COHb at various concentrations. Solid lines in the left panel and dashed lines in the right panel represent scenarios with COHb concentrations at 1%, 6%, and 14%, respectively. The graphs were generated based on eq. 1 by using Mathematica 12 (codes provided in Supplemental Appendix 2).

(Beard, 1969); 6%, representing a COHb level commonly seen in smokers and an approximate COHb level likely achievable in human subjects after CO administration (Sheps et al., 1991; Fazekas et al., 2012); and 14%, representing the highest threshold level of COHb allowable in humans by the US Food and Drug Administration. Although COHb levels above 14% can be achieved, they will not be discussed in detail in the context of current review for lack of therapeutic relevance. It should be emphasized again that eq. 1 and the derivative plots are based on a binary (Hb vs. target) system by considering only CO without considering binding by other species such as NO, H_2S, and O_2. Thus, the numbers are only quantitative reference points for consideration before designing experimental studies. Obviously, experimental data will be needed to inform therapeutic decisions.

A careful analysis of Fig. 7 shows that in the high-affinity R state of COHb (K_d 0.7 nM), very little transfer of CO from COHb to Mb would happen, even when the COHb level is high. For example, 14% COHb in the high-affinity R state is expected to induce only 0.4% myoglobin CO saturation. However, in its low-affinity state (K_d 4.5 μM), 1% COHb can lead to 61% saturation of Mb and 5% COHb can lead to nearly 90% saturation of Mb. Such analysis also means that the partitioning of CO between Hb and Mb is a dynamic process and is dependent on the physiologic and pathologic states of the tissue/location in question, including perturbation of the local pH, oxygenation level, the presence of other ligands (Egan and Zierath, 2013), and ultimately the affinity of Hb for CO. At this point, we would like to raise one question for readers to ponder. In considering CO's endogenous signaling roles and therapeutic actions, often the discussions are focused on the amount of CO available, either through upregulation of HO-1 or external delivery. If one looks at the plots in Fig. 7, it is very clear that changes of local conditions such as pH or oxygenation level could play a very important role in regulating the level of target engagement (i.e., Mb in this case), even if COHb level does not change. For example, it is well known that exercise leads to production of lactic acid in the skeletal muscle and thus acidification (Robergs et al., 2004), which could in turn lead to a decrease of Hb's affinity for CO and thus increased transfer of CO to Mb without increasing the level of COHb. This scenario could be applicable to many pathophysiological conditions. In another word, CO could play regulatory roles without a change of the COHb level as a prerequisite.

Although the major function of Mb is to store and increase the diffusion rate of oxygen to myocytes, from an evolutionary perspective the aforementioned conformational changes indicate that it should have other secondary functions as well. Indeed, it was revealed by Frauenfelder et al. (2001) that Mb has allosteric enzymatic functions, including those similar to that of peroxidase and cytochrome P450. Due to the spatially congested nature of the heme-binding motif, substrates for Mb are limited to small molecules such as O_2, CO, and NO, and H_2O_2, among others. Nature has shaped Mb like a micro redox chemical reactor for such molecules, with the iron center being an electron transport and/or catalytic center. It is known that Mb can mediate redox reactions involving O_2, NO, and nitrite (Richards, 2013).

During this process (Scheme 1), deoxymyoglobin (Mb) reacts with O_2 to produce ferric metmyoglobin

$$Mb + O_2 \longrightarrow metMb^+ + O_2^{\bullet-} \quad (I)$$

$$Mb + O_2 \longrightarrow MbO_2 \quad (II)$$

$$MbO_2 + H^+ \longrightarrow metMb^+ + HO_2^{\bullet} \quad (III)$$

$$MbO_2 + NO \longrightarrow metMb^+ + NO_3^- \quad (IV)$$

$$MbO_2 + NO_2^- \xrightarrow{H^+\ H_2O} metMb^+ + NO_x \quad (V)$$

Scheme 1. Redox reactions mediated by myoglobin.

(MetMb) and superoxide radical (I). Deoxymyoglobin binds with oxygen to form oxymyoglobin (MbO_2, II); the bound O_2 in MbO_2 can be protonated and undergo one-electron oxidation of the ferrous iron to produce MetMb and hydroperoxyl radical (III). MbO_2 also readily reacts with nitric oxide to form nitrate anion and MetMb (IV); this reaction contributes to the metabolism of NO and affects NO concentration gradient with signaling implications (Liu et al., 1998a). Similarly, MbO_2 can react with nitrite to generate peroxynitrite species (V) (Liu et al., 1998a). By the same token, MbO_2 can react with nitrite to generate peroxynitrite species (V). The generated reactive oxygen species (ROS) such as superoxide, hydroperoxyl radicals, and peroxynitrite can lead to oxidative damage to the cell. However, when Mb is bound to CO, the redox catalysis is inhibited. This mechanism partially contributes to CO's antioxidative activity in myocytes. Indeed, CO was found to abolish the oxidation of low-density lipoprotein (LDL) by horseradish peroxidase (HRP) (Natella et al., 1998). CO was also found to trap the heme iron in HRP in its ferrous state, therefore preventing its redox activity. Along the same line, upon rhabdomyolysis or traumatic muscle damage, the released ferrous Mb can mediate redox reactions and cause oxidative damage. Shaklai et al. found that CO sequestered the ferrous Mb and completely arrested Mb-mediated oxidation of LDL (Sher et al., 2014). CO has also been found to attenuate Hb-induced LDL oxidation by blocking heme oxidation and the transfer of heme from Hb to LDL. Unlike Mb, Hb's oxidative activity results from a weakening of the binding between ferric heme and globin (Bunn and Jandl, 1968; Natella et al., 1998). If Hb is released from the red blood cell due to hemolysis, then transfer of the hemin molecule to other proteins such as LDL is possible; this can lead to in situ oxidation catalyzed by hemin. In this aspect, Hb-sequestering proteins such as haptoglobin and hemopexin are more efficient than CO in arresting hemin released from Hb. However, myoglobin, on the other hand, has stable binding with heme, contributing very little to hemin transfer to other proteins. Therefore, CO generated by the HO-1 pathway or given exogenously is capable of arresting Mb's oxidative toxicity (Sher et al., 2014). At the molecular level, Shaklai et al. demonstrated that CO promotes the reduction of the oxidized hemoproteins such as methemoglobin (MetHb) and MetMb by using peroxides as electron donors (Sher et al., 2012). This mechanism adds another possible aspect of the vascular protection effect of the HO/CO axis. From another point of view, the food industry also utilizes CO's ability to sequester ferrous iron in myoglobin to preserve the red color of meat that comes from ferrous Mb and to avoid the dull brown color from oxidized MetMb (Sher et al., 2012).

Therefore, Mb is a target of CO with high affinity to allow almost "lateral" transfer of CO from COHb. Further, because Mb also has some enzymatic functions, CO binding may lead to modified reactivity and other implications (Jue and Chung, 2003; Chung et al., 2006; Huysal et al., 2016; Postnikova and Shekhovtsova, 2018).

C. Neuroglobin and Cytoglobin

Neuroglobin (Ngb) was discovered by Burmester in 2000. It only shares less than 25% similarity with Mb and Hb, and its evolutionary origin may trace back to nerve globins of invertebrates (Dubey and Dubey, 2019). As the third heme-containing globin in mammals, it is mainly expressed in the central and peripheral nervous system, including cerebrospinal fluid, retina, and endocrine tissues. The physiologic level of Ngb is about the equivalent of $\sim$0.2 μM, which is much lower than those of Hb or Mb. Different from Hb and Mb, the ferrous atom in Ngb is hexa-coordinated with an additional distal histidine residue (H64). Similar to Mb, Ngb is a monomeric protein with a high binding affinity to oxygen (K_d, 3.2 nM), which is about 30–100 times higher than that of Hb (Dewilde et al., 2001). Therefore, such a high affinity can increase oxygen availability and protect neuron cells under hypoxic or ischemic conditions. Ngb is significantly upregulated under hypoxic conditions (Schmidt et al., 2004). Upon formation of a disulfide bond between Cys46 and Cys55 on the protein surface under oxidative stress, Ngb undergoes conformational changes, which transfer the hexa-coordinated structure to a penta-coordinated one, leading to an increase in its nitrite reductase activity (Omar and Webb, 2014). In addition to oxygen binding activity, Ngb has also been reported to allosterically modulate nitro reductase, NO dioxygenase, and peroxidase activities. Further, evidence seems to be emerging that supports the involvement of Ngb in redox sensing, oxidative stress, ischemia damage, and inflammatory responses (Mathai et al., 2020). In fact, all of the mammalian heme-associated globins have been shown to possess nitrite reductase activity in their deoxygenated state. The reaction has been very well characterized (Scheme 2).

The reduction of nitrite generates NO and ferric Ngb. The increased NO leads to inhibition of mitochondrial respiration, oxygen consumption, and ROS production (Raub and Benignus, 2002; Tiso et al., 2011; Qiu and Chen, 2014). The ferric Ngb, but not the ferrous Ngb, acts as guanine nucleotide dissociation inhibitor (GDI) and binds to the GDP-bound form of the α-subunit of G protein with a K_d of 0.6 μM,

$$\text{DeoxyFe(II)} + NO^{2-} + H^{+} \longrightarrow \text{Fe(III)} + NO + OH^{-}$$

Scheme 2. Nitrite reductase activity of ferrous heme-associated globins.

leading to protection against neuronal death (Wakasugi et al., 2003). On the other hand, ferrous Ngb also binds with ferric cytochrome c and acts as reductase with a K_d of about 10 μM (Tiwari et al., 2015). Ferric cytochrome c (cyt c), but not ferrous cyt c, can initiate apoptosis. Ferrous Ngb may, on the other hand, function as an antiapoptotic molecule to offer cytoprotective effects to neuron cells (Fago et al., 2006). These findings led to the suggestion of Ngb being a neuroprotective molecule against stroke.

There have been studies of CO's affinity to Ngb (Azarov et al., 2016). The K_d of Ngb was determined to be 0.2 nM (Dewilde et al., 2001; Azarov et al., 2016). In contrast, the K_d of CO was 1.7 nM for the R state of Hb and 1.8 μM for the T state of Hb. Such results mean that Ngb should be able to "extract" CO from the high-affinity R state of Hb, let alone the "average ensemble" of the dynamic equilibrium of the various states. Further, the high affinity of Ngb for O_2 (K_d, 3.2 nM) means that it would take a higher relative concentration of CO to achieve the same effect of CO "poisoning" against Ngb than Hb. However, there has not been a study of the interplay among CO, O_2, and Ngb and the associated biologic significance. In our opinion, the colocalization of Ngb and HO-2 in neuron cells and the hypoxia-inducible nature of Ngb (Fiocchetti et al., 2019) and HO-1 (Motterlini et al., 2000) may indicate a potential link between CO and Ngb functions, which deserves in-depth studies.

Figure 8 presents a picture of the partitioning of CO between Ngb and COHb in a binary form based on published K_d values. It is clear that the high affinity of Ngb for CO means that transferring CO from Hb is an energetically favorable process, regardless of whether Hb is in its high-affinity R state or low-affinity T state. For example, even at its high-affinity state, it would only take 14% of COHb to allow for 36.3% saturation of Ngb. At the low-affinity state (μM K_d), COHb at 1% would allow 99.6% saturation of Ngb. Under such a circumstance, it is almost certain that the transfer is not under equilibrium conditions and is limited by CO availability. The high affinity of Ngb for CO help to partially explain why reversal of CNS damage after CO intoxication takes a much longer time than the time needed to decrease COHb levels in the blood (Bleecker, 2015; Rose et al., 2017). Further, if the K_d of COHb in the CNS, especially after some pathologic changes such as pH decrease, is much higher than the 0.7 nM for the high-affinity R state, then it may present a kinetic barrier in clearing CO from the CNS. One way to bridge this kinetic barrier is the use of a "catalytic amount" of a circulating intermediary binder that has a comparable or higher affinity for CO when compared with Ngb. A cyclodextrin-encapsulated heme (Kitagishi et al., 2016; Kitagishi and Minegishi, 2017) and an engineered Ngb may play such a role as described below.

A very interesting Ngb-related study is the engineering of a Ngb mutant with an even higher affinity for CO than Ngb itself, which can be used as a scavenger for treating CO intoxication (Azarov et al., 2016). Specifically, Gladwin and coworkers found that mutation of the distal histidine (H64) to glutamine led to a significant increase in binding affinity with CO to a K_d of 2.6 pM. As a result, this H64Q-Ngb is able to extract CO from COHb and Ngb and thus can function as an antidote for CO poisoning (Azarov et al., 2016; Rose et al., 2020).

In addition to Hb, Mb, and Ngb, there are other heme-containing globin proteins, including cytoglobin and androglobin. These two relatively "newcomers" actually have evolutionary longevity and diversity among metazoan species (Hoogewijs et al., 2012), although the detailed functions for these two have not been fully elucidated. As the fourth member of the vertebrate globin family, cytoglobin shares structural similarities with neuroglobin. The heme iron is also six-coordinated with a distal histidine (His81), and binding to a ligand displaces the distal histidine. CO is known to bind with cytoglobin and disassociate the distal histidine ligand (Makino et al., 2011). The dissociation constants of CO to the cytoglobin dimer and monomer were determined to be 0.29 μM and 68 nM,

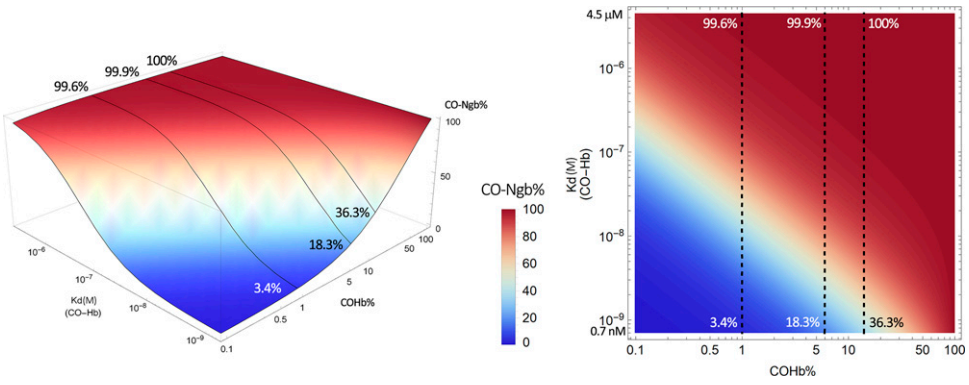

Fig. 8. Estimated CO saturation levels of neuroglobin in the presence of COHb at various concentrations. Solid lines in the left panel and dashed lines in the right panel represent scenarios with COHb concentrations at 1%, 6%, and 14% COHb, respectively. The graphs were generated based on eq. 1 by using Mathematica 12 (codes provided in Supplemental Appendix 2).

respectively (Tsujino et al., 2014; Beckerson et al., 2015). The conformational changes of cytoglobin upon CO binding are more pronounced compared with Ngb, indicating potential gas-sensing functions. Similar to Ngb, cytoglobin also has cysteine residues (Cys38, Cys83) that can form intramolecular and intermolecular disulfide bonds, leading to further conformational changes. Such properties also indicate a potential redox sensing function (Mathai et al., 2020). However, further studies are needed to understand its cellular functions.

V. Carbon Monoxide Binding to Heme-Containing Enzymes

Targets for carbon monoxide binding go beyond proteins important for oxygen transport and storage. CO is known to bind to a number of enzymes with diverse functions. Below we describe those targets that have been extensively studied.

A. Activation of Guanylyl Cyclase: An Intersection with the NO Signaling Pathway?

The three gasotransmitters are known to have overlapping activities and molecular targets, partially because of their ability to bind to metal centers. These interactions are complex, and the overall outcome likely depends on the interplay of many factors, including their relative affinities, relative concentrations, the presence of other proteins that can bind the same gasotransmitter(s), and maybe even on-off rates. The story of guanylyl cyclase is an especially important one for many reasons. Below we describe this molecular target and its interactions with CO and NO in detail.

To start, guanylyl cyclase is responsible for the synthesis of second messenger cyclic GMP (cGMP) from GTP (Fig. 9). There are two enzymes that catalyze the production of cGMP: particulate guanylate cyclase (pGC) and soluble guanylate cyclase (sGC). pGC is membrane bound and responds to extracellular signal molecules such as natriuretic peptides. Second, guanylate cyclase (GC) is cytosolic and exists in two forms: NO-dependent heme-containing form and NO-independent heme-free/oxidized form. Because sGC is known to be sensitive to NO as well as CO, this is the focus of this discussion. In the presence of a ferrous heme moiety, sGC constitutively catalyzes cGMP production at a low rate. Upon binding with NO, an intrinsic sGC stimulant, sGC increases the catalytic activity by at least 200-fold through allosteric regulations (Ma et al., 2007).

Structurally speaking, sGC is a heterodimeric complex consisting of two subunits, α and β, each of which has two isoforms (Derbyshire and Marletta, 2012). The most common sGC combination is $\alpha1/\beta1$, but $\alpha2/\beta1$ is highly expressed in some tissues (e.g., brain) (Koglin et al., 2001). Each subunit contains three

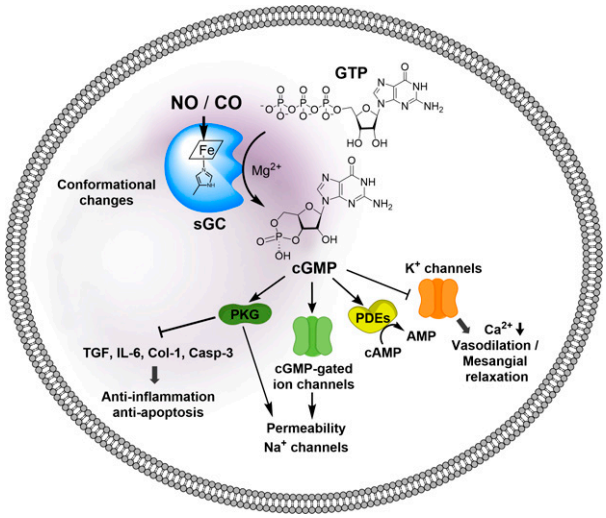

Fig. 9. NO/cGMP signaling pathways. NO or CO binding to the heme prosthetic group induces conformational changes of the catalytic domain, thus increasing the catalytic activity to produce cGMP from GTP. cGMP as a second messenger binds to intracellular target proteins; activation of protein kinase G inhibits expression of profibrotic genes, including transforming growth factor $\beta1$ (TGF-$\beta1$), Type-I collagen (Col-1), proinflammatory cytokine interleukin-6 (IL-6), activation of proapoptotic protein Caspase 3 (Casp-3), activation of cGMP-gated ion channels, activation of phosphodiesterases (PDEs), and inhibition of K^+ channels, thus decreasing intracellular Ca^{2+} concentrations.

common domains: 1) the N-terminal heme-binding domain (HBD) that mediates the NO sensitivity of the enzyme; 2) a dimerization domain, which is found in the middle of the structure of each subunit and is required for basal or NO-stimulated sGC activity; and 3) the C-terminal catalytic domain, which is the most highly conserved region between the subunits and is responsible for the conversion of GTP to cGMP (Priviero and Webb, 2010). The N-terminal HBD structurally belongs to the H-NOX (heme-nitric oxide/oxygen binding) family (Derbyshire and Marletta, 2012). The ability of NO to regulate the activity of sGC plays a critical role in various physiologic processes. As a secondary messenger, cGMP mediates three major pathways, including cGMP-dependent protein kinase, cGMP-regulated phosphodiesterase (PDE), and cGMP-gated ion channels (Fig. 9) (Denninger and Marletta, 1999). These signaling pathways in turn lead to various effects, including inhibition of smooth muscle proliferation, blockade of leukocyte infiltration and inhibition of platelet aggregation, anti-inflammation, antifibrosis, antiapoptosis, and vasodilation (Derbyshire and Marletta, 2012; Hoffmann et al., 2015; Friebe et al., 2020). Activation of the GC/cGMP signaling pathway offers protective effect in cardiovascular diseases (Hoffmann et al., 2015) and kidney injury (Chen and Burnett, 2018; Yang et al., 2020b), among others (Ingi et al., 1996; Feil and Kemp-Harper, 2006; Derbyshire and Marletta, 2012).

NO was found to bind to the five-coordinated ferrous iron of the heme located in the $\beta1$ subunit of sGC, where one of the coordinating groups is His105.

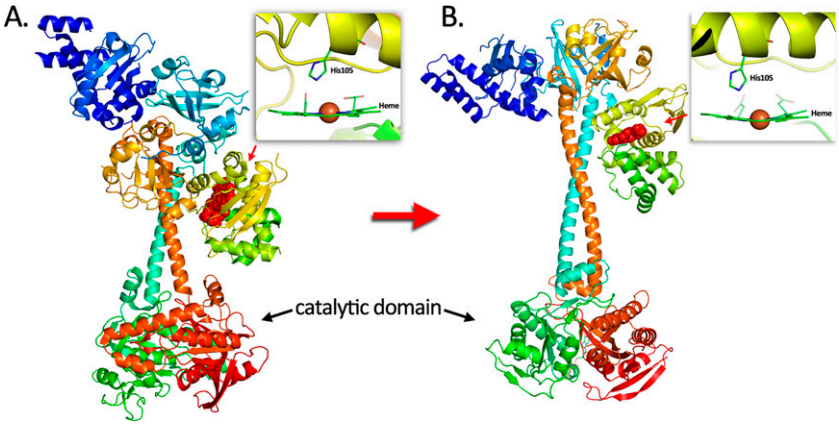

Fig. 10. Conformational changes before (A) and after (B) NO binding with heme (figure generated from PDB 6jt0 and 6jt2 by PyMOL).

NO binding leads to a six-coordinated heme (Fig. 10A). Subsequent binding with another NO on the proximal side of the heme followed by dissociation of the distal NO would further push the His105 sideways. All of these conformational changes allosterically induce large conformational changes of the catalytic H-NOX domain, favoring enzyme activation by 200-fold through enhanced GTP binding and thus catalytic activity (Fig. 10B). A cryo-electron microscopy (cryo-EM) study was able to show the drastic changes of protein conformation upon NO binding (Kang et al., 2019). The same N-terminal HBD of sGC that mediates the NO sensitivity of the enzyme also responds to CO binding, leading to activation by about 3- to 6-fold based on in vitro studies (Stone and Marletta, 1994; Friebe et al., 1996; Ma et al., 2007). To understand the mechanism of action of CO on sGC and its relationship to NO activation, the following section discusses the mechanistic aspects in brief.

Intuitively, it is easy to understand that the conformation of the hexa-coordinated CO-bound form is different from that of the penta-coordinated NO-bound form. As a result, the allosteric effects of these two gasotransmitters are also different. One quantitative factor is very important. In one report based on binding kinetics, it was said that the ratio of K_d values for NO:CO:O_2 stays at about $1:10^3:10^6$ for a range of heme-containing targets, including sGC, cyt c, and a bacterial hemoprotein *Nostoc* sp (Ns) heme nitric oxide/oxygen binding (H-NOX) protein (Ns H-NOX) (Ma et al., 2007; Tsai et al., 2012). The same study also deduced a "sliding scale rule" for predicting binding affinity of a hemoprotein, in which the proximal ligand is a histidine and the distal site is an apolar environment. The influence of the distal amino acid residue on the binding affinity was also discussed; thiolate, tyrosinate, and imidazolate were said to exert a "leveling" effect on ligand binding affinity (Tsai et al., 2012), though specifics may differ depending on the enzyme in question and conditions. The large differences in binding affinity already raise the issue of "nonequal" targets for CO, even though they all bind CO. If we examine some specific numbers, the picture becomes more complex, but the implications are the same. The K_d for sGC binding is 4.2 pM for NO and 240 μM for CO (Martin et al., 2006). This is a huge difference in binding affinity and probably means that CO does not play a physiologic role under nonpathologic conditions, when the COHb level is about 1% or lower and unlikely to afford a CO level that is close to its K_d with sGC. Further, the K_d for CO binding to the α- and β-subunits of Hb, even in the low-affinity T state, is 1.8 μM and 4.5 μM, respectively, which are far below the K_d for CO binding with sGC. In the R state, the K_d of CO binding to Hb is 1.7 nM for the α-subunit and 0.7 nM for the β-subunit. As such, the likelihood for sGC to "extract" CO from COHb is very small under physiologic conditions, and the maximum saturation level of sGC in an equilibrated binary system would only reach about 0.3% at a COHb level of 14%. The large difference between the K_d values for CO binding with sGC and Hb probably means that unless the CO level is very high in the systemic circulation and the pH is very low at a particular location, binding to sGC is unlikely to be a major regulating or toxicity factor for CO. The extremely large difference between NO and CO in their K_d values in binding with sGC probably also suggests that the proposed overlapping activity between NO and CO in activating sGC likely only comes into play at very high levels of CO and/or when NO synthesis is severely inhibited (Vogel et al., 1999). In this context, it is important to note that most of the studies in determining the 4-fold activation of sGC by CO were conducted in vitro. In the very first report of CO's effect on sGC, elegant work was performed by studying CO's inhibitory effect on platelet aggregation and 10,000 *g* supernatant from platelet homogenates was used (Brüne and Ullrich, 1987). Most of the experiments were done with pure CO; and it was found that platelet inhibition effects were observed in the range of 20–80 μM for CO. Such numbers are consistent with the known K_d of 240

μM for sGC for CO. Further, in determining the activation of sGC from bovine lung by NO (128 ± 17-fold) and CO (4.4 ± 0.4-fold), these experiments were performed using 0.5% of NO in argon and 100% CO, respectively (Stone and Marletta, 1994). One wonders whether the CO concentration created with 100% CO can be realized in vivo. As a result, even the modest 4-fold activation of sGC by CO might only be the biochemical maximum and is likely a significant overestimation of what is achievable in vivo. Of course, one also needs to keep in mind the short-lived nature of NO, which may come into play when examining the competition for binding with sGC between CO and NO.

In an effort to allow visualization of the partitioning of CO between Hb and sGC in a binary setup, we present a 3-D and a contour plot for the theoretically estimated sGC occupancy level in the presence of various levels of COHb with varying K_d values (Fig. 11). It is very clear that even at its low-affinity state, the transfer of CO to sGC is negligible. One would certainly not expect to see a regulatory role for CO under such circumstances. If CO indeed helps to activate sGC in vivo, there must be other factors at play in order for CO to overcome the known barrier of transferring from COHb to the low-affinity sGC.

The picture described above in terms of the intricate relationship in binding affinity and signaling molecule stability may only represent a small part of the complex signaling network. For example, H_2S is also known to stabilize sGC in its NO-responsive form (Szabo, 2017; Cao et al., 2018). Are there other endogenous molecules that may come into play? One would think the likelihood is real (Beuve, 2017; Kollau et al., 2018; Dai et al., 2019). Along a similar line, there are also synthetic small molecules that have "stimulating" effects on sGC and have regulatory roles in this intricate relationship (Fig. 12). For example, at 100 μM, the synthetic small molecule lificiguat (YC-1) has been shown to potentiate CO's stimulatory effect of bovine sGC to the similar magnitude of NO (using CO solution) (Stone and Marletta, 1998). It is worth noting that YC-1 alone can stimulate sGC activity by 12-fold even without NO or CO (Friebe et al., 1996). Further, in mice-derived sGC, YC-1 analogs such as BAY 41-2272 and PF-25 were found to increase CO's binding affinity to sGC and vice versa (Purohit et al., 2014). The affinity of sGC for these stimulators is also drastically augmented by CO. For example, YC-1 binds sGC with a K_d of $9-21$ μM in the absence of CO and $0.6-1.1$ μM in the presence of CO. PF-25 binds to sGC ~10-fold weaker than YC-1 in the absence of CO, whereas compound BAY 41-2272 binds particularly tightly in the presence of CO (K_d = $30-90$ nM). Surface plasmon resonance (SPR) binding studies showed that these YC-1 analogs bind to the N-terminal portion of the β1 chain near the heme domain and repress the allosteric inhibition effect from the α1 chain, which leads to expulsion of NO or CO from heme. Therefore, with YC-1, sGC retains its high-affinity binding conformation for NO or CO (using CO solution) (Purohit et al., 2014). However, how the β1 H-NOX domain switches from low to high affinity for CO and NO is still unknown. Some sGC stimulators have been studied in clinical trials for various indications (Armstrong et al., 2018; Xiao et al., 2019).

With of all of the discussions of the intricacy of CO's effects on sGC, it is important to examine experimental results using CO in vivo. In one case using sGC inhibitor NS2028, Zhang et al. showed that a ruthenium-based CORM, CORM-3, at a dosage of 4 mg/kg post-treatment was able to protect rats against neuronal pyroptosis in the cortical tissue after hemorrhagic shock and resuscitation. CORM-3 was also shown to partially restore sGC activity and cellular cGMP level, whereas pretreatment with NS2028 abolished the restoration effect. Restoration of the mitochondrial membrane potential was observed with CORM-3 treatment but not iCORM-3. This in turn

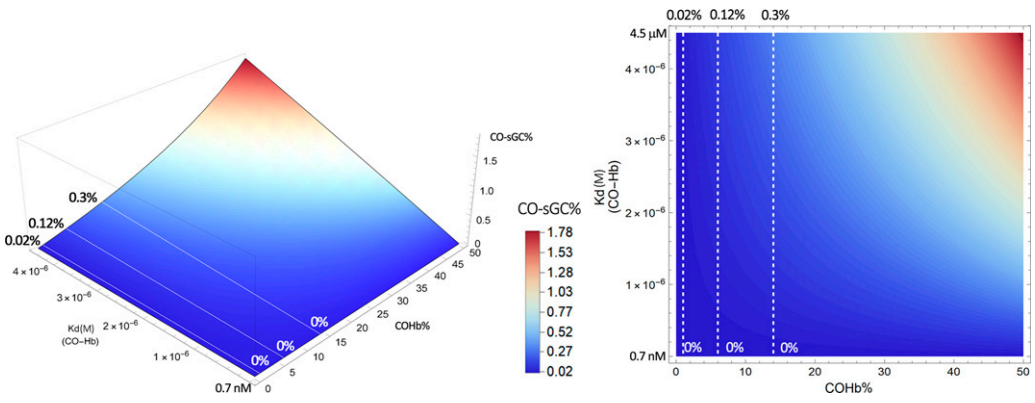

Fig. 11. Estimated CO saturation levels of sGC in the presence of various levels of COHb in a binary system. Solid lines in the left panel and dashed lines in the right panel represent scenarios at COHb concentrations of 1%, 6%, and 14%, respectively; scales are different from that of Fig. 8 due to the low affinity of sGC for CO and the need to expand the low-saturation level region to present a meaningful figure. The graphs were generated based on eq. 1 by using Mathematica 12 (codes provided in Supplemental Appendix 2).

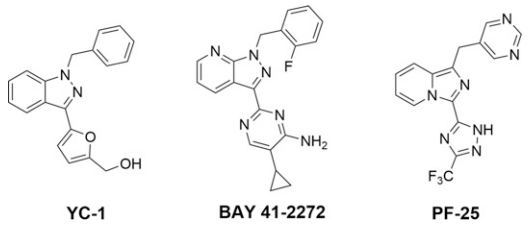

Fig. 12. Allosteric stimulators of sGC. YC-1: 3-(5′-hydroxymethyl-2′-furyl)-1-benzylindazole; BAY 41-2272: 3-(4-amino-5-cyclopropylpyrimidin-2-yl)-1-(2-fluorobenzyl)-1H-pyrazolo[3,4-b]pyridine; PF-25: 1-(pyrimidin-5-ylmethyl)-3-(3-(trifluoromethyl)-1H-1,2,4-triazol-5-yl)imidazo[1,5-a]pyridine.

reduced ROS generation after resuscitation, related mitochondrial damage and thus pyroptosis (Zhang et al., 2019). In terms of possible mechanism(s) of action, activating the sGC/cGMP/PKG pathway is known to activate the mitochondrial large-conductance calcium-activated potassium (BK_{Ca}) channel and thus regulate ROS generation (Walewska et al., 2018). This was proposed as one possible explanation. In the gastric system, Magierowski and coworkers (2019) also showed that pretreatment with 5 mg/kg CORM-2 was able to prevent ischemia-reperfusion–induced gastric mucosal injury in rats. sGC inhibitor ODQ (1H-[1,2,4]oxadiazolo[4,3-a]uinoxaline-1-one) was able to block the protective effect, which is consistent with sGC activation being a factor. Carretero and coworkers took the studies one step further to understand the mechanism of CO's effect in renal microcirculation. It was found that CORM-3 at 50 μM led to a decrease of tubuloglomerular feedback (TGF), which is the sensing mechanism that induces constriction of the afferent arteriole upon increased luminal NaCl concentration (Ren et al., 2008). Later, in isolated rabbit afferent arterioles (Af-Art, with glomerulus and adherent tubular segments), microperfusion with 50 μM CORM-3 was found to attenuate TGF levels by one-third to one-half, whereas this effect was blocked with the addition of 1 μM sGC inhibitor LY-53583. Such results are consistent with the attenuation of TGF by CORM-3 being mediated by activation of the (sGC)/cGMP system. Further studies with a cGMP-dependent protein kinase (PKG) inhibitor KT-5823, phosphodiesterase 2 (PDE2) inhibitor BAY-60-7550, and a cAMP analog dibutyryl-cAMP led to the finding that the attenuation of TGF by CORM-3 was via reduction in cAMP level. It was proposed that CORM-3 activation of the cGMP pathway and PKG, but not PDE2, led to the reduced cAMP levels (Ren et al., 2012). All such results are consistent with CO's role in activating sGC in vivo. However, ruthenium-based CORMs such as CORM-2 and -3 have been found to have biologic effects that are independent of their ability to donate CO (Dong et al., 2008; Santos-Silva et al., 2011b; Nielsen and Garza, 2014; Wareham et al., 2015; Nobre et al., 2016; Gessner et al., 2017; Southam et al., 2018, 2021; Juszczak et al., 2020; Nielsen, 2020a,b; Nielsen et al., 2020; Rossier et al., 2020; Stucki et al., 2020a; Yuan et al., 2020). Further, they have also been found to undergo chemical reactions under physiologic conditions (Gessner et al., 2017; Southam et al., 2018, 2021; Nielsen, 2020a; Yuan et al., 2020, 2021a,b). There have been several recent reports of the biologic effects of such CORMs being CO-independent after years of acceptance of their roles solely as CO donors (Southam et al., 2018; Juszczak et al., 2020; Nielsen, 2020a,b; Nielsen et al., 2020; Stucki et al., 2020a). Coupled with the relative low affinity of CO with sGC, it seems that the effect of CO on sGC in a physiologically relevant setting still needs more studies. More experimental work may be needed to truly understand the implications, if any, of these new findings in the interpretation of the above results related to sGC and CORM-2 and -3. As a result, the question of whether sGC is a key target for NO and CO to intersect under near physiologic conditions still faces a great deal of uncertainty. If they intersect, could there be possible indirect/secondary and/or tertiary pathways or a third player as a modulator? Could there be one or more endogenous "YC-1"-like compounds capable of augmenting CO binding to sGC? On a related note, the effect of CO on vasodilation is supported by results from many studies, though the proposed mechanism of actions varies (Wang, 1998; US-EPA, 2000; Ryan et al., 2006; Decaluwé et al., 2012a,b; Bae et al., 2021; Kaczara et al., 2021), including the attenuation of ROS-related responses (Lamon et al., 2009).

B. Cystathionine β-Synthase: An Intersection with Sulfur Signaling Pathways

Cystathionine β-synthase (CBS), an enzyme found in the cytosol and mitochondrial outer membrane (Szabo et al., 2013), is a key player in mammalian sulfur metabolism, specifically in methionine cycling and transsulfuration pathways (Hishiki et al., 2012; Suematsu et al., 2016). Through its action as a hydro-lyase, CBS commits L-homocysteine to the transsulfuration pathway by catalyzing the beta-replacement reaction between L-serine and L-homocysteine to form L-cystathionine (Scheme 3A). CBS is a major player in maintaining the intracellular homeostasis of L-homocysteine, which is considered as a risk factor for vascular diseases (Graham et al., 1997). CBS also catalyzes several other reactions that produce H_2S (Scheme 3B). In mammalian tissues, CBS funnels methionine from methionine metabolism pathways to the transsulfuration pathway as it commits L-homocysteine to forming cysteine and other vital sulfur metabolites such as H_2S and glutathione (GSH). Under oxidizing conditions, CBS is fully activated, thus favoring the formation of glutathione, a

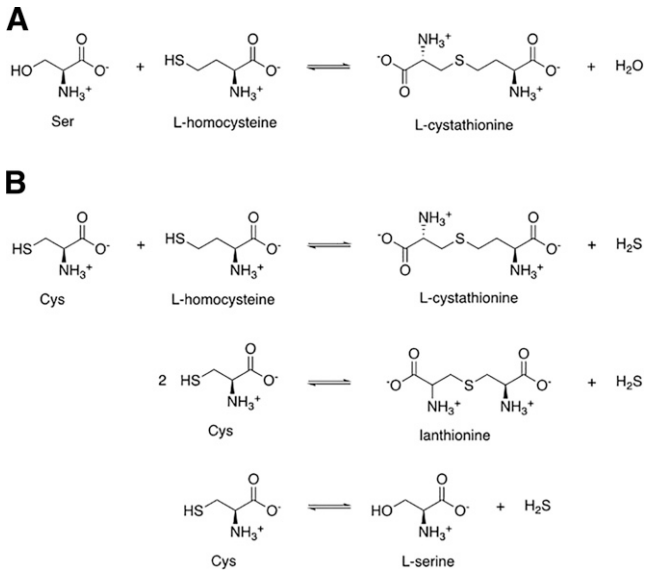

Scheme 3. Reactions catalyzed by CBS. (A) A beta-replacement reaction to produce L-cystathionine and (B) H_2S-producing reactions catalyzed by CBS.

key antioxidant present at high concentrations in the cellular milieu (Fig. 13). On the other hand, when CBS is in the resting state, L-homocysteine is directed to the transmethylation pathway, recycling methionine and providing precursors for methylation reactions. CBS regulation sustains the redox buffering capacity of the cell.

CBS is the only known hemoprotein that requires both heme and PLP (pyridoxal phosphate or vitamin B_6) for its functions (Kery et al., 1994). The active form of CBS is tetrameric, wherein each 63-kDa subunit consists of three structural domains: the N-terminal domain, the central catalytic core domain, and the C-terminal regulatory domain (Fig. 14) (Banerjee and Zou, 2005). The C-terminal regulatory domain includes the dimeric Bateman domain, consisting of a tandem repeat of two CBS motifs. This regulatory domain also binds the allosteric activator S-adenosylmethionine (SAM). The N-terminal domain binds the cofactor heme through cysteine 52 and histidine 65, whereas the active site in the catalytic core binds to pyridoxal phosphate (PLP) as another cofactor through imine formation with lysine-119. These two cofactors are 20 Å away from each other, pointing to a regulatory role for heme instead of catalytic (Meier et al., 2001). In the ferrous state, the heme moiety binds gaseous ligands such as CO and NO, leading to CBS inhibition. As a result, CBS sits at a point of convergence linking the three gasotransmitters (Vicente et al., 2018). Furthermore, from the involvement of multiple cofactors and various metabolic pathways, CO binding touches more than sulfur signaling per se.

1. CO Binding to Cystathionine β-Synthase. The heme cofactor in CBS exists in a low-spin and six-coordinated state with the axial ligands being thiolate and histidine (Omura et al., 1984; Ojha et al., 2002). In the ferrous state of CBS, CO binds heme by displacing its thiolate ligand, Cys52, leading to the stabilization of the six-coordinated complex. It is postulated that cysteine thiolate is preferentially displaced instead of histidine because of the presence of a salt bridge between Cys52 and Arg266, which helps to stabilize the thiolate after dissociation and thus impede rebinding to heme (Puranik et al., 2006). In wild-type (WT) human CBS, noncooperative CO binding was observed with K_d values of 1.5 ± 0.1 μM and 68 ± 14 μM, resulting in CBS inhibition with an inhibition constant (K_i) of 5.6 ± 1.9 μM (Taoka et al., 1999; Puranik et al., 2006). The slow on-rate for CO binding (18 $\mu M^{-1}s^{-1}$) is attributed to the slow dissociation of Cys52 from the ferrous heme with a dissociation rate of 0.0166 $seconds^{-1}$ at 24.5°C (Puranik et al., 2006). As a consequence of this slow on-rate for CO binding, a relatively high concentration of CO is needed to achieve physiologic relevance. This was postulated to prevent wasteful response to background fluctuations in local CO concentration (Puranik et al., 2006). As another example of CO and NO binding to the same target, it is important to note that nitric oxide binds to CBS to form a stable five-coordinated ferrous complex, displacing both the cysteine and histidine ligands. In a 2001 report using both NO gas-saturated buffer and

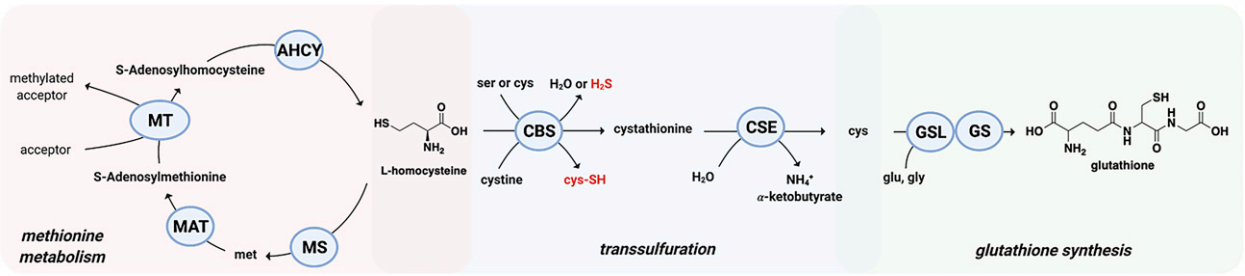

Fig. 13. CBS is a redox-sensitive enzyme at the junction of important pathways: methionine metabolism, transsulfuration, and glutathione synthesis. AHCY, adenosylhomocysteinase; CSE, cystathionine gamma-lyase; GCL, glutamate cysteine ligase; GS, GSH synthetase; MAT, methionine adenosyltransferase; MS, methionine synthase; MT, methyl transferase.

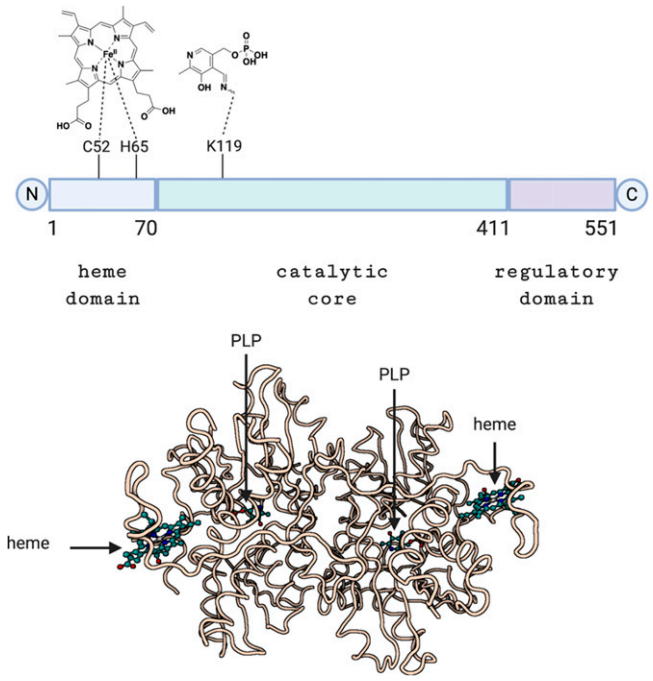

Fig. 14. A linear depiction and a 3-D representation of human cystathionine β-synthase showing the heme binding domain and the cofactor pyridoxal 5′-phosphate (PLP) (PDB 1jbq) (Meier et al., 2001).

DEA-NONOate as NO sources, the K_d for NO binding was determined to be 281 ± 50 μM with a K_i of 320 ± 60 μM (Taoka and Banerjee, 2001). As both native ligands are displaced upon NO binding, the question of maintaining the heme moiety enzyme bound was addressed by exposing NO-bound enzyme to air, which led to spectral changes consistent with the replacement of NO with the native ligands. However, in 2014, it was reported that NO binds ~1000-fold more tightly than previously reported and >100-fold faster than CO (Vicente et al., 2014). Using NO gas instead of an NO donor and static and stopped flow absorption spectroscopy, the apparent K_d was measured to be <0.23 μM at 25°C. Kinetic measurements revealed that NO gas quickly binds CBS with an association rate constant (k_{on}) of ~8×10^3 M^{-1} s^{-1} forming the Fe(II)-NO· adduct, whereas dissociation occurs at a slow rate with a dissociation rate constant of (k_{off}) of ~0.003 seconds^{-1}. In contrast to CO, NO binding is not hampered by the slow dissociation of cysteine 52 from the ferrous heme. In the presence of oxygen, inactivated ferrous CBS readily reacts with oxygen (1.11 ± 0.07 $\times$ 10^5 M^{-1} s^{-1}), yielding the enzymatically active ferric CBS (Carballal et al., 2008).

CO binding abolishes CBS activity via an Arg266-Thr257/260 helix segment that transduces the signal from the heme site to the PLP active site. Initially, it was postulated that CO binding releases Cys52, leading to the reorientation of the helix lever and thus the misalignment of the PLP cofactor, which eventually disturbs the optimal geometry in the active site (Fig. 15) (Puranik et al., 2006). Through Raman spectroscopy that allows for differentiation between the inactive enolimine PLP tautomer and the active ketoenamine tautomer, it was found that CO binding is followed by the protonation of the thiolate, which disrupts the salt bridge between Cys52 and Arg266, leading to the displacement of the helix. This ultimately disrupts the stabilizing hydrogen bond between Asn149 and the ketoenamine tautomer of PLP, shifting the equilibrium In favor of the inactive enolimine tautomer (Weeks et al., 2009). Interestingly, in a study using recombinant full-length human CBS, AdoMet, a known CBS activator, sensitized CBS to NO and CO, decreasing the K_i of CO from 9.5 ± 1 μM in the absence of AdoMet to 0.7 ± 0.1 μM in the presence 500 μM AdoMet (Vicente et al., 2016). Such findings suggest that CO inhibition is very unique in terms of how to classify this inhibitor. It is clearly a noncompetitive inhibitor because it functions as an allosteric inhibitor. However, it also has some characteristics of an uncompetitive inhibitor in that binding of a cofactor analog presumably at a remote site enhances its inhibitory activity. As demonstrated in various studies, the inhibitory potential of CO on CBS is modulated by several factors such as pH, AdoMet binding, and redox status of the environment. The heme cofactor in CBS has a very low reduction potential of −350 mV (Singh et al., 2009). Then there is the question as to how CBS is converted to the ferrous form under physiologic conditions. In 2011, a physiologic reducing system, human methionine synthase reductase (MSR), was demonstrated to be the reducing partner in the carbonylation of CBS (Kabil et al., 2011).

2. CBS as a CO Therapeutic Target. Because of the important role that CBS plays and because of CO's inhibitory effect on CBS, there have been efforts in using externally applied CO or induced production of CO as a way to elicit pharmacological actions for therapeutic purposes by targeting CBS. In a 2009 study, the effect of CO overproduction was examined in mice through metabolomic analysis of hepatic tissues after HO-1 induction or exogenous administration of CO (Shintani et al., 2009). Specifically, hemin (40 μmol/kg) was used to induce HO-1 expression, which presumably led to over production of CO. However, HO-1 has other functions of its own in addition to CO production. Nevertheless, HO-1 overexpression led to perturbed metabolomic profiles, wherein metabolites from the methionine/remethylation pathway are upregulated whereas a global decrease in metabolites from the transsulfuration pathway such as cystathionine was observed. Acetaminophen-induced overproduction of CO also led to the suppression of H_2S production. These observations were reproduced in HepG2 cells treated with 50 μM CORM-2, wherein levels of metabolites such as cystathionine were suppressed whereas methionine pools were maintained. Since CBS is the

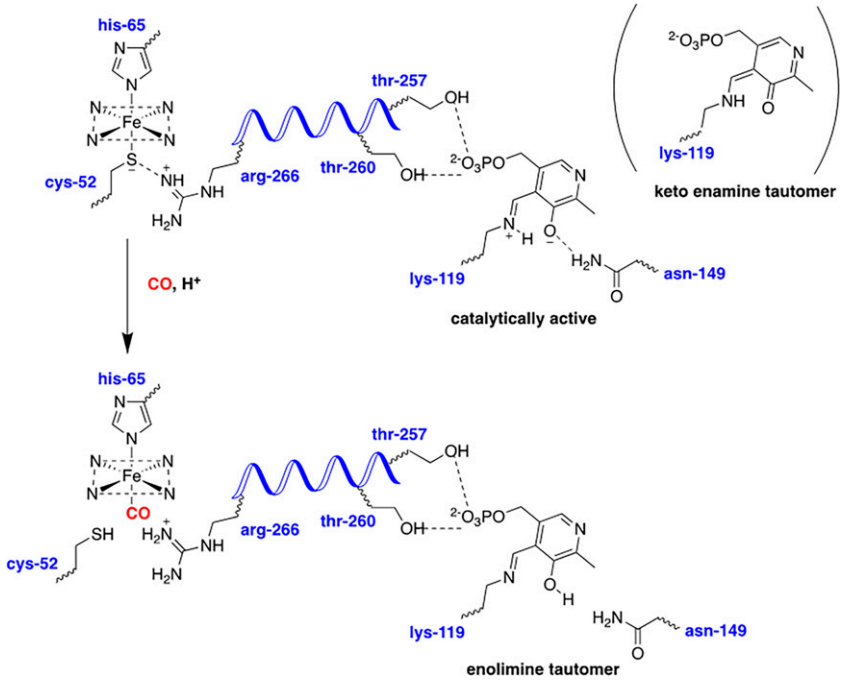

Fig. 15. CO inhibition of CBS. CO binds to the heme prosthetic group in the active form of CBS, leading to the release of the thiolate of Cys52 followed by protonating and breaking the salt bridge of Arg266. Consequently, the orientations of the helix domain and the PLP cofactor change in favor of the inactive enolimine tautomer. Therefore, the catalytic activity is inhibited upon CO binding.

rate-limiting enzyme in the transsulfuration pathway, these findings were interpreted as further support of the significance of CO's effects on CBS. Using a rat recombinant CBS, application of either CO or NO (both at 100 μM) led to spectroscopic changes indicating binding. However, at the concentration tested, only CO binding, but not NO, resulted in inhibition of CBS activity, as measured by conversion of homocysteine to cystathionine (Shintani et al., 2009). Although in certain instances, these gases have similar or sometimes shared biologic propensities, these results emphasize the distinct regulatory role of CO independent from the effects of NO. It needs to be noted that HO-1 leads to the production of biliverdin, bilirubin, and iron in addition to CO. The accompanying products have their own effects (Vítek, 2020). Further, ruthenium-based CORM-2 is known to have activities of its own that are independent of its ability to donate CO (Yang et al., 2020b,c; Southam et al., 2021). Very importantly, CO has many molecular targets as discussed earlier. All of these mean that one has to exercise caution in attributing the observed effects to that of CO binding to CBS.

CO has been demonstrated to cause vasodilation in peripheral circulation; however, in cerebral microcirculation, CO is a vasoconstrictor (Ishikawa et al., 2005b). This reversal in vasoaction cannot be explained by the vasodilatory effect of sGC and potassium channels, which are both known CO sensors. CO's cerebral vasoconstriction effects were shown to be a protective mechanism against hypoxia and are mediated through the CO/HO-2 and H_2S/CBS axes (Morikawa et al., 2012). First, it was established that the presence of HO-2 inhibitors led to dilatation of arterioles by 50% and that this effect was reversed after addition of 100 μM CORM-2. The dilatation observed with HO-2 inhibition was mirrored by the addition of 30 μM NaHS, a known vasodilator. Furthermore, HO-2 inhibition in CBS-null mice no longer caused vasodilation, indicating that at basal levels when O_2 is abundant and HO-2 action is not hampered, the generated CO inhibits CBS-derived production of H_2S, thus preventing vasodilation. Under hypoxic conditions, cerebral slices of WT mice exhibited arteriolar vasodilation, whereas cerebral slices from HO-2–null and CBS-null mice had reduced vasodilation. These effects were also observed in in vivo models, wherein hypoxia-induced vasodilation was impaired in HO-2–null mice and completely abolished in CBS-null mice. With impaired CO production, CBS is uninhibited, thereby producing H_2S, which in turn dilates arterioles, allowing more O_2 and glucose to the hypoxic brain. The constitutively produced CO from HO-2 under normoxic conditions serves as a "respiratory lock" that is unraveled in times of hypoxia.

CO inhibition of CBS redirects the metabolic flow from transsulfuration to alterations in the methionine/remethylation pathway, leading to global protein methylation (Shintani et al., 2009). In human monoblastic leukemia cell line U937, treatment with

100 μM CORM-2 as a CO source led to a statistically significant decrease in cystathionine concentration, from 0.02 to 0.15 nmol/g protein, whereas methionine and S-adenosylmethionine (SAM) concentrations increased from 0.1 to 0.28 μmol/g protein and from 0.4 to 0.55 nmol/μg protein, respectively (Yamamoto et al., 2011). CORM-2 treatment and hemin-induced CO production both led to global protein arginine methylation. These studies show that CORM-2, presumably through CBS inhibition by CO, not only perturbs sulfur-metabolism pathways but also the methionine/remethylation pathway, wherein activation of protein methylation can lead to various biologic effects.

One protein target for arginine methylation as a result of CO/CBS inhibition was identified as phosphofructokinase/fructose bisphosphatase type 3 (PFKFB3) through differential metabolome/fluxome analyses of $^{13}C_6$-glucose utilization (Yamamoto et al., 2014). HO-1 induction by hemin (25 μM for 6 hours) or CO supplementation through CORM-2 (100 μM for 60 minutes) in human leukemia cell line U937 caused a change in glucose utilization from glycolysis to the pentose phosphate pathway (PPP). Relative to basal control, a 50% decrease in ^{13}C-labeled glycolytic metabolites and a 3-fold increase in ^{13}C-labeled PPP metabolites were observed. This was thought to be due to inhibition of CBS by CO, leading to the reduced methylation of PFKFB3 (6-phosphofructo-2-kinase/fructose-2,6-biphosphatase 3). Unmethylated PFKFB3 is recognized by the ubiquitin proteasome system, leading to its degradation. Because fructose-2,6-bisphosphate is downregulated, phosphofructokinase-1, the rate limiting enzyme of glycolysis, is also negatively affected, leading to a metabolic shift from glycolysis to the PPP. Though CBS inhibition by CO decreases GSH synthesis (total amount of GSH), this CO-mediated shift to the PPP increases NADPH production, which in turn raises the glutathione/oxidized glutathione (GSH/GSSG) ratio. This increase in the GSH/GSSG ratio confers chemoresistance to cancer cells against oxidative stress (Fig. 16). Further CBS knockdown experiments using xenograft transplantation of HCT116 cells in superimmunodeficient NOG mice also revealed that glutathione synthesis is compensated, increasing the ratio of GSH/GSSG to stimulate tumor growth due to this shift to the PPP. However, as discussed above, HO-1 expression and the use of CORM-2 may have effects beyond simply donating CO. There are other factors that should be considered in interpreting the data.

In direct contrast to the increase in the GSH/GSSG ratio mediated by CBS inhibition in human breast cancer cell line , a 2017 study reported that CO-mediated CBS inhibition (using a photo-sensitive Mn-based CORM) in three human breast cancer cell lines (MCF-7, MDA-MB-468, and Hs 578T) led to a decrease

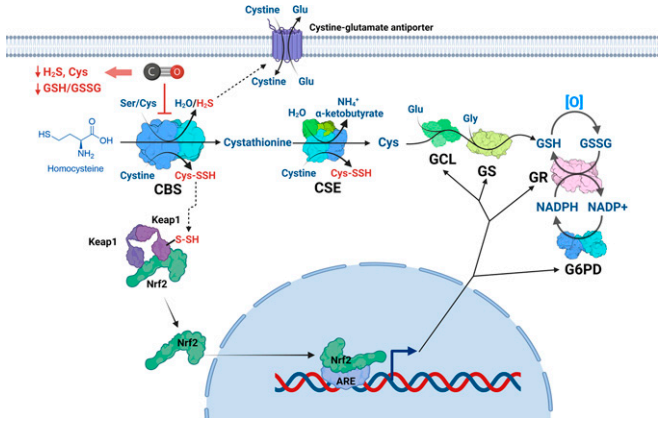

Fig. 16. CO inhibition of CBS leads to decreased concentration of sulfur species such as H_2S, cysteine persulfides, and glutathione, resulting in impairment of cancer cells' ability to neutralize ROS. CBS synthesizes cystathionine from homocysteine and serine to generate H_2S. Cystathionine is further converted to cysteine by cystathionine gamma-lyase (CSE). Cystine can be converted to cysteine persulfide by CBS and CSE. Cysteine persulfide induces Keap1 persulfidation and dissociation of the Keap1-Nrf2 complex. Nrf2 translocates to the nucleus and binds to ARE to express antioxidative proteins such as glutamate cysteine ligase (GCL), glutathione synthetase (GS), glutathione reductase (GR), and glucose-6-phosphate dehydrogenase (G6PD). GCL and GS use the cysteine produced by CBS/CSE to synthesize GSH, which acts as the major antioxidative resolution in the cell. GR reduces oxidized glutathione with NADPH, which can be regenerated from NADP+ by G6PD.

in GSH/GSSG ratio and other processes that promote GSH synthesis or regeneration from GSSG (Kawahara et al., 2017). Furthermore, silencing CBS led to suppression of nuclear factor erythroid-related factor 2 (Nrf2) gene expression, whereas metabolic products of CBS such as H_2S partially reverse some of these effects, indicating a direct correlation between CBS expression and Nrf2 gene expression. It is postulated that H_2S prevents repression of Nrf2 gene expression through persulfidation of Kelch-like ECH-associated protein 1 (Keap1) (Hourihan et al., 2013). Transient overexpression of CBS in normal human breast epithelial cell line MCF-10A, which has been previously shown to possess undetectable levels of CBS mRNA and protein (Sen et al., 2015), led to increased GSH/GSSG ratio, total GSH, glutathione, and cysteine. Establishment of the key role of CBS in maintaining the antioxidant capacity in breast cancer cells prompted the authors to examine CO as a way to perturb this chemoresistance tactic. Using a visible light–activated Mn-containing CORM (120 μM, [$Mn(CO)_3$]), CO-mediated CBS inhibition was demonstrated by a decrease in steady state levels of total GSH, GSH, and cysteine. The impairment of the antioxidant capacity of breast cancer cells during CO-mediated CBS inhibition was hypothesized to sensitize breast cancer cell lines toward chemotherapeutic drugs such as doxorubicin (DOX) that rely on ROS damage for its action (Kawahara et al., 2017). MCF-7 cells exposed to combination treatment of the [$Mn(CO)_3$] (121 μM) and DOX (1 μM) exhibited around 50% decrease in viable cell count that was accompanied by a 37% increase in apoptosis compared with the DOX-only treatment.

In epithelial ovarian cancer cell lines, overexpression of CBS to produce cytoprotective metabolites such as H_2S and glutathione was identified as a possible mechanism for the development of cisplatin resistance (Bhattacharyya et al., 2013). Using cisplatin-resistant cell lines, pharmacological CBS inhibition using light-induced CO treatment from an Mn-containing photoCORM (30 μM, $[Mn(CO)_3(phen)(PTA)]CF_3SO_3$), together with 20 μM cisplatin, led to a 2-fold decrease in cell viability compared with cisplatin-only treatment (Kawahara et al., 2019b). Addition of *N*-acetylcysteine (3 mM) to supply increased levels of cysteine reversed the sensitization observed, indicating that cysteine is key in conferring cisplatin resistance. Steady-state levels of cystathionine, cysteine, and glutathione after CO treatment all decreased, indicating CO inhibition of CBS. Levels of metallothionein, a cysteine-rich peptide that binds and inactivates cisplatin, were also downregulated. Ultimately, it was proposed that CO inhibition "hijacks" the cancer cell's ability to accumulate antioxidant equivalents, thereby making it more sensitive toward ROS-based anticancer therapies. The results described are consistent with this proposal. However, cancer is a complex disease, and there have been other hypotheses on how CO affects cancer (Zuckerbraun et al., 2007; Wegiel et al., 2013). Additional studies in unifying various postulates will be beneficial to the field.

3. CBS Target Engagement Relative to COHb Levels. In the case of CBS, the level of this hemoprotein is enhanced in specific tissues such as liver and pancreas. In the blood, it is known to be enriched in immune cells, specifically only in neutrophils. Under normal physiologic conditions, COHb levels hover between 1% and 2%. In assessing the partitioning of CO between COHb and CBS using a binary model, Fig. 17 presents a visual representation of the relative CO saturation levels using the K_d of 1.5, 4.5, and 45 μM for CBS. These three numbers are from different publications (Table 1). In the first scenario of K_d of 1.5 μM (Puranik et al., 2006), the results are presented in the upper panel of Fig. 17. In areas where the T state is predominant, CBS will be 16% occupied at COHb level of 6%. While in locations where the R state is favored such as in neutrophils in oxygenated blood, CBS target occupancy by CO is nearly 0% even when the COHb level is as high as 100%. These calculations of binary portioning indicate low target engagement even at supraphysiological concentration of CO in the blood. Using a K_d of 45 μM described from a different study, the occupancy picture becomes very different (Vicente et al., 2016) (Fig. 17, lower panel). At the capillary ends in the vicinity of peripheral tissues wherein the T state is predominant, there will only be 1.4% occupancy of CBS even at a COHb level of 14%. While in locations where the R state is favored such as in neutrophils in oxygenated blood, CBS target occupancy by CO is nearly 0% even when the COHb level is as high as 100%. These calculations of binary portioning indicate low target engagement even at supraphysiological concentration of CO in the blood. However, the presence of an endogenous sensitizer as in the case of AdoMet for CBS may drastically alter its affinity toward CO. It was reported that in the presence of AdoMet, 90% of AdoMet-bound CBS exhibited lower K_d values (4.5 μM), whereas in the absence of AdoMet, 80% of AdoMet-free CBS exhibited higher K_d values of (45 μM) (Vicente et al., 2016) (Fig. 17, middle panel). Under those circumstances, CBS occupancy by CO is enhanced 10-fold. For example, at 6% COHb, occupancy is raised to 6% in the presence of AdoMet compared with only 0.6% in the absence of AdoMet. Although AdoMet is an allosteric activator of CBS, it also renders CBS more prone to CO inhibition. Therefore, it is entirely possible that the CBS-CO signaling axis is an important mechanism for regulatory effects. Furthermore, contributions from HO-derived CO in the extravascular tissue may result in drastically higher local CO levels. Much more work is needed to fully understand the relationship of the varying K_d value for COHb at a particular location, the affinity of CBS for CO, and the presence of a sensitizer and its concentration.

C. CO and Cytochrome c Oxidase: Intersection with ROS Generation and the Mitochondrial Respiration Chain

Cytochrome c oxidase (COX) is complex IV in the cellular respiratory chain (Wharton and Tzagoloff, 1967). It functions by transferring electrons and protons for the reduction of O_2 to water. Mammalian COX consists of 13 subunits and 4 redox centers (heme a, heme a_3, Cu_A, and Cu_B) and 3 other redox-inactive metal ions (Mg^{2+}, Zn^{2+} and Na^{1+}) (Tsukihara et al., 1995). Cu_A is located in subunit II, which is bound to the membrane surface on the cytosolic side (Tsukihara et al., 1995). Heme a, heme a_3, and Cu_B are located in subunit I, which is also attached to the cytosolic side (Fig. 18).

The electron flow pathway has been determined as: cytochrome c $\rightarrow$ Cu_A $\rightarrow$ heme a $\rightarrow$ heme a_3-Cu_B binuclear center, which is the reduction site of oxygen. In the absence of a conjugation ligand between heme a_3 iron and Cu_B, electron transfer was suggested to involve the participation of nearby and coordinated amino acids (His and Tyr) or a direct electron transfer between two metal ions, as the distance is only 4.5 Å (Tsukihara et al., 1995).

The binding site of small molecules such as O_2, NO, and CO is the heme a_3 iron atom. For understanding the structural features of COX upon binding with these ligands, there have been detailed studies of conformational changes by using CO as the representative ligand. In one study using serial femtosecond X-ray crystallography at room temperature (Ishigami et al., 2017), it

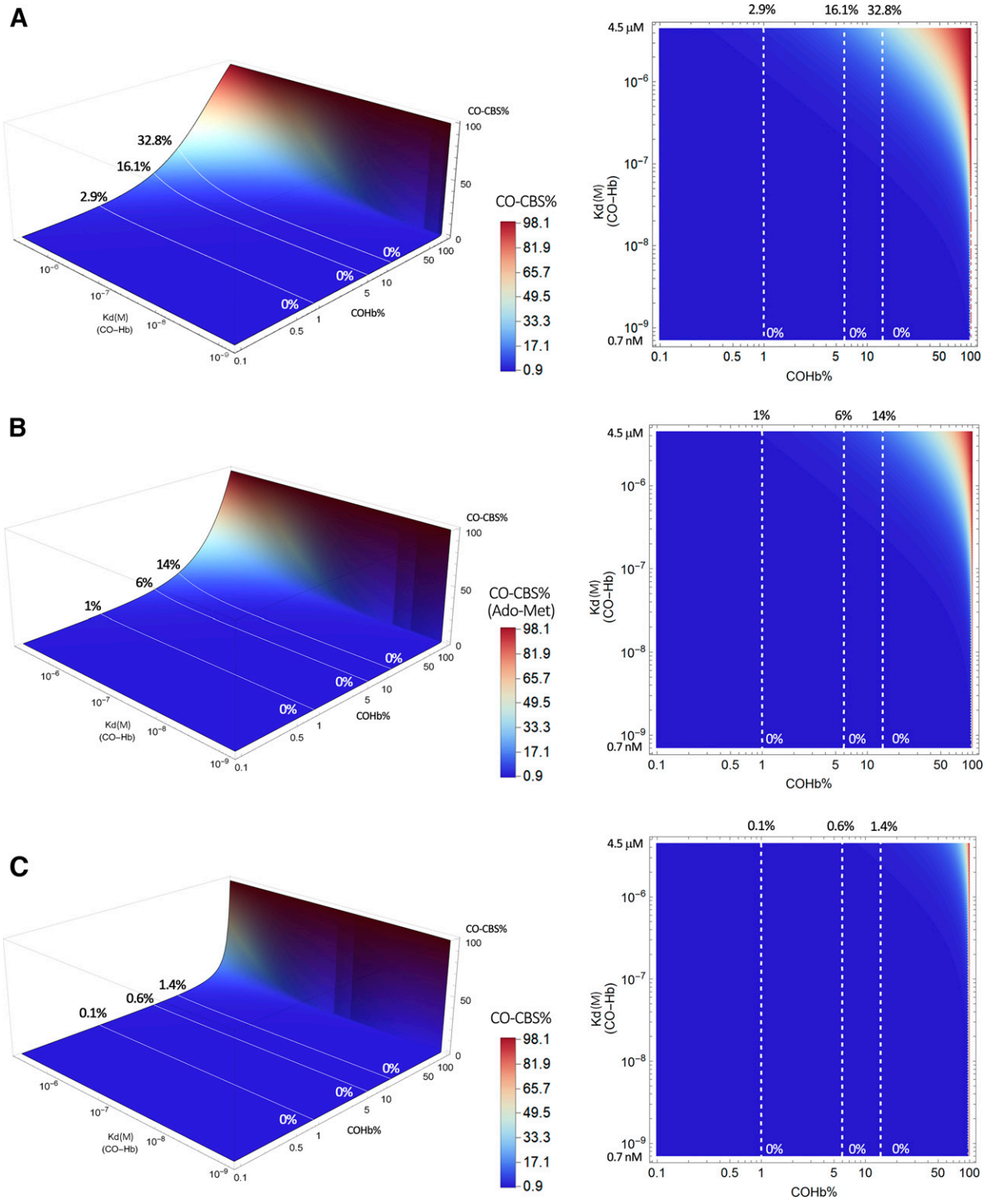

Fig. 17. Estimated CBS saturation levels as a function of the conformational state of COHb and COHb levels. (Upper panel, K_d = 1.5 μM; middle panel, K_d = 4.5 μM, with AdoMet; bottom panel, K_d = 45 μM, AdoMet-free CBS. Solid lines in the left panel and dashed lines in the right panel represent scenarios in the presence of 1%, 6%, and 14% COHb, respectively.) The graphs were generated based on eq. 1 by using Mathematica 12 (codes provided in Supplemental Appendix 2).

was found that the Fe-C-O angle is bent to around 142°, which is possibly due to the close proximity between the heme a_3 iron center and Cu_B (Fig. 19). Under synchrotron radiation at 100 K, CO was dissociated from the iron center and moved close to Cu_B. The distance between Cu_B and the iron center (heme a_3) decreased from 5.30 Å to 4.92 Å compared with that when CO was bound to heme a_3. At the same time, Cu_B also moved out from the planar position supported by three nearby histidine residues. Another significant structural

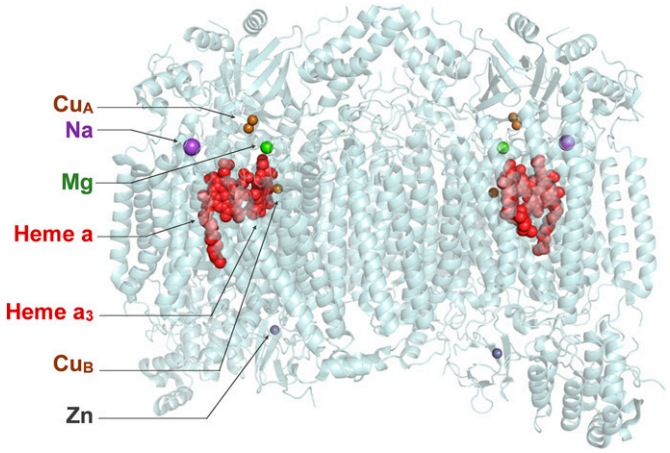

Fig. 18. Distribution of heme and metal centers (shown as spheres) in oxidized COX complex [figure generated from PDB 1v54 (Tsukihara et al., 2003) using PyMOL]. Legends only show the metals and heme in one part of the complex, which mirrors the distribution on other side.

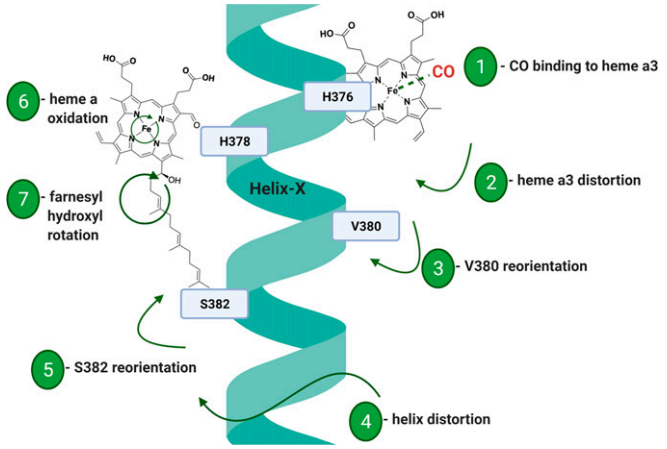

Fig. 20. Structural changes of Helix-X induced by heme a_3-CO binding. The heme a and heme a_3 bind to the imidazole axial ligands of H378 and H376, respectively. CO binds to the heme a_3, which induces conformational changes to the helix domain, allowing for the interaction of S382 and the OH group on the farnesyl side chain of the oxidized heme a.

change was observed on Helix-X, which is located between heme a and heme a_3 and contains H378 and H376 as axial ligands for the two heme domains (Fig. 20). CO binding to heme a_3 was observed to induce heme distortion, leading to the movement of the C pyrrole ring in heme a_3 and therefore resulting in movement of the V380 residue (on Helix-X) to trigger the Helix-X distortion as well as reorientation of the attached S382 residue. Upon oxidation of heme a, the OH group on the farnesyl side chain was observed to rotate by 160°, decreasing the distance between S382 and the OH group from ~8 A° to ~3 A° and enabling their interactions (Fig. 20).

O_2 and CO can only bind to the fully reduced heme a_3-Cu_B center, which is different from the cases of NO and H_2S. NO can bind to both the reduced and oxidized states of COX, whereas H_2S can only interact with the oxidized state of the enzyme. Therefore, CO is a strictly competitive inhibitor of COX toward O_2. There have been extensive studies of the binding constants of CO with COX. For the reduced form of COX from mammalian heart muscle, the rate constant with CO was determined by stopped-flow and flow-flash methods. By using the Yonetani preparation method (Yonetani, 1960, 1961), the second-order rate constant for the on-reaction was determined to be 7.2×10^4 to 7.8×10^4 M^{-1} s^{-1} at around 21°C in PBS (pH = 7.4) (Gibson and Greenwood, 1963). The dissociation constant between reduced COX and CO was measured through displacement by NO by taking advantage of the higher affinity (K_d, = 0.2 nM) of NO toward reduced COX and its known rate constant of approximately 4×10^7 M^{-1} s^{-1}. As such, the off-rate constant for CO was determined to be 0.023 $seconds^{-1}$ (Gibson and Greenwood, 1963), which is similar to that of NO (0.02 $seconds^{-1}$). The K_d between CO and COX was calculated to be around 0.3 μM. By monitoring the oxygen-binding kinetics under various partial pressures of CO, the K_i of CO for COX toward O_2 (lower than 4 μM) was determined to be 0.32 μM (Petersen, 1977). Due to competitive inhibition of COX by CO, it was proposed that besides hemoglobin, COX is also a target of human acute CO poisoning (Miró et al., 1998).

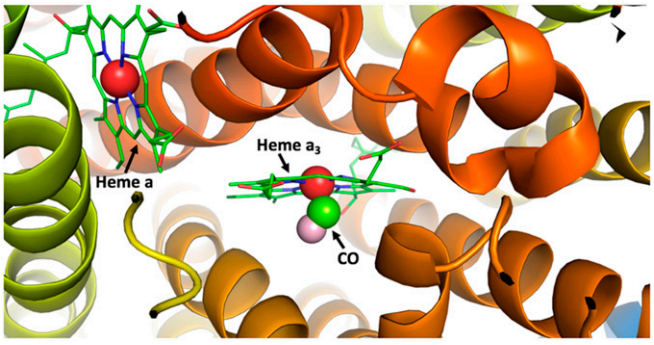

Fig. 19. Structure of CO-bound COX determined by serial femtosecond X-ray crystallography at room temperature. CO is found to bind to the heme a_3 prosthetic group of COX (figure generated from PDB 5w97 using PyMOL).

Along the subject of CO poisoning, the activities of COX and other mitochondrial respirational complexes were analyzed from lymphocytes of three patients suffering from CO poisoning (Miró et al., 1998). In this particular study, when the average COHb level was around 17% during the acute phase, the COX activity was inhibited by 70%. After 3 days, the COHb level decreased to around 2.1%, whereas the COX activity was still ~60% of the basal levels. Some symptoms, including nausea and weakness, still existed. After 12 days, all symptoms disappeared, COX activity recovered, and the COHb level was 1.9%, which was almost the same as that on day 3. It should be noted that the activity of complexes I–III was normal during the study. Such results reinforce the idea that COX

inhibition by CO is one of the reasons for CO poisoning-related symptoms, which are not synchronized with the normalization of the COHb level. Further, the authors suggested that such persistent inhibition of COX by CO might be due to CO-induced reduction of cytochrome a_3 and Cu_B (Ellis et al., 1986).

Inhibition of COX by CO was also studied using isolated mitochondria from human muscle. Specifically, samples were incubated with various concentrations of CO for 5 minutes followed by measuring the activities of the four complexes in the respiratory chain. Exposure to 50, 100, and 500 ppm of CO for 5 minutes led to decreases of COX's activity by 20%, 42%, and 55%, respectively (Alonso et al., 2003). However, the same treatment (50–500 ppm CO) did not show any effects on the activities of complexes I–III. Similar inhibitory effects were also observed at the cellular level. For example, in human embryonic kidney (HEK)293 cells, exogenous CO solutions (5–20 μM prepared using CO gas) showed inhibition of cellular respiration in a concentration-dependent manner (D'Amico et al., 2006). Upon treatment with 20 μM CO solution, the oxygen consumption rate decreased by 40% under ambient oxygen conditions. The inhibition lasted for at least 30 minutes after addition of CO solution. Under hypoxic conditions (1% oxygen), the same concentration (20 μM) of CO solution inhibited the respiration by 75%. Consequently, the K_i values of CO in inhibiting COX in HEK293 cells were determined to be 1.44 μM and 0.35 μM under normal and hypoxic conditions, respectively. To study the effect from endogenous CO production, tetracycline was used to induce the expression of HO-1 in HEK293 cells, which led to a 12% decrease in the rate of respiration compared with noninduced HEK293 cells under ambient conditions. COX activity in cells with induced HO-1 overexpression was also measured. A 23% reduction was observed under normoxic conditions. Under hypoxic conditions, the inhibitory effect on respiration was decreased by 70%, whereas HO-1 expression still remained at the same level compared with the cells under ambient conditions. Such results suggest that the enhanced inhibitory effects on respiration under hypoxic conditions might come from the increased binding between CO and COX at lower oxygen concentrations.

The effect of CO on COX was also studied in isolated nonsynaptic mitochondria from rat cerebral cortex and astrocytes. In one study, CO gas dissolved in solution was employed. Upon incubation in 10 μM CO solution, the activity of COX in isolated mitochondria from rat cerebral cortex slightly dropped (by around 5%) within 5 minutes and then reverted and increased by around 20% and 5% at the 30-minute and 60-minute timepoints, respectively, compared with the control group (Almeida et al., 2012). For astrocytes, the cells were first treated with 50 μM CO solution for 3 or 24 hours followed by isolation of the mitochondria and determination of the COX activity. It was found that at such CO concentrations, the activity of COX in astrocytes increased by around 10% and 40% at the 3- and 24-hour timepoints, respectively. Along with activation of COX in astrocytes, 50 μM CO solution also increased the oxidative metabolism, as revealed by a decreased level of lactate production/glucose consumption ratio and increased oxygen consumption rate after 36 hours of treatment. Additionally, stimulation of mitochondrial biogenesis was also observed in astrocytes after CO treatment by monitoring the amount of mitochondrial coding gene for cytochrome b. Specifically, studies using quantitative real-time PCR showed that mitochondrial cytochrome b DNA increased by 50% 3 hours after treatment with CO solution. A slight drop of the cytochrome b DNA quantity was also observed at the 24-hour timepoint. However, the overall increase was still around 50%. Furthermore, B-cell lymphoma 2 (Bcl-2) protein expression was found to be essential in modulating COX activity by CO. By transfecting the small interfering RNA (siRNA) for Bcl-2 to astrocytes, no increase of the COX activity was observed after the same treatment with a CO solution. However, the detailed mechanism on how Bcl-2 is involved in CO and COX interactions in astrocytes was not discussed. In isolated mitochondria from mouse liver, CO was also found to show time-dependent biphasic effect on COX activity. In the presence of 10 μM CO solution, COX activity first decreased by 50% in the first 10 minutes and then increased by around 20% at the 30-minute timepoint.

In RAW 264.7 macrophages, treatment with exogenous CO gas was shown to elevate the level of ROS by suppressing the activity of COX (Zuckerbraun et al., 2007). Specifically, RAW 267.4 cells were incubated with 250 ppm of CO gas for 1 hour followed by determination of the COX activity. As indicated by a microtiter assay (reduced cytochrome c was used as the substrate) (Chrzanowska-Lightowlers et al., 1993), the COX activity was inhibited by 50%. Under the same conditions, the ROS level in cells also increased in a dose-dependent fashion in the range of 50–500 ppm CO. To investigate if the generation of ROS was caused by CO's inhibitory effect on COX, RAW 264.7 cells were pretreated with various inhibitors of components of the respiration chain or NADPH oxidase before CO exposure. It was found that only antimycin A, a known complex III inhibitor, decreased the ROS level after CO treatment as revealed by a dichlorofluorescein (DCF) fluorescence assay, whereas inhibitors of other components of the electron transport chain or NADPH oxidase did not show any effects. Such results suggest that CO-induced generation of ROS is due to its inhibitory effects on COX.

LPS is known to stimulate p38 MAPK phosphorylation and tumor necrosis factor alpha (TNF-α) secretion. In this study, it was found that the increased p38 phosphorylation (2.37 ± 0.55-fold) induced by LPS was further elevated to 5.7 ± 0.87-fold upon exposure to CO gas. Pretreatment with polyethylene glycol-superoxide dismutase (PEG-SOD) and PEG-catalase led to a reduction of this augment to 3.6 ± 0.64-fold, suggesting that the effect of CO on LPS-induced p38 MAPK phosphorylation might be related to the generation of ROS. Additionally, elimination of ROS by PEG-SOD and PEG-catalase also affected the inhibition of LPS-induced TNF-α secretion by CO. Under normal conditions, CO treatment was able to reduce TNF-α secretion in LPS-stimulated RAW 264.7 cells from 900 pg/ml to 300 pg/ml. However, in the presence of PEG-SOD and PEG-catalase, TNF-α concentration only decreased to around 700 pg/ml after the same CO treatment. Complex III inhibitor antimycin A also attenuated CO's effects on LPS-induced p38 phosphorylation and TNF-α secretion. Based on these results, it was suggested that the inhibition of COX by CO stimulated ROS production, which is an important regulator for CO to elevate p38 phosphorylation and diminish TNF-α secretion in LPS-treated RAW 264.7 cells.

In addition to CO gas or dissolved CO solution, CORMs were also used as CO surrogates to evaluate their effects on COX. In isolated mitochondria from rat heart, 100 μM CORM-3 reduced the activity of COX by 50% and no effect was observed from 20 μM CORM-3 or 100 μM iCORM-3 (Lo Iacono et al., 2011). Additionally, neither 20 μM nor 100 μM CORM-3 showed any effects on complexes I–III. However, 20 μM CORM-3 led to an increase of State-2 respiration rate by almost 100% and a decrease of State-3 respiration by around 20%, which indicate the involvement of other molecular targets during the regulatory process of mitochondrial respiration by CORM-3. In human endothelial cell line EA.hy926, CORM-2 was reported to elevate the production of ROS in mitochondria through inhibition on COX (Yeh et al., 2014). In the presence of 25 μM CORM-2, intracellular ROS formation significantly increased, as revealed by a peroxide-sensitive fluorescent probe known as 6-carboxy-2',7'-dichlorodihydrofluorescein diacetate (carboxy-DCFDA). A lucigenin-based chemiluminescence method also showed an increase of around 2.5-fold based on the chemiluminescence intensity induced by superoxide species after 1 hour of incubation with 25 μM CORM-2. Pretreatment with complex III inhibitor (antimycin A) decreased CORM-2–induced chemiluminescence to the same level as that in the control group; an NADPH oxidase inhibitor, apocynin, did not induce any changes on the superoxide level. All of these were proposed to suggest that ROS might come from the inhibition of COX by CORM-2. Intracellular concentrations of GSH and GSSG were also measured after incubation with CORM-2 for 1–12 hours. The concentrations of both GSH and GSSG increased. However, the overall GSH/GSSG ratio decreased by around 20%, which led to an overall elevated level of protein glutathionylation. Upon incubation with CORM-2 for 1 hour, the level of glutathionylated p65 increased for the period between 1 and 12 hours. It was also found that glutathionylation was related to inhibition of NF-κB. Transfection of the cells with mutant Cys38 p65 diminished the inhibitory effect on NF-κB. To further probe the effect from CORM-2–induced oxidative stress, cells were pretreated with the antioxidant enzyme catalase before addition of CORM-2. A significant decrease of p65 glutathionylation and nuclear translocation was found. Such results were proposed to suggest that ROS formation due to COX inhibition is an important factor in CORM-2–mediated biologic effects. However, all of these will also need to be examined in the context of the newly discovered chemical reactivity of ruthenium-based CORMs, as described earlier (Southam et al., 2018, 2021; Yuan et al., 2020, 2021a).

For visualization of the relative CO saturation levels, we have created 3-D and contour plots to allow for intuitive assessment, using a K_d value of 0.3 μM for binding between reduced COX and CO (Fig. 21). Under normal physiologic conditions, when COHb level is around 1%, CO-COX percentage can reach up to around 13% when Hb is in the T state (K_d = 4.5 μM). When COHb level is at 14%, which is the highest level approved for human use of CO, around 70% of the reduced COX can be bound with CO, assuming Hb is in the low-affinity T state (K_d = 4.5 μM) and the amount of available CO is not a limiting factor. If COHb is in the high-affinity R state (K_d = 0.7 nM), then there is minimal inhibition of COX (~0.03% CO-COX percentage) by CO even at 14% COHb level. This indicates that exogenous delivery of CO may allow for a substantial level of COX inhibition under certain conditions that allow Hb to stay mostly in the low-affinity T state.

In summary, the structure of CO-bound COX has been extensively studied and characterized. As summarized in Table 2, the effects of CO on COX activity seem to be different under various conditions. Studies also suggest that CO has more than one target/pathway in regulating COX activity. Recently, several studies reported that ruthenium-based CORMs are chemically reactive and have their own activities that are independent from CO (Southam et al., 2018, 2021; Yuan et al., 2020, 2021a,b). Such findings might suggest the need to reassess the results from studies using CORM-2/CORM-3 as CO donors in the context of their effects on COX. At this point, it is also important to point out the difference in time-dependent studies between CO in solution and nonvolatile small organic molecules (as ligands). In the latter case, the concentration

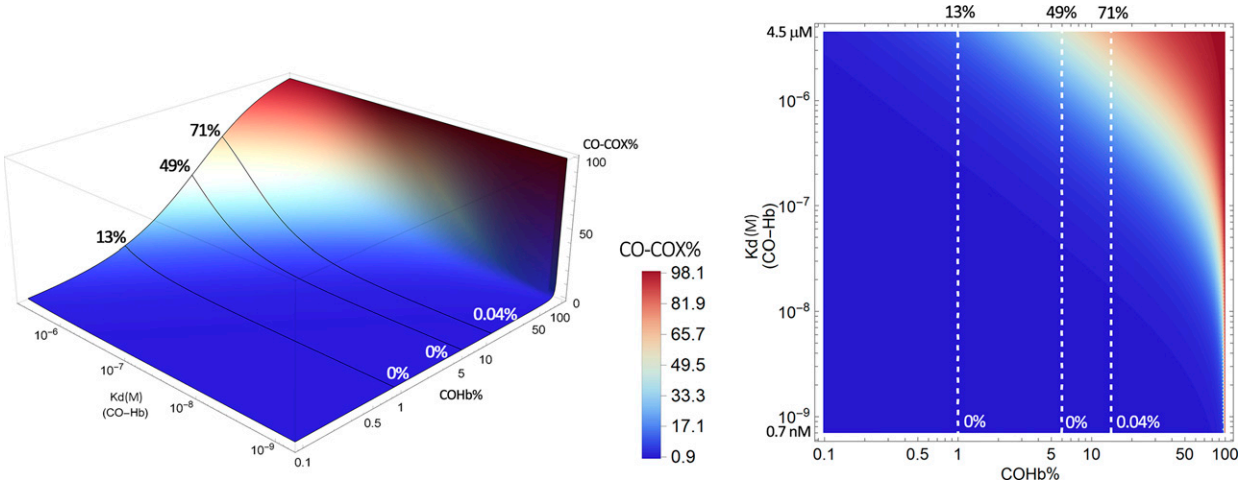

Fig. 21. Estimated COX saturation levels as a function of the conformational state of COHb and COHb levels. Solid lines in the left panel and dashed lines in the right panel represent scenarios in the presence of 1%, 6%, and 14% COHb, respectively. The graphs were generated based on eq. 1 by using Mathematica 12 (codes provided in Supplemental Appendix 2).

of the small-molecule ligand in solution is not expected to change. However, in the case of a volatile molecule such as CO, the concentration is sustained only for a short period of time and is expected to decrease rapidly with time due to exchanges with the atmosphere. Therefore, the treatment time concepts are different for these two scenarios. Along a similar line, studies using CO gas are also different. Most of the time, incubation while exposed to a constant level of CO in air does allow for a sustained exposure concentration. Therefore, target exposure is not expected to change under such circumstances. These differences also show the complexity in interpreting and comparing data of CO experiments when CO treatment conditions or CO sources are different.

TABLE 2
The effects of CO and CORMs on COX

Study Reference	CO Source	Preparation	Effect
(Miró et al., 1998)	CO gas	Analysis of lymphocytes from acute CO poisoning patients	Inhibition by 76% at 17% of COHb
(Alonso et al., 2003)	CO gas	Incubation of isolated human muscle mitochondria with 50–500 ppm of CO	Inhibition level: 20%-55%
(D'Amico et al., 2006)	Dissolved CO	HEK293 cells were incubated with 5–20 μM CO solution.	CO gas solution incubation for 5 min: normoxic conditions = inhibition by 40% (20 μM CO); hypoxic conditions (1% oxygen) = inhibition by 75% (20 μM CO)
(D'Amico et al., 2006)	Induced HO-1	HO-1 expression was induced by tetracycline in HEK293 cells.	HO-1 induction: normoxic conditions = inhibition by 23%; hypoxic conditions (1% oxygen) = inhibition by 70%
(Almeida et al., 2012)	Dissolved CO	Isolated mitochondria from rat cerebral cortex and astrocytes were incubated with CO gas solution of various concentrations.	Incubation with CO gas solution led to a slight inhibition for a short term (first 5 min) and a long-term activation (up to 60 min in isolated mitochondria and 24 h in astrocytes).
(Queiroga et al., 2011)	Dissolved CO	Isolated mitochondria from mouse liver were treated with CO gas solution.	10 μM CO gas solution inhibited COX activity by 50% in the first 10 min and increased COX activity by 20% at 30 min.
(Zuckerbraun et al., 2007)	CO gas	RAW 267.4 cells were exposed to 250 ppm CO gas for 1 h.	COX activity was inhibited by 50%.
(Lo Iacono et al., 2011)	CORM-3	Isolated mitochondria from rat heart were incubated with CORM-3.	100 μM CORM-3 reduced the activity of COX by 50%. However, 20 μM CORM-3 did not show any effects.
(Yang et al., 2020a)	CORM-2	Human endothelial cells (EA.hy926) were incubated with 25 μM CORM-2.	COX activity was not directly measured. Cellular ROS production induced by CORM-2 was diminished by incubating with antimycin A.

D. CO and Cytochrome P450: The Effect on Drug Metabolism?

In using CO as a therapeutic agent, one question that often comes up is the potential effect on the major metabolizing enzyme, cytochrome P450, inhibition of which could pose major drug-drug interaction issues. With P450 being a heme-containing enzyme, this concern is natural. Indeed, carbon monoxide has been reported to inhibit CYP450 (Wang, 1998). However, most such studies were conducted using purified enzymes or enzyme preparations (Kuthan and Ullrich, 1982; Krikun and Cederbaum, 1985) under nonphysiologic conditions (Ortiz de Montellano and Correia, 2005; Nakao et al., 2008). For example, Leemann reported CO's inhibition of P450DB1, P450TB, and P450NF with Warburg partition coefficients of 0.35, 1.1, and 3.9 μM, respectively (Leemann et al., 1994). One important issue to consider with regard to possible P450 inhibition is to quantitatively examine the binding constant(s) or dissociation constant(s) (K_d) of the various CO targets in the context of COHb levels. CO binds to CYP450 with K_d values in the range of 3–10 μM (Debey et al., 1973). In comparison, the K_d is 1.7 and 0.7 nM for CO binding with the α- and β-subunits of Hb in its high-affinity R state, respectively; 29 nM with Mb; 0.2 nM with WT Ngb; 1–2 μM with neuronal PAS domain protein 2 (NPAS2) in Per-Arnt-Sim (PAS)-A; 21 μM with PAS-B; and about 1 μM with CBS, as discussed earlier. Considering the high abundance of Hb (mM range) and the high relative (and absolute) affinity of Hb over CYP450 (2700- to 14,000-fold) for CO, the proportion of CO that is bound to CYP450 is expected to be small under nonsaturating conditions and therapeutically relevant COHb levels. Therefore, the extent of P450 inhibition is expected to be minimal under normal physiologic conditions. Of course, nitrosylation (Fago et al., 2013) and allosteric effectors (Gong et al., 2006; Song et al., 2008; Yonetani and Laberge, 2008; Kanaori et al., 2011; Lal et al., 2017) are known to affect Hb's affinity for CO and O_2 and could complicate the actual effects of these numerical relative affinities in vivo. One specific example probably also helps to indicate P450's tolerance of CO; P450 itself is known to catalyze lipid peroxidation, leading to CO production (Archakov et al., 2002). Overall, we do not feel that therapeutic levels of COHb would pose meaningful CYP450 inhibition issues, especially if the high-affinity R state is the dominant population.

E. Carbon Monoxide Inhibits Indoleamine-Pyrrole Dioxygenase: Another Pathway in Regulating Immune Responses?

Indoleamine-pyrrole dioxygenase (IDO) is the rate-limiting enzyme that transforms tryptophan to kynurenine (Kyn) in immune cells such as macrophages, monocytes, and dendritic cells. It has been reported that up to 90% of dietary L-Trp is catabolized via the kynurenine pathway (Bertazzo et al., 2001). IDO-induced tryptophan degradation inhibits the proliferation of T cells and promotes T cell cycle arrest and apoptosis. Inhibition of IDO activity in graft-tolerant rats has been shown to lead to rapid graft rejection.

Catabolites of L-Trp are capable of promoting immunosuppression and tumor tolerance in cancer, formation of cataracts, human immunodeficiency virus (HIV)-related neurologic damages, and ischemic brain injury (Kolawole et al., 2015). For example, tumor cells that overexpress IDO are known to suppress host T cell immunity in the tumor microenvironment by depleting tryptophan and generating cytotoxic Kyn to suppress T lymphocytes and natural killer (NK) cells (Frumento et al., 2002). As an immune checkpoint protein, IDO is recognized as a promising drug target for cancer therapy, autoimmune diseases, and immunosuppression for transplantation. Along this line, inhibition of IDO has been shown to induce T cell proliferation and tumor regression in animal models. As such, there have been dozens of IDO inhibitors clinical trials for various cancer treatments (Moon et al., 2015).

IDO is a heme-containing oxidase that uses molecular oxygen to oxidize tryptophan, leading to *N*-formyl-L-kynurenine (NFK), which undergoes hydrolysis to release Kyn (Fig. 22).

The catalytic mechanism for the oxidation reaction has been studied in detail by Smirnov et al. (Kolawole et al., 2015). It was found that this is a random bisubstrate reaction and would yield the desired product regardless of the binding sequence (Kolawole et al., 2015). CO is known to bind to IDO (Yanagisawa et al., 2010), either in the free form or tryptophan bound form, to inhibit its catalytic activity. However, there has been no report of the binding affinity for CO or the biologic implications of such binding. Therefore, it is hard to assess the physiologic and/or pathologic significance of CO binding to IDO or conditions needed for such binding to be biologically significant in vivo. However, it is certain that due to the importance of IDO in immunoregulation and tumorigenesis, there is a need to study the possible regulatory role of CO and

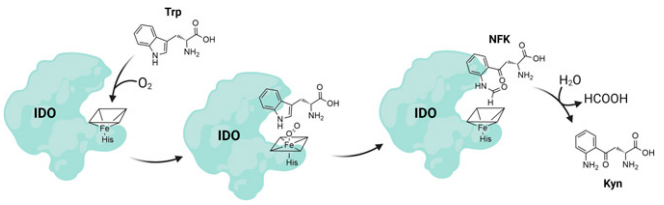

Fig. 22. IDO catalyzes the formation of kynurenine from tryptophan. IDO is a heme-containing oxidase that uses molecular oxygen to oxidize tryptophan leading to *N*-formyl-L-kynurenine (NFK), which undergoes hydrolysis to release kynurenine (Kyn).

its associated therapeutic effect by inhibiting IDO (Zhang et al., 2020).

VI. Neuronal PAS Domain Protein 2: Intersection with the Circadian Clock

NPAS2 belongs to the basic helix-loop-helix (bHLH) family of transcription factors that dimerizes with brain and muscle Arnt-like protein 1 (BMAL1) to bind DNA and initiate the transcription of hundreds of genes, including those for circadian rhythm regulation (Zhou et al., 1997). Consisting of 824 amino acids, NPAS2 contains the bHLH DNA-binding region in the N-terminal domain and the two PAS domains named PAS-1 and PAS-2 (Ascenzi et al., 2004). Both domains bind heme, which controls DNA binding (Dioum et al., 2002). NPAS2, similar to the circadian locomotor output cycles kaput (CLOCK) transcription factor, takes cues from the environment such as light to regulate gene expression. Both transcription factors share closely similar primary sequences and form heterodimers with BMAL1 as a response to intracellular redox potential changes. NPAS2/CLOCK-BMAL1 heterodimers then bind to the E-box region, activating the transcription of molecular clock components such as period (Per) and cryptochrome (Cry). Per and Cry translocate to the cytosol and propagate the circadian rhythm cascade. To close the loop, accumulated Per and Cry are either ubiquitinated or form heterodimers that act as negative regulators of CLOCK/NPAS2-BMAL1, completing the transcriptional-translation feedback loop (TTFL) that maintains the rhythmic ~24-hour expression (Fig. 23).

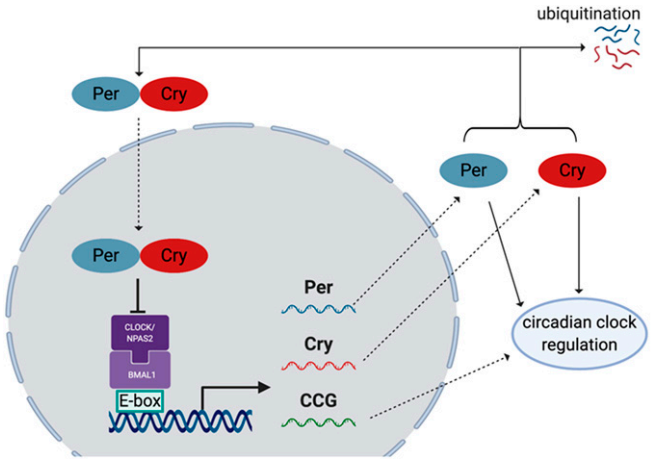

Fig. 23. The transcription-translation feedback loop in the CLOCK/NPAS2-BMAL1 and Per-Cry circadian clock system. NPAS2/CLOCK-BMAL1 heterodimer binding to the E-box region transactivates circadian clock proteins such as Period (Per), Cryptochrome (Cry), and other clock-controlled genes (CCGs). Per and Cry translocate to the cytosol and propagate the circadian rhythm cascade. Accumulated Per and Cry are either ubiquitinated or form heterodimers, which negatively regulate the function of NPAS2/CLOCK-BMAL1.

A. CO Binding to NPAS2

Because of the ability of NPAS2 to bind to heme in both domains, low micromolar concentrations of carbon monoxide were shown to inhibit binding activity of holo-NPAS2 but not apo-NPAS2 (Dioum et al., 2002). Prior to the first report of CO binding to the heme domains in NPAS2, it was already known that brain regions expressing NPAS2 exhibit enhanced expression of HO-2 (Vincent et al., 1994). Furthermore, aminolevulinic acid synthase, the rate-limiting step in heme biosynthesis, is under circadian control (Kaasik and Lee, 2004). In 2002, NPAS2 was serendipitously found to include an HBD that influenced the activity of another domain of the protein. For each monomer of NPAS2, there are two heme groups with deoxy absorption spectral characteristic of six-coordinated heme-iron complex with two axial ligands from amino acid side chains. Resonance Raman spectroscopy identified histidine as the axial ligand trans to CO in the PAS domain (Tomita et al., 2002). In vitro, CO binds to these HBDs with K_d of 1–2 μM for NPAS2 in PAS-A and 21 μM for PAS-B (Dioum et al., 2002). Further probing through an in vitro DNA binding assay revealed that at least 3 μM CO impairs DNA binding by blocking heterodimer formation of NPAS2 with BMAL1 favoring unproductive homodimerization of BMAL1 (Fig. 24). Inhibition by CO at this concentration agrees well with CO saturation of heme in NPAS2. In addition to CO regulation, the transcriptional activity of NPAS2-BMAL1 heterodimerization is also regulated by the cellular redox balance (Fig. 24). Low NADPH/NADP ratio also has the same effect as CO-heme–mediated inhibition of DNA binding. Under reducing conditions, NPAS2 disrupts the unproductive homodimeric BMAL1 complex to form the DNA-binding NPAS2-BMAL1 heterodimer. NPAS2's ability to sense cellular redox state occurs to the same extent with or without heme. This indicates that NPAS2 has a separate redox-sensing mechanism distinct from that mediated by heme. Notably, NO, another common heme ligand, did not bind NPAS2 at physiologic concentrations, whereas O_2 reacted irreversibly (Dioum et al., 2002). In 2018, CO was also shown to bind to the heme prosthetic of the CLOCK transcription factor with an association rate constant (k_{on}) of 3.1×10^6 $M^{-1} \cdot s^{-1}$ (Lukat-Rodgers et al., 2010), and the K_d was estimated to be about 0.1 mM in a study by Minegishi et al. (2018).

B. CO Modulation of the Circadian Clock

In 2009, using a yeast model, CO's role as an endogenous cue in the control of metabolic state and biologic rhythm was demonstrated (Tu and McKnight, 2009). Pulsed administration of CO in the temporal window when it was predicted to be generated induced a phase advancement into the oxidative phase and respiratory metabolism. After this, robust metabolic cycles of temporal dimensions resumed. Targeted deletion of HO revealed that HO-deficient yeast, despite being fully

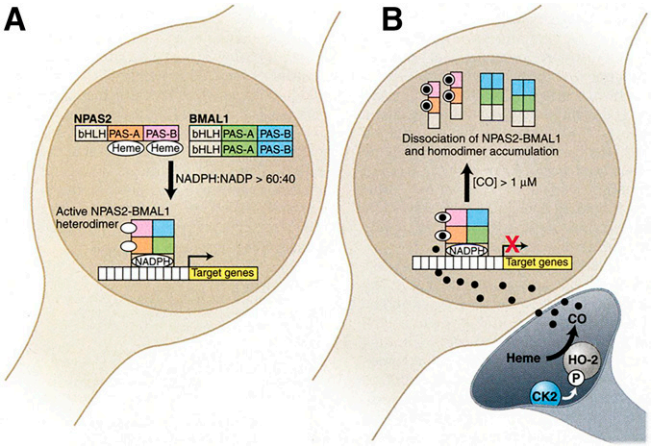

Fig. 24. Cellular redox status and CO-mediated regulation of circadian gene transcription. (A) Reducing redox status favors the heterodimerization of NPAS2 and BMAL1, forming an activated transcriptional complex for various circadian clock genes. (B) HO-2–generated CO (represented by the black dots) diffuses through cell membrane into the nucleus to bind to the heme domain of NPAS2, thereby deactivating the transcriptional complex. Figure reprinted with permission from Boehning and Snyder (2002).

capable of chemostat growth, exhibited prolonged period length by 25% compared with wild-type cells.

The effects of sunlight-induced release of CO in ophthalmic venous blood on the expression levels of clock genes in hypothalamic structures were studied in domestic pig and wild boar crossbreeds. Infusion of autologous plasma with elevated levels of CO (three times the control, exact concentration not defined) through a catheter to the right dorsal nasal veins of the crossbreeds alters the expression of clock genes (Per1 and 2, Cry1 and 2, and Rev-erb α and β) and the genes of their regulators (Bmal1, Npas2, Clock, and Retinoic acid-related orphan receptor β). The response to elevated CO levels varied between the gene involved, type of hypothalamic region, time of day and season. Among the genes tested, only Per1 expression (light-regulated) increased with treatment of CO regardless of time of day and season (Gilun et al., 2013). In this study, it was also noted that the master clock machinery of the experimental animals was deregulated after CO treatment.

The role of heme catabolism and thus CO in circadian transcription and dynamics was revealed in a study in 2016 (Klemz et al., 2017). A firefly luciferase assay for a Bmal1 promoter fragment in dexamethasone-synchronized human osteosarcoma cell line (U2-OS) indicated that HO inhibitor cobalt protoporphyrin (CoPP), but not hemin, resulted in a CoPP-dependent lengthening of circadian period by 1.5 hours relative to the control. Because both treatments would increase heme levels, it was surmised that it was not heme but heme degradation products that could be the link to circadian dynamics. Measurement of the circadian transcript levels of CLOCK/NPAS2-BMAL1 target genes in primary fibroblast isolated from HO-1 knockout mouse revealed the upregulation by 1.5- to 6-fold of the target genes. To verify that the observed upregulation of circadian clock genes was due to CO, primary fibroblasts from wild-type mice were treated with either continuous exposure to 6% CO from 0 to 48 hours or acute exposure using 100 μM (CORM-2). Very little difference was observed with both CO treatments versus control. In contrast, a substantial decrease in the transcript levels was observed with both treatments when HO-1 knockout mice were used. Furthermore, it was shown that depleting endogenous CO from both HO-1 and HO-2 led to upregulation of target genes of CLOCK-BMAL1 and also increased gluconeogenesis in human and mouse hepatocytes. These observations even broaden the potential impact of CO encompassing circadian clock regulation, metabolism, and behavior. In a recent study, CO level changes in female volunteers in response to sunlight was reported (Oren et al., 2020).

In 2017, Otterbein and colleagues showed that subarachnoid hemorrhage (SAH) disrupts the naturally occurring oscillation of circadian rhythm. In SAH, clock genes such as Per1 and 2 and NPAS2 were significantly elevated, leading to the disruption of central and peripheral organ rhythmicity. The dysregulation of clock gene expression observed after SAH was alleviated by the addition of exogenous CO (200 ppm every 24 hours for 7 days), with the restoration of Per1, Per2, and NPAS2 expression and reduction of neuronal apoptosis (Schallner et al., 2017). In a bilateral kidney ischemia reperfusion injury (IRI) model, CO in various delivery forms—CO gas (250 ppm), HBI-002 (0.2 mg/kg by mouth), and CO prodrug BW-CO-101 (100 mg/kg i.p.)—was shown to abolish kidney IRI and accelerate tissue recovery (Correa-Costa et al., 2018). This effect was shown to occur through purinergic signaling involving increased cluster of differentiation (CD)39 ectonucleotidase expression, which in turn leads to a greater than 20-fold increase in the expression of Per2 and 5-fold increase in serum erythropoietin (EPO) (Fig. 25). CO-mediated increase in Per2 expression via downregulation of A1 receptor expression and upregulation of A2 receptor signaling led to stabilization of HIF-1α. This cascade ultimately results in increased circulating levels of its target gene EPO, which ultimately imparts renoprotective effects. Interestingly, EPO has been previously shown to positively regulate HO-1 expression, suggesting a feed-forward loop amplification of CO (Burger et al., 2009; Correa-Costa et al., 2018).

In some of the studies, the role of CO in circadian clock regulation has been explored through HO-1 inhibition. However, other components of the HO-1 system such as heme itself have also been reported to affect the circadian rhythm (Kaasik and Lee, 2004). Moreover, NADPH, a key regulator of the circadian

clock (Yoshii et al., 2015), is consumed as HO catabolizes heme to CO. Therefore, a pseudo-knockdown approach using hemoCD1, an iron(II)porphyrin with per-O-methyl-β-cyclodextrin dimer that effectively scavenges CO (K_d of 0.02 nM), was used to study the effect of removal of endogenous CO on the circadian clock system. Intraperitoneal administration of hemoCD1 led to the transient decrease in endogenous CO levels. Under these lower-than-normal CO levels, the transcriptional activities of BMAL1: CLOCK(-NPAS2) was enhanced, resulting in the upregulation of E-box–controlled clock genes such Per, Cry, and Rev-erb (Minegishi et al., 2018). As hemoCD1 strips CO from hemoproteins, oxyHb is readily oxidized by plasma ROS to MetHb. Because MetHb is prone to heme dissociation, free heme accumulates, which in turn induces HO-1 activation. After a short CO-depleted state, the amount of endogenous CO significantly increases through HO-1 activity, leading to the eventual downregulation of the E-box–regulated clock genes.

Although it has been established that CO indeed plays a role in the modulation of the circadian clock, more studies are needed to establish NPAS2/CLOCK as viable molecular targets of CO. Further, the circadian rhythm is known to have significant impacts on various pathologies (Musiek and Holtzman, 2016; Nagarajan et al., 2017; Aziz et al., 2021; Rouzbahani et al., 2021; Wang and Li, 2021) and treatment outcomes (Qian et al., 2021; O'Brien and Dolan, 2022). One wonders how consideration of the link between the circadian clock and CO's effects might be incorporated into future studies. Detailed mechanistic studies are needed to elucidate how CO binding leads to conformational changes in NPAS2 and how this in turn leads to alteration in protein function.

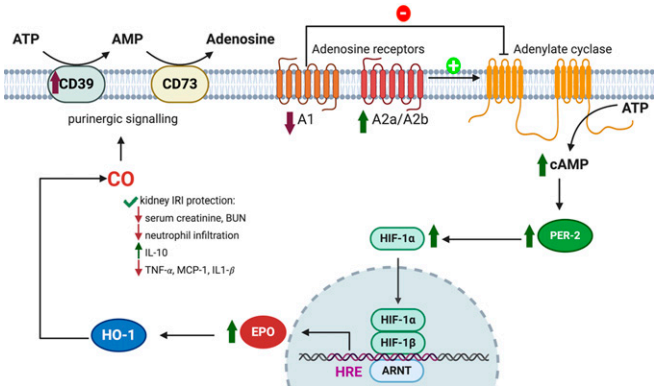

Fig. 25. During tissue hypoxia, the upregulated ectonucleotidases CD39 and CD73 convert extracellular ATP to adenosine as an adaptive response. Adenosine activates adenosine receptors, including A1 and A2a/A2b, which differentially act on the adenylate cyclase. Activation of A1 inhibits adenylate cyclase through coupled inhibitory G protein, whereas activation of A2a/A2b stimulates adenylate cyclase to generate cAMP from ATP. CO is protective in mouse models of kidney IRI through upregulation of CD39 ectonucleotidase expression, decreasing A1 expression, and increasing A2 expression, which lead to cAMP-mediated stabilization of Per2 and HIF-1α and upregulation of EPO gene transcription. A feed-forward loop is postulated, wherein EPO stimulates expression of HO-1, which can further increase CO through heme degradation.

VII. CO and Ion Channels

CO has been reported to modulate the activity of various ion channels. Mechanistic studies show different pathways by which CO inhibits or activates ion channels. The ruthenium-based CORMs known as CORM-2 and CORM-3 were widely used as surrogates of CO in related mechanistic studies. However, some published work suggests that these CORMs regulate the activity of ion channel in a CO-independent mechanism (Jara-Oseguera et al., 2011; Gessner et al., 2017). As such, the following discussions draw a distinction between the results from CO gas and CORMs and focus more on the studies on the former.

A. CO Interacts with Heme and the Heme-Binding Domain on Ion Channels

Heme binding motifs (HBMs) have been identified within ion channels, including large conductance calcium-activated potassium (BK_{Ca}) channels (Tang et al., 2003), ATP-sensitive K^+ (K_{ATP}) channels (Burton et al., 2016), and voltage-gated potassium (Kv) channels (Burton et al., 2020). Several studies have shown that CO can modulate ion channel activities via heme binding.

BK_{Ca} channels transfer potassium ions across the cellular membrane in a calcium-dependent fashion. The channel consists of four pore-forming subunits that are encoded by the Slo1 gene. Three functional domains (the voltage-sensing domain, pore-gate domain, and cytosolic domain) are located on either the membrane or the cytosolic side. The cytosolic domain contains two calcium-binding sites and a conserved heme-binding amino acid sequence motif (CXXCH), which is a c-type cytochrome, where heme and hemin can bind to the channel, leading to inhibition. In an early study, Leffler and coworkers used a thin-layer chromatography (TLC) approach to study the disruption of the binding between heme and the BK_{Ca} channel HBD by CO (Jaggar et al., 2005). Specifically, heme was immobilized on a TLC plate, and the heme-binding peptide (HBP) was in the mobile phase. Under N_2 atmosphere, only around 12% of the peptide was found to migrate through the heme area, whereas in a CO atmosphere around 63% of the peptide was able to pass through. If hemin was fixed as the barrier on a TLC plate, CO gas failed to increase the proportion of the peptide capable of passing through. Such results suggest that the interaction between heme and BK_{Ca} channel HBD can be disrupted by CO. The activities of BK_{Ca} channels from a single cerebral artery smooth muscle cell were also measured in the presence of heme or hemin. When partial pressure of oxygen (pO_2) was 20 mm Hg, 100 nM hemin or heme was able to keep the BK_{Ca} channel almost

completely in the open form. However, after subsequent treatment with 10% CO, the inhibitory effect caused by heme was decreased to the point that only 30% of the channel remained open. No activity change induced by CO was observed in the hemin-treated group. It should be noted that without pretreatment with exogenous heme or hemin, 10% of CO atmosphere was able to increase the probability for the channel to stay open by 2-fold. Interestingly, subsequent addition of 100 nM heme was able to further enhance this activation, whereas 100 nM hemin decreased the open probability to the original level. Such results are hard to explain and suggest the possibility of multiple roles for the CO-heme complex. Mutation of the BK_{Ca} channel HBM eradicated the ability of heme and CO to regulate the BK_{Ca} channels. Ragsdale et al. found that the redox state of two cysteine residues (Cys612 and Cys615) on HBM (the CXXCH motif) are essential for regulation of the binding affinity of HBM to heme and CO (Yi et al., 2010). In addition to the two cysteine residues on HBM, there are also another two cysteine residues located at positions 628 and 630 on the HBD. Upon reduction by dithiothreitol (DTT), four thiols per mole of protein were detected on the HBD by the 5,5'-dithiobis-(2-nitrobenzoic acid) (DTNB) test. Under oxidized conditions, C612S and C615S mutants had only one thiol per mole of protein, and C612S/C615S mutant did not show the existence of free thiol groups, indicating the formation of intramolecular disulfide bonds. The HBP, which contains residues 601–623 of the BK channel, was prepared and used to study its dissociation constants with heme under different redox conditions. The K_d of the oxidized HBP for heme was measured to be 14.5 ± 4.6 μM, which is much higher than that under reduced conditions (0.16 ± 0.05 μM). Additionally, the C612S/C615S mutant was shown to have similar affinity regardless of oxidation states, with K_d being 1.5 and 1.7 μM under oxidized and reduced states, respectively. Such results suggest that the redox states of Cys612 and Cys615 are important regulators for heme binding. Replacement of these cysteine residues eliminated their sensitivity to redox states. Furthermore, the K_d of the heme-HBD complex for CO was determined to be 50 nM, which is less than that of the C612S/C615S variant (K_d = 2.7 μM). Given the fact that the native HBD and the C612S/C615S variant have similar K_d values (0.29 and 0.49 μM, respectively), Cys612 and Cys615 residues may also play a role in CO binding with the heme-HBD complex.

The $CXXHX_{16}H$ motif on the cytoplasmic region of sulfonylurea receptor 2A (SUR2A) was identified as the heme-binding site on the K_{ATP} channel. Raven and coworkers showed that the effects of CO on K_{ATP} channel activity relied on the interaction among CO, heme, and the HBD (Kapetanaki et al., 2018). In an inside-out patch experiment, CO was found to further increase channel activation by heme (channel open probability: within the range of 0.013 ± 0.002 to 0.051 ± 0.017) to 0.303 ± 0.064. Without heme, CO alone failed to increase the channel activity. Mutation of the HBD $CXXHX_{16}H$ led to abolishment of the effects from heme and CO-heme combination. For a more detailed study of the heme-CO-SUR2A interaction, the SUR2A subunit was expressed and purified. Through a spectrophotometric titration method, the K_d of CO for the ferrous heme–SUR2A complex was determined to be 0.6 ± 0.3 μM, which is comparable to other known heme proteins. The rate constants for the on- and off-processes were measured to be 0.27 ± 0.1 μM^{-1} s^{-1} and 0.05 $seconds^{-1}$, respectively. Resonance Raman spectroscopy was further used to study the structure of heme-CO-SUR2A complex. Compared with the heme-CO complex, heme-CO-SUR2A exhibited a stronger ν(Fe-CO) stretching vibration at 494 cm^{-1} and a weaker vibration at 525 cm^{-1}. No significant bending mode was shown in the region of 550–570 cm^{-1}, which suggests a nearly linear Fe-C-O geometry in the binding complex. The results from this work are consistent with an earlier study on BK_{Ca} channel (Jaggar et al., 2005).

Recently, Raven and coworkers also identified a PAS domain located on Kv channel Kv11.3 that can interact with heme in regulating channel activities (Burton et al., 2020). To study the binding event between heme and the PAS domain, the N-terminal cytoplasmic region (hERG3-eag) of the Kv channel bearing a Cap domain and a PAS domain was generated from an *Escherichia coli* expression system. By utilizing titration techniques, the K_d of hemin was determined to be 7.02 ± 0.35 μM. The binding affinity for heme was not addressed. CO also exhibited tight binding affinity toward to the heme-hERG3-eag complex with a K_d of 1.03 ± 0.37 μM. The K_d of the preformed CO-heme complex to the HBD was determined to be 10.55 ± 1.34 μM. In the presence of NO, CO was found to be easily replaced from the heme-hERG3-eag, with a k_{off} of 0.03 $seconds^{-1}$. Such results suggest NO being a competitive inhibitor toward the binding between CO and heme-hERG3-eag.

In summary, the HBM on the BK_{Ca}, K_{ATP}, and Kv channels can bind to heme to form the heme-HBM complexes as CO's molecular targets. Based on in vitro studies, CO showed binding affinity toward these complexes, with K_d values ranging from 0.05 to 1 μM, indicating the possibility for such interaction to alter activities of ion channels in vivo.

B. Direct CO Interactions with Amino Acid Residues on Ion Channels?

Some studies showed that the presence of some amino acid residues (histidine, aspartic acid, and

cysteine) located on ion channels are essential for CO's activities.

In 1997, a study found that chemical modifications of the histidine residues on the external portion of BK_{Ca} channels could affect CO's activity. In rat smooth muscle cells, 3–30 μM CO solution increased the probability for the channel to remain open in a dose-dependent manner in both outside-out and inside-out patch experiments. Diethyl pyrocarbonate (DEPC) can chemically modify the imidazole ring on histidine residues. In this case, upon preincubation of the ion channel with 0.5 mM DEPC in an outside-out membrane patch experiment, CO exposure failed to activate the BK_{Ca} channels. However, CO's activity was reversed in the presence of hydroxylamine, which can remove the modification of histidine by DEPC in outside-out patches. In contrast, treatment of DEPC using inside-out patches did not show any effects on CO-induced increased probability for the BK_{Ca} channels to stay in the open state. In terms of chemical reactions or binding, there is no known mechanism for CO to chemically modify the histidine residues in BK_{Ca} channels. One explanation of the observed effects related to histidine might be with HBD on the external side of BK_{Ca} channels.

Another proposed molecular mechanism of CO's action on BK_{Ca} channels is the participation of an aspartic acid and two histidine residues on the cytosolic RCK1 domain (Hou et al., 2008). It should be noted that in this mechanistic study, instead of CO gas, CORM-2 was used as a CO surrogate. In HEK cells, CORM-2 increased the expression of Slo1 BK_{Ca} channel current by around 1-fold under 100 mV conditions. However, after pretreatment with 2 mM DEPC on the intracellular side for 5–10 minutes, CORM-2 failed to increase the current. It might suggest the importance of histidine residues on the cytoplasmic side of the BK_{Ca} channel in regulating the channel activity by CORM-2. Four histidine residues near the channel's Ca^{2+} sensors (H350, H365, H394, and H379) were further investigated to see if they are possible CO's targets. The results show that mutation of H350 or H379 to arginine failed to abolish CO's activation of the channel. However, mutation of H365 or H394 fully abolished the effects of either CORM-2 or CO gas. Additionally, mutation of an aspartic acid residue (D367) near the H365 also eliminated the sensitivity of the channel to CORM-2. Such results indicate that H365, H394, and D367 are important targets for CO/CORM-2 sensitivity on the BK_{Ca} channel. However, a different study suggested that CORM-2 was able to directly form $Ru(CO)_2$ adducts with histidine residues (Gessner et al., 2017). In terms of the chemistry, the likelihood is extremely low for CO to directly act on one or more amino acid residues to regulate channel activities. Some kind of involvement of a transition metal is essential. Therefore, the results with CORM-2 may require additional studies to achieve a good mechanistic understanding.

L-type calcium channels belong to the family of voltage-gated calcium channels. They are widely expressed in skeletal, cardiac, endocrine, and smooth muscle cells as well as in neurons. In rat ventricular cardiomyocytes, both CORM-2 (30 μM) and dissolved CO solution (concentration not indicated) inhibited the activity of the L-type calcium channels (Scragg et al., 2008). The structural requirements for human cardiac L-type Ca^{2+} channels (HEK293 cells) for CO's actions were examined by using CORM-2. Through evaluating the effect of CORM-2 on various mutants, it was found that the region spanning residues 1787–1818 on the C-tail insert region was necessary for the inhibitory effects of CORM-2. CO is known to produce mitochondrial ROS, which act as secondary mediators and play important roles in CO-related signaling. Preincubation of mitochondria-targeted antioxidant mitoquinone mesylate (MitoQ) for 1 hour efficiently reduced the inhibitory effects by CORM-2 on the Ca^{2+} current. In the presence of complex III inhibitors stigmatellin (1 μM) and antimycin A (3 μM), the effects of CORM-2 on the channels were also significantly reduced. Such results suggest that ROS production triggered by CORM-2 might interact with the redox-sensitive cysteine residues on the channel to modulate their activity. Thus, three cysteine residues located on the C-tail region were targeted for further studies. Mutations of one of them abolished the sensitivity of the channel to CORM-2. N(G)-nitro-L-arginine methyl ester (L-NAME) (1 mM), a nitric-oxide synthase inhibitor, was also added during the 20-minute preincubation to see if the reactivity is due to CO-stimulated NO production. However, no effect was observed on the inhibitory effects caused by CORM-2. Such results suggest that the action is independent of NO's effects. In a study using CO gas, Farrugia and coworkers found that 0.2% of CO gas significantly activated human intestinal L-type calcium channels in HEK cells by increasing NO production and cGMP levels (Lim et al., 2005). CO gas solution of 0.2% and 0.38% reversibly increased the current from human intestinal Ca^{2+} by 18% and 21%, respectively. Such effects were diminished upon washing out CO. Further experiments were conducted to examine whether this effect was due to cGMP and NO formation. Preincubation of cells with 10 μM ODQ, which is an sGC inhibitor, for 15 minutes decreased the activity enhancement induced by CO from 18% to 4%. Various NO synthase (NOS) inhibitors such as N-[3-(aminomethyl)benzyl]acetamidine (1400 W), 3-bromo-7-nitroindazole (3-Br-7NI), and N5-iminoethyl-l-orthinine (L-NIO) were also evaluated during the pretreatment. It was found that only selective endothelial NOS inhibitor L-NIO reduced the activation effect of CO (0.2%) from 18% to 11%. cGMP can activate PKG for the

downregulated protein phosphorylation. Considering this aspect, the effect from a PKG inhibitor (KT-5823) was further examined. However, no sensitivity change of the channel to CO was observed, suggesting the nonessential nature of the cGMP/PKG pathway. cGMP is known to activate cAMP-dependent protein kinase A (PKA). Along this line, PKA inhibitor KT-5720 was shown to diminish CO's activation effect from 18% to only 5%. cGMP can increase the cAMP level by inhibiting PDE III, leading to the activation of PKA. However, selective PDE III inhibitor milrinone diminished the current increase caused by 0.2% CO from 18% to 11%. This leaves the question of how PDE III played a role in the cGMP/PKA pathway mediated by CO. Overall, there are extensive experimental findings. However, the mechanistic implication at the molecular level is not entirely clear. Much more work is needed.

C. CO Activates NO Formation and S-Nitrosylation

CO is known to induce NO formation by activating NO synthase (NOS). Protein S-nitrosylation is an important posttranslational modification through reaction between NO and the thiol group on cysteine residues and is known to regulate the activities of a broad range of cellular proteins. In cardiac myocytes, Peers et al. found that elevation of NO levels and S-nitrosylation on voltage-gated sodium channel (Nav)1.5 is essential for the proarrhythmic effects of CORM-2 or CO (Dallas et al., 2012). Activation of the late Na^+ current was commonly associated with arrhythmias. In the presence of 30 μM CORM-2 or 87.6 μM dissolved CO, the late Na^+ currents were increased by $\sim$100% and $\sim$140%, respectively. However, upon preincubation with 1 mM NOS inhibitor L-NAME such effects from CORM-2 on Na^+ currents were almost completely abolished, suggesting NO formation being essential for CORM-2 to regulate the channel activity. The question of whether NO formation led to protein modifications on the channel was further investigated. By using a modified biotin-switch assay, it was found that CORM-2 or NO donor CysNO, but not iCORM-2, increased the S-nitrosylation of cardiac Na^+ channel in cardiac myocyte extracts. As a positive control, treatment of myocytes with 2,2'-dithiobis(5-nitropyridine) (DTNP), a known inducer of TRPC5 channel S-nitrosylation, led to an increase of the late Na^+ current. These results suggest the possibility for the modulation of Nav1.5 channel activity by CORM-2 to go through elevation of NO production and S-nitrosylation. However, a later study found that addition of NO donors did not mimic the effects from CORM-2 on the peak Na^+ current (Elies et al., 2014), indicating the need for additional mechanistic studies. At this point, it might also be important to discuss the affinity of CO for NOS. In a study using neuronal NOS, the dissociation constant (K_d) for CO was determined to be less than 10^{-3} μM in the absence of the substrate and cofactor, 1 μM in the presence of L-Arg, and 100 μM in the presence of inhibitors such as N(G)-nitro-L-arginine methyl ester (L-NAME) or 7-nitroindazole (7-NI) (Sato et al., 1998). The effects of the cofactor and substrate on CO binding make it hard to model the distribution CO between COHb and NOS without knowing the precise concentration of the cofactor and substrate.

D. CO-Independent Reactivities from CORMs

Heinemann and coworkers showed that CORM-2 was able to directly form $Ru(CO)_2$ adducts with histidine residues to modulate the activities of the BK_{Ca} and voltage-gated K^+ channels through a CO-independent mechanism (Gessner et al., 2017). In BK_{Ca} channels in HEK293T cells, it was found that mutations of H365 and H394 were able to abolish the channel modulating activity of CORM-2 but not from CO gas. Such results suggest that the histidine residues on the BK_{Ca} channels be related to the channel modulation activity of CORM-2. To study the molecular interaction between CORM-2 and histidine residues, a peptide corresponding to the pore-loop histidine residues of the voltage-gated K^+ channel was synthesized. After incubation of CORM-2 with four equivalents of this peptide for 15 minutes, high-performance liquid chromatography (HPLC) showed a decrease of the original peptide peak and appearance of a new stable peak at a longer elution time in a reverse-phase column. Liquid chromatography-electrospray ionization-tandem mass spectrometry (LC-ESI-MS/MS) analysis of the new peak identified a mass change matching the formation of an adduct between $Ru(CO)_2$ and the histidine-containing peptide. For the control peptide without the histidine moiety, neither formation of a new peak nor direct modification was observed. Thus, it was suggested that the modulation of the potassium ion channels by CORM-2 was through the formation of histidine-$Ru(CO)_2$ adduct(s) in a CO-independent fashion.

P2X receptors are ATP-gated ion channels commonly expressed on mammalian cell membranes. Coded by different genes, seven subunits of P2X receptors ($P2X_1$ to $P2X_7$) have been identified (Khakh and North, 2006). Each subunit contains two membrane-spanning domains (TM1 and TM2) and intracellular C and N termini. It was found that most of the subunits form homotrimeric or heterotrimeric receptors. For example, $P2X_{2/3}$ receptors are composed of $P2X_2$ and $P2X_3$ subunits. P2X receptors are widely distributed throughout mammalian cells and tissues, with demonstrated physiologic functions (North, 2002; Surprenant and North, 2009). In $P2X_2$/$P2X_3$ double knockout mice, neurons were found to have weak response to ATP (Cockayne et al., 2005). The activities of ATP-gated $P2X_2$ receptor were also reported to be regulated by CO and CORM-2. Wilkinson and coworkers found that 30% CO gas increased the currents through the $P2X_2$ receptor from 1049 ± 219 to 1183 ± 240 picoamperes (pA) upon coincubation with 10 μM ATP (Wilkinson et al., 2009). It was also shown that

0.3–100 μM CORM-2 activated the $P2X_2$ receptors in the presence of 10 μM ATP with EC_{50} and Hill coefficient of 3.1 ± 0.6 μM and 1.8 ± 0.4 (n = 3), respectively. The effects of CORM-2 on other P2X receptor–expressing HEK cells were also evaluated in this study. For example, for the $P2X_4$ receptor, CORM-2 showed a slight inhibitory effect. Upon preincubation with CORM-2 for 10 seconds, the ATP-induced current density decreased from 6.51 ± 1.27 to 5.39 ± 1.26 $pA{\cdot}pF^{-1}$. To probe the activation mechanism of CORM-2 on $P2X_2$, cells were treated with a cGMP derivative to mimic the activation of sGC by CO. However, no augmentation on the ATP-evoked channel currents was observed. ODQ, an inhibitor of sGC, also failed to abolish channel activation on ATP-evoked $P2X_2$. In a different study from the same research group, it was found that CORM-2, but not CO gas, inhibited the activity of ATP-gated $P2X_4$ channel. In HEK293 cells, 30 μM CORM-2 decreased the ATP-enhanced currents on the channel to around 45.3% of the control group. However, treatment with 20% CO gas for up to 4 minutes failed to exhibit any effects on the currents evoked by ATP. Such results indicate the possibility that the regulation of the $P2X_4$ channel by CORM-2 is CO-independent.

CORM-2 also showed CO-independent effects toward mitochondrial BK_{Ca} channels, according to a recent study by Rotko et al. (2020). In isolated mitochondria from U-87 MG human astrocytoma cells, after 1 minute perfusion, 30 μM CORM-2 increased the probability for the channel to open from 0% to 12% ± 7% at −40 mV and from 7% ± 3% to 46% ± 17% at +40 mV in the presence of 1 μM Ca^{2+}. At the 5-minute point, the initial activation was diminished to the original level. However, under the same conditions, saturated CO gas solution failed to alter the activity of the channel. Such results may suggest the CO-independent nature of the mechanism by which CORM-2 modulates the activities of mitochondrial BK_{Ca} channel. Alternatively, CO concentration or specific experimental conditions may also make a difference.

In this section, we have discussed the regulation of ion channels by CO and described several reported mechanisms of actions (Fig. 26). In a cellular environment, CO may form a complex with heme, which can interact with an HBD located on the ion channel to regulate the channel's activity, or it may directly target the heme-HBD of the channel. In addition to these direct pathways, CO may also modulate ion channels by its secondary messenger molecules, including NO and ROS. Several studies indicated that CORM-2 exhibited CO-independent activities on ion channels. For future mechanistic studies, experiments using CO gas should be included as a CO source to corroborate results from CO donors.

VIII. CO and the Cytochrome C-Cardiolipin Complex

Cytochrome c (cyt c) is a hemoprotein, containing heme c as a prosthetic group. It is responsible for transferring electrons from complex III to COX in the cellular respiratory chain (Bushnell et al., 1990; Zaidi et al., 2014). Mammalian cyt c is composed of around 100 amino acid residues with several key residues involved in heme binding, including two cysteine residues (Cys14 and Cys17), His18, Met80, and Tyr67 with His18 and Met80 axially coordinating with the iron (Bushnell et al., 1990). Anchored by these amino acid residues, less than 10% of the heme moiety is exposed to the outside environment. The nearby positively charged Lys and Arg residues produce a hydrophilic area around the heme moiety.

As such, it is hard for CO to directly bind to the heme moiety on cyt c under physiologic conditions. However, several charged Lys residues on cyt c enable its interaction with phospholipids. A well known case is the binding between cyt c and cardiolipin, which is one type of phospholipid located on the inner mitochondrial membrane and responsible for fixing cyt c onto the same inner membrane, allowing its participation in the respiratory chain reactions (Kagan et al., 2014). Additionally, this interaction can activate the peroxidase activity of cyt c, which in turn oxidizes and translocates the bound cardiolipin from the mitochondrial inner membrane to the outer membrane and initiates the activation of caspases in apoptosis processes (Kagan et al., 2014). Cardiolipin binds to cyt c by electrostatic interactions with three lysine residues (Lys72, Lys78, and Lys86) on site A (Rytömaa and Kinnunen, 1995). The cyt c–cardiolipin

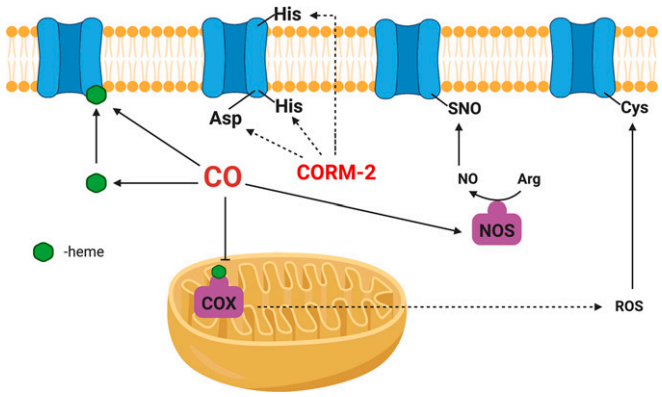

Fig. 26. Possible molecular mechanisms for the actions of CO and CORM-2 on ion channels. CO released from CORM-2 binds to heme-containing ion channels through two possible mechanisms: 1) direct binding to the heme prosthetic group in the ion channel and 2) binding to the free heme first before engaging the ion channel. CO binding modulates the function of ion channel; CO inhibits COX, thus increasing intracellular ROS production, which acts on redox-sensitive ion channels; CO interacts with NOS, thus affecting NO production, leading to direct modulation of NO-sensitive ion channels or through a second messenger pathway to regulate ion channels; CORM-2 itself exhibits CO-independent activities on ion channels as well.

complex is also stabilized by a hydrogen bond between the acyl side chain of cardiolipin and Asn52 in site C. At the same time, the hydrogen bond between nearby His26 and Pro44 is disrupted (Sinibaldi et al., 2008; Amacher et al., 2015). Upon binding with cardiolipin, the coordination of the iron center with Met80 is disassociated and cyt c is transformed into a more open conformation. These structural changes allow CO to bind with the cyt c–cardiolipin complex.

Vos et al. first studied such binding properties by using time-resolved absorption spectroscopy. Ferric cyt c and cardiolipin complex were reduced to the ferrous form by adding sodium dithionite (Kapetanaki et al., 2009). The ferrous native cyt c alone did not show binding affinity with CO at pH 7. However, coincubation of ferrous cyt c–cardiolipin complex with a CO solution produced an absorption pattern of CO-bound heme at pH 7.4 and 6.1. Binding of 1 Eq cyt c to CO required 30 Eq cardiolipin for saturation in this in vitro study. The dissociation constant for CO binding was determined to be around 20 nM at 37°C, which is comparable to the binding affinity between CO and myoglobin. The CO inhibitory effects on the peroxidase activity of the cyt c–cardiolipin complex were also studied. In the presence of 1- or 0.1-mM CO gas solution, the H_2O_2-induced heme degradation rate of the cyt c–cardiolipin complex was measured to be in the range of 0.0003–0.001 seconds^{-1}, which is similar to that of cyt c alone. Such results show significant inhibition of the peroxidase activity of the cyt c–cardiolipin complex by CO. In a newborn mouse model of isoflurane-induced apoptosis in the developing brain, Levy and coworkers found that CO exposure exhibited protective effects by inhibiting the cyt c peroxidase activity and reducing the cyt c release from forebrain mitochondria (Cheng and Levy, 2014). Compared with the control group, isoflurane treatment caused a ~7% increase of cytochrome c peroxidase activity. Exposure to 5 ppm or 100 ppm of CO gas for 1 hour decreased the cyt c peroxidase activity by 30% and 50% in both isoflurane treated and nontreated groups, respectively. Cyt c release was assessed by comparing the amount of heme c in mitochondrial and cytosolic fractions. It was found that the heme c concentration in cytoplasmic (isoflurane-treated) was decreased by ~30% and ~50% after treatment with 5 ppm and 100 ppm CO gas, respectively. Without isoflurane treatment, 5 or 100 ppm CO gas was also able to decrease the cytosolic heme c concentration by about 30%. In contrast, in the presence of isoflurane, the level of mitochondrial heme c significantly increased after exposure to 100 ppm CO but not 5 ppm. Along this line, the COHb level was also determined after CO gas exposure. After 1-hour exposure to 5 ppm CO of gas, only a minimal increase of COHb level (from ~0.3% to ~0.5%) was observed. Under the same conditions, exposure to 100 ppm of CO gas for 1 hour led to an increase of COHb level to 4%. Compared with CO, NO can bind to both ferrous and ferric cyt c–cardiolipin complexes. The K_d for NO binding to the ferrous cyt c–cardiolipin complex was determined to be around 0.02 nM (calculated from given k_{on} and k_{off}), which is much lower than that of CO (Silkstone et al., 2010).

With all of the analyses above, it is important to be able to correlate COHb availability with observable pharmacological efficacy. For example, small changes of COHb levels by 5 ppm of CO exposure was shown to lead to significant effects on cytochrome c peroxidase activity (Kapetanaki et al., 2009). To present an intuitive picture of the occupancy level of the cyt c–cardiolipin complex by CO relative to that of COHb, we have generated a 3-D and contour plot (Fig. 27) of the relationship between COHb and target binding under various conditions. This is based on the K_d (20 nM) of the cyt c–cardiolipin complex for CO and the varying K_d of COHb, depending on the environment. When the COHB level is at 1% and K_d of Hb is 4.5 μM at the low-affinity T state, the percentage of CO saturation of the cyt c–cardiolipin complex can reach 95%. When COHb level is elevated to 14%, the percentage of CO saturation of the cyt c–cardiolipin complex can be nearly 100%. However, if the competition is between the high-affinity R state (K_d = 0.7 nM) of COHb and the cyt c–cardiolipin complex, then the picture is very different. The percentage of CO saturation of the cyt c–cardiolipin complex is expected to be 5% when COHb level is at 14%. Therefore, the dependence of target engagement on the COHb level is heavily influenced by whether COHb is at the low-affinity or high-affinity state, which in turn is affected by local pH, oxygenation level, and the presence of other metabolites.

IX. Two Long-Standing Issues in the CO Field: Possible Explanations at the Molecular Level

With all of the detailed analyses of various molecular targets, what are their implications in addressing some long-standing issues related to CO research and clinical observations? In the CO field, there is the famous Ron Coburn experiment in an anesthetized dog (Coburn, 1970). When the inspired gas progressively decreased in oxygen partial pressure from 200 to a low of 40 mm Hg, a decline of its basal COHb level was observed (from 0.8% to 0.5%). Interestingly, the CO "reappeared" in the blood in the form of COHb after the oxygen pressure was brought back to 200 mm Hg. Such observations were interpreted as the result of distribution of CO to tissues (mostly Mb) when the oxygen partial pressure was low and redistribution back to the blood/Hb when the oxygen partial pressure was normal. Understanding this experiment in

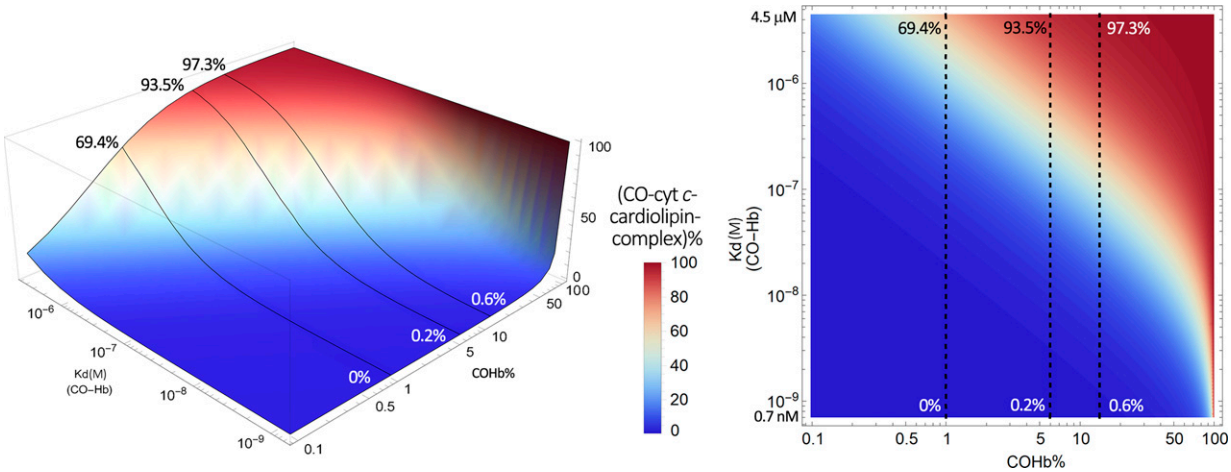

Fig. 27. Estimated CO-saturation levels of the cyt c–cardiolipin complex as a function of the conformational state of COHb and COHb levels. Solid lines in the left panel and dashed lines in the right panel represent scenarios with COHb at 1%, 6%, and 14% levels, respectively. The graphs were generated based on eq. 1 by using Mathematica 12 (codes provided in Supplemental Appendix 2).

depth is very important to the analysis of CO pharmacokinetics under pathophysiological conditions. Further, understanding the observations described is also important for assessing the efficacy of CO and itis relationship to the level of COHb under various conditions. First of all, oxygen content has profound effects on human physiology. Even high oxygen content has toxic effects (Shykoff and Lee, 2019). One can envision respiratory and metabolic acidosis under low oxygen partial pressure (Epstein and Singh, 2001; Kao and Nañagas, 2005; Cho et al., 2008; Swenson, 2016; Kuniavsky et al., 2018; Joffe et al., 2020). It is known that hypoxia (and low pH) would lead to a shift of Hb from its high-affinity R state to the low-affinity T state. As a result, CO is expected to partition from Hb to Mb and other targets with K_d below 4.5 μM (the K_d of low-affinity COHb). Figure 7 shows the effect of COHb K_d on CO's distribution to Mb. In its high-affinity R state, very little CO is expected to be transferred to Mb. However, at its low-affinity state (4.5 μM), even 0.4% of COHb could be in equilibrium with over 90% COMb levels. In an otherwise healthy dog, hypoxia (Swenson, 2016) can be readily reversed upon administration of oxygen, leading to the restoration of COHb to its high-affinity state in the blood and thus "reappearance" of CO in the blood.

Figure 28 shows in a schematic fashion how changes in O_2 partial pressure may affect CO redistribution through the switching of COHb between its high-affinity and low-affinity states. This would help to explain the observations by Coburn in his famous experiments, though this is only our analysis. Under normoxia (left side in both Figs. A and B), the pressure gradient in O_2 and CO_2 drives O_2 diffusion into the red blood cells (RBCs) in the pulmonary alveoli, whereas CO_2 (through bicarbonate system) and CO diffuse out shifting Hb equilibrium toward the R state. In the peripheral tissues, pO_2 is lower whereas pCO_2 is higher, creating a lower pH environment (through bicarbonate buffering system) in the interstitial fluid as well as in the RBCs. Together, these two factors favor Hb equilibrium toward the T state, wherein CO may dissociate from Hb and bind to hemoprotein targets with $K_d < 4.5$ μM, such as Mb. The dynamic balance between CO endogenous production, CO inhalation and exhalation, and CO partitioning to extravascular tissues maintains the blood COHb level saturation around 1%. Under hypoxia such as in Coburn's dog experiments, once the arterial pO_2 (controlled by inspired pO_2) becomes equivalent to the venous pO_2 (which is $\approx$ 40 mmHg), the pressure gradient is abolished, leading to no (or minimal) net exchange in gases in the pulmonary alveoli. The lack of gas exchange, along with pH lowering in both plasma and RBCs because of excess CO_2 accumulation in the absence of effective exhalation, may lock the circulating Hb in the T state. In the extravascular tissues, a metabolic shift to fermentation due to lack of oxygen decreases pH as well. Because of these compounding effects, Hb remains and is circulated in the T state, allowing for CO to move out of the blood into the extravascular tissues such as muscles, which is manifested as lowered blood COHb but increased COMb. Once arterial pO_2 is restored and the pressure gradient is reestablished, more Hb in the high-affinity R state is circulated, leading to rebinding of CO to Hb and thus the "reappearance" of COHb.

A second and very clinically relevant issue is the difficulty of reversing CO intoxication (Prockop and Chichkova, 2007). Theoretically, upon removal of the affected individuals from an environment with elevated CO levels, exhalation of CO should happen, leading to decreased COHb levels. Further, the rapid exchange of CO between Hb and various targets should lead to clearance of CO from peripheral tissues and extravasculature targets. Indeed, blood COHb

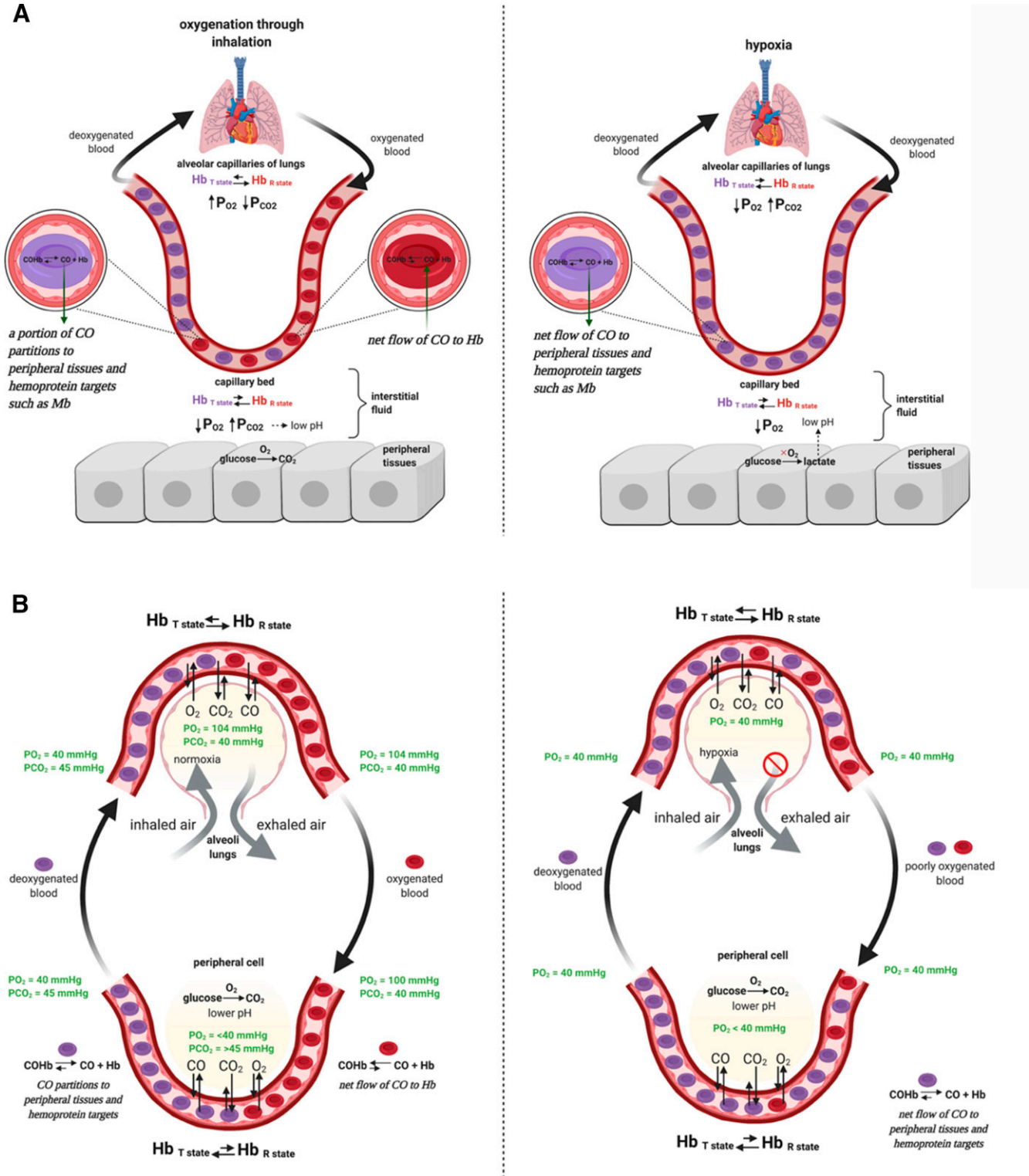

Fig. 28. CO distribution is dependent on the dynamic change of the ratio between high affinity and low affinity of COHb. (A) A brief description of the idea of the shifting distribution of CO from the cardiovascular circulation to peripheral tissues when O_2 pressure is low and Hb largely exists in the low-affinity T state because of the change in pH and O_2 partial pressure, among other factors. (B) A detailed description of the processes leading to CO redistribution depending on O_2 partial pressure.

recovery often does happen quickly, at least to a level that is no longer considered an acute problem. However, it seems that clearance of CO from extravasculature targets takes a much longer time (days) than one would expect based on the binding kinetics and respiration, and recovery of CNS impairments does not always correlate with decreased levels of COHb (Miró et al., 1998). There could be many convoluted clinical

reasons for this, but one can envision persistent CO binding to molecular target(s) in the CNS being a key factor. If one looks at the kinetics and thermodynamics of CO exchange between Hb and key CNS target Ngb, it becomes very clear that efficient exchange would happen only when Hb is in the high-affinity R state. If it is in the low-affinity T state, with K_d for CO being in the low μM range, the ability of Hb to "extract" CO from Ngb is almost nonexistent, with a K_d difference on the order of 10^7. The lack of a high-affinity carrier (Hb) could present a kinetic barrier to clearing CO from the CNS. One of the clinical features of CO intoxication is the metabolic acidosis as a result of hypoxia and perturbed metabolism. This drop in pH is expected to shift Hb to its low-affinity state. As a result, the ability of Hb to help clear CO from Ngb becomes very weak. This could be a key reason for the delayed recovery of CNS impairments in patients with severe CO intoxication. During recovery, the blood pH normally gradually returns to normal, which is also expected to allow Hb to exist in its high-affinity state. With a K_d of 0.7–1.7 nM, Hb at its R state is expected to compete for CO binding with Ngb (K_d of 0.2 nM) very effectively, especially considering the high abundance of Hb. As a result, CO clearance could very much depend on the overall physiologic state of the patients in addition to the use of oxygen for CO replacement.

X. Conclusions

With all of the analyses, there are several key messages that we hope will be helpful to the field. First, studies of dose dependency are essential for any effort in developing therapeutics. With CO having so many targets, dose dependency is more than an issue of potency; it also affects the analysis of side effects and the involvement of targets beyond the intended ones. However, at this stage, the CO field is in real need of rigorous studies of dose-dependent effects.

Second, with K_d values spanning seven orders of magnitude (ranging from sub-nM to high μM) for binding between CO and identified hemoprotein targets, there is a need to examine the effect of a given target in the context of all of the targets, with attention to the convoluted relationship among binding affinity, CO concentration (free and in the form of COHb), and the affinity state of COHb. If the intended target is a low-affinity one, then there need to be analyses of how the same concentration of CO would affect the other targets with a higher affinity than the intended target.

Third, CO transport, CO binding to Hb, and local conditions are all important factors to consider in analyzing the ability of Hb to unload CO locally. Future studies will need to consider local environments and their effects on CO's affinity for various hemoproteins.

Fourth, development of appropriate formulations and donors for controlled delivery of CO has been very critical to the CO field. However, the release rates of CO donors play an important role in the peak and sustained concentrations of CO (Yang et al., 2021a,b). Along this line, it is important to emphasize that donor concentration does not equate CO concentration because of CO's volatility. Therefore, comparison of CO dosage goes beyond comparing the concentration of the donor used; it also needs to consider the release rate and peak and sustained CO concentrations because of CO's volatility. This aspect also impacts dose-response studies.

Fifth, one might ask the question as to which molecular targets are the most important ones to consider for CO. There is no simple answer. Here we provide our views of issues to consider. Naturally, molecular targets that have higher affinity for CO than Hb will need to be considered because of their ability to "extract" CO from Hb. This list includes neuroglobin, myoglobin, some isoforms of P450, and cytochrome c oxidase, all of which have been widely recognized as CO's targets. Along this line, sGC stands out as an outlier because it has a very low affinity but is often cited as a target for CO in attributing CO's pharmacological effects. We are not sure of what the answer is. Another way of looking at this issue is based on the biologic problem at hand. For example, if P450 mediated metabolism is the question at hand, then P450 is important, even though it may not have the highest affinity for CO.

Sixth, all of the mathematical model work is based on binary analyses, and in reality that binary scenario only represents a simplified estimate for intuitive assessments of the competition in binding with CO between Hb and a given target. Therefore, all of the analyses can be considered as starting points to inject a quantitative sense into studying the various relationship among targets. For in-depth studies of a particular target for a given indication, more extensive multivariable analyses will be required for information, with enhanced relevance to a particular application. As more experimental data become available, they will also help the refinement of the computational work. We hope that the holistic approach of analyzing the binding with all relevant targets in a quantitative fashion will help the understanding of binding and pharmacokinetic factors that are important for the eventual development of CO-based therapeutics.

At this point, the analyses of the interplay among molecular targets, binding affinity, dosage, and effects of local conditions on binding affinity are complete. However, there are two points that are important for the development of CO-based therapeutics, which are pertinent to the subject of this review. First, are there ways to deliver CO selectively to achieve site-specific

enrichments? This would allow for the ability to overcome limitations by the intrinsic affinity of various targets. It is easy to think of selective delivery to the GI (Steiger et al., 2017; Bakalarz et al., 2021). However, selective CO delivery toward intended organs, tissues, cell types, or organelles is much harder (Berreau, 2022). Along this line, there have been reports of mitochondria-targeted delivery of CO (Zheng et al., 2018; Lazarus et al., 2022) leading to improved potency in animal models (Zheng et al., 2018). Future work along the lines of tissue- and/or organ-targeted delivery will be very important. A recent publication on a free radical-triggered CO donor also offers an approach for selective activation and enrichment (Xing et al., 2022). Second, understanding the pathophysiological effects of endogenous CO as well as the relationships between heme oxygenase and abnormality in CO levels and diseases will be very important for designing CO-based therapeutics. However, this is a complex subject; readers are referred to reports on CO production in sickness and in health as well as the protective effects of HO-1 for more in-depth analyses of these subjects (Coburn et al., 1966; Otterbein et al., 2003; Kishimoto et al., 2019; Wang et al., 2021; De La Cruz and Wang, 2022). We hope that with the discussions of these last two points, the review allows for putting the discussions of CO targets, binding affinity, and dose-response relationship in the context of developing new therapeutic agents and in understanding CO's targets in health and sickness.

Authorship Contributions

Participated in research design: Yuan, De La Cruz, Yang, Wang.

Contributed new reagents or analytic tools: Yang.

Performed data analysis: Yang, Wang.

Wrote or contributed to the writing of the manuscript: Yuan, De La Cruz, Yang, Wang.

Acknowledgments

Figures 1, 13, 14, 16, 20, 23, 25, 26, and 28 were created with Biorender.com.

References

Abe T, Yazawa K, Fujino M, Imamura R, Hatayama N, Kakuta Y, Tsutahara K, Okumi M, Ichimaru N, Kaimori JY, et al. (2017) High-pressure carbon monoxide preserves rat kidney grafts from apoptosis and inflammation. *Lab Invest* **97**:468–477.

Abu-Soud HM and Hazen SL (2001) Interrogation of heme pocket environment of mammalian peroxidases with diatomic ligands. *Biochemistry* **40**:10747–10755.

Ahmed MH, Ghatge MS, and Safo MK (2020) Hemoglobin: structure, function and allostery. *Subcell Biochem* **94**:345–382.

Akeson A, Biörck G, and Simon R (1968) On the content of myoglobin in human muscles. *Acta Med Scand* **183**:307–316.

Alam J, Igarashi K, Immenschuh S, Shibahara S, and Tyrrell RM (2004) Regulation of heme oxygenase-1 gene transcription: recent advances and highlights from the International Conference (Uppsala, 2003) on Heme Oxygenase. *Antioxid Redox Signal* **6**:924–933.

Almeida AS, Queiroga CSF, Sousa MFQ, Alves PM, and Vieira HLA (2012) Carbon monoxide modulates apoptosis by reinforcing oxidative metabolism in astrocytes: role of Bcl-2. *J Biol Chem* **287**:10761–10770.

Alonso J-R, Cardellach F, López S, Casademont J, and Miró O (2003) Carbon monoxide specifically inhibits cytochrome c oxidase of human mitochondrial respiratory chain. *Pharmacol Toxicol* **93**:142–146.

Amacher JF, Zhong F, Lisi GP, Zhu MQ, Alden SL, Hoke KR, Madden DR, and Pletneva EV (2015) A compact structure of cytochrome c trapped in a lysine-ligated state: loop refolding and functional implications of a conformational switch. *J Am Chem Soc* **137**:8435–8449.

Andersen CC and Stark MJ (2012) Haemoglobin transfusion threshold in very preterm newborns: a theoretical framework derived from prevailing oxygen physiology. *Med Hypotheses* **78**:71–74.

Ansari A, Jones CM, Henry ER, Hofrichter J, and Eaton WA (1994) Conformational relaxation and ligand binding in myoglobin. *Biochemistry* **33**:5128–5145.

Antony LA, Slanina T, Šebej P, Šolomek T, and Klán P (2013) Fluorescein analogue xanthene-9-carboxylic acid: a transition-metal-free CO releasing molecule activated by green light. *Org Lett* **15**:4552–4555.

Archakov AI, Karuzina II, Petushkova NA, Lisitsa AV, and Zgoda VG (2002) Production of carbon monoxide by cytochrome P450 during iron-dependent lipid peroxidation. *Toxicol In Vitro* **16**:1–10.

Armstrong PW, Roessig L, Patel MJ, Anstrom KJ, Butler J, Voors AA, Lam CSP, Ponikowski P, Temple T, Pieske B, et al. (2018) A multicenter, randomized, double-blind, placebo-controlled trial of the efficacy and safety of the oral soluble guanylate cyclase stimulator: the VICTORIA trial. *JACC Heart Fail* **6**:96–104.

Ascenzi P, Bocedi A, Leoni L, Visca P, Zennaro E, Milani M, and Bolognesi M (2004) CO sniffing through heme-based sensor proteins. *IUBMB Life* **56**:309–315.

Azarov I, Wang L, Rose JJ, Xu Q, Huang XN, Belanger A, Wang Y, Guo L, Liu C, Ucer KB, et al. (2016) Five-coordinate H64Q neuroglobin as a ligand-trap antidote for carbon monoxide poisoning. *Sci Transl Med* **8**:368ra173.

Aziz IS, McMahon AM, Friedman D, Rabinovich-Nikitin I, Kirshenbaum LA, and Martino TA (2021) Circadian influence on inflammatory response during cardiovascular disease. *Curr Opin Pharmacol* **57**:60–70.

Bae H, Kim T, and Lim I (2021) Carbon monoxide activates large-conductance calcium-activated potassium channels of human cardiac fibroblasts through various mechanisms. *Korean J Physiol Pharmacol* **25**:227–237.

Bakalarz D, Surmiak M, Yang X, Wójcik D, Korbut E, Śliwowski Z, Ginter G, Buszewicz G, Brzozowski T, Cieszkowski J, et al. (2021) Organic carbon monoxide prodrug, BW-CO-111, in protection against chemically-induced gastric mucosal damage. *Acta Pharm Sin B* **11**:456–475.

Balny C and Debey P (1976) Low temperature studies of microsomal cytochrome P450. determination of dissociation constant of the [Fe2+-CO] form. *FEBS Lett* **62**:198–201.

Banerjee R and Zou CG (2005) Redox regulation and reaction mechanism of human cystathionine-β-synthase: a PLP-dependent hemesensor protein. *Arch Biochem Biophys* **433**:144–156.

Bani Hashemi S, Braun J, Bernhardt WM, Rascher W, Dötsch J, and Trollmann R (2008) HIF-1alpha subunit and vasoactive HIF-1-dependent genes are involved in carbon monoxide-induced cerebral hypoxic stress response. *Eur J Appl Physiol* **104**:95–102.

Barr I, Smith AT, Chen Y, Senturia R, Burstyn JN, and Guo F (2012) Ferric, not ferrous, heme activates RNA-binding protein DGCR8 for primary microRNA processing. *Proc Natl Acad Sci USA* **109**:1919–1924.

Beard RR (1969) Toxicological appraisal of carbon monoxide. *J Air Pollut Control Assoc* **19**:722–727.

Beckerson P, Reeder BJ, and Wilson MT (2015) Coupling of disulfide bond and distal histidine dissociation in human ferrous cytoglobin regulates ligand binding. *FEBS Lett* **589**:507–512.

Bengea S, Araki Y, Ito O, Igarashi J, Sagami I, and Shimizu T (2004) Analysis of the kinetics of CO binding to neuronal nitric oxide synthase by flash photolysis: dual effects of substrates, inhibitors, and tetrahydrobiopterin. *J Inorg Biochem* **98**:1210–1216.

Bengea S, Sagami I, and Shimizu T (2003) CO binding to the isolated oxygenase domain of neuronal nitric oxide synthase: effects of inhibitors and mutations at the substrate-binding site. *J Inorg Biochem* **94**:343–347.

Berg JM, Tymoczko JL, and Stryer L (2002) Hemoglobin transports oxygen efficiently by binding oxygen cooperatively, in *Biochemistry*, 5th ed, W.H. Freeman, New York.

Berreau L (2022) Targeted delivery of carbon monoxide, in *Carbon Monoxide in Drug Discovery: Basics, Pharmacology, and Therapeutic Potential* (Wang B and Otterbein LE, eds) John Wiley and Sons, Hoboken, NJ.

Bertazzo A, Ragazzi E, Biasiolo M, Costa CV, and Allegri G (2001) Enzyme activities involved in tryptophan metabolism along the kynurenine pathway in rabbits. *Biochim Biophys Acta* **1527**:167–175.

Beutler E and Waalen J (2006) The definition of anemia: what is the lower limit of normal of the blood hemoglobin concentration? *Blood* **107**:1747–1750.

Beuve A (2017) Thiol-based redox modulation of soluble guanylyl cyclase, the nitric oxide receptor. *Antioxid Redox Signal* **26**:137–149.

Bhattacharyya S, Saha S, Giri K, Lanza IR, Nair KS, Jennings NB, Rodriguez-Aguayo C, Lopez-Berestein G, Basal E, Weaver AL, et al. (2013) Cystathionine beta-synthase (CBS) contributes to advanced ovarian cancer progression and drug resistance. *PLoS One* **8**:e79167.

Bilban M, Haschemi A, Wegiel B, Chin BY, Wagner O, and Otterbein LE (2008) Heme oxygenase and carbon monoxide initiate homeostatic signaling. *J Mol Med (Berl)* **86**:267–279.

Bleecker ML (2015) Carbon monoxide intoxication. *Handb Clin Neurol* **131**:191–203.

Boehning D and Snyder SH (2002) Circadian rhythms. Carbon monoxide and clocks. *Science* **298**:2339–2340.

Borisov VB and Siletsky SA (2019) Features of organization and mechanism of catalysis of two families of terminal oxidases: heme-copper and bd-type. *Biochemistry (Mosc)* **84**:1390–1402.

Bostelaar T, Vitvitsky V, Kumutima J, Lewis BE, Yadav PK, Brunold TC, Filipovic M, Lehnert N, Stemmler TL, and Banerjee R (2016) Hydrogen sulfide oxidation by myoglobin. *J Am Chem Soc* **138**:8476–8488.

Brückmann NE, Wahl M, Reiß GJ, Kohns M, Wätjen W, and Kunz PC (2011) Polymer conjugates of photoinducible CO-releasing molecules. *Eur J Inorg Chem* **2011**:4571–4577 DOI: 10.1002/ejic.201100545.

Brüne B and Ullrich V (1987) Inhibition of platelet aggregation by carbon monoxide is mediated by activation of guanylate cyclase. *Mol Pharmacol* **32**:497–504.
Brunori M, Bonaventura J, Bonaventura C, Antonini E, and Wyman J (1972) Carbon monoxide binding by hemoglobin and myoglobin under photodissociating conditions. *Proc Natl Acad Sci USA* **69**:868–871.
Bunn HF and Jandl JH (1968) Exchange of heme among hemoglobins and between hemoglobin and albumin. *J Biol Chem* **243**:465–475.
Burger D, Xiang F, Hammoud L, Lu X, and Feng Q (2009) Role of heme oxygenase-1 in the cardioprotective effects of erythropoietin during myocardial ischemia and reperfusion. *Am J Physiol Heart Circ Physiol* **296**:H84–H93.
Burton MJ, Cresser-Brown J, Thomas M, Portolano N, Basran J, Freeman SL, Kwon H, Bottrill AR, Llansola-Portoles MJ, Pascal AA, et al. (2020) Discovery of a heme-binding domain in a neuronal voltage-gated potassium channel. *J Biol Chem* **295**:13277–13286.
Burton MJ, Kapetanaki SM, Chernova T, Jamieson AG, Dorlet P, Santolini J, Moody PCE, Mitcheson JS, Davies NW, Schmid R, et al. (2016) A heme-binding domain controls regulation of ATP-dependent potassium channels. *Proc Natl Acad Sci USA* **113**:3785–3790.
Bushnell GW, Louie GV, and Brayer GD (1990) High-resolution three-dimensional structure of horse heart cytochrome c. *J Mol Biol* **214**:585–595.
Calderazzo F (2006) Carbonyl complexes of the transition metals, in *Encyclopedia of Inorganic Chemistry* (Scott RA, ed) John Wiley and Sons, New York.
Campbell Jr BN, Araiso T, Reinisch L, Yue KT, and Hager LP (1982) A kinetic study of the binding of carbon monoxide to ferrous chloroperoxidase. *Biochemistry* **21**:4343–4349.
Cao X, Wu Z, Xiong S, Cao L, Sethi G, and Bian JS (2018) The role of hydrogen sulfide in cyclic nucleotide signaling. *Biochem Pharmacol* **149**:20–28.
Carballal S, Madzelan P, Zinola CF, Graña M, Radi R, Banerjee R, and Alvarez B (2008) Dioxygen reactivity and heme redox potential of truncated human cystathionine β-synthase. *Biochemistry* **47**:3194–3201.
Carter EL, Gupta N, and Ragsdale SW (2016) High affinity heme binding to a heme regulatory motif on the nuclear receptor Rev-erbβ leads to its degradation and indirectly regulates its interaction with nuclear receptor corepressor. *J Biol Chem* **291**:2196–2222.
Carter EL, Ramirez Y, and Ragsdale SW (2017) The heme-regulatory motif of nuclear receptor Rev-erbβ is a key mediator of heme and redox signaling in circadian rhythm maintenance and metabolism. *J Biol Chem* **292**:11280–11299.
Chakraborty S, Balakotaiah V, and Bidani A (2004) Diffusing capacity reexamined: relative roles of diffusion and chemical reaction in red cell uptake of O2, CO, CO2, and NO. *J Appl Physiol* **97**:2284–2302.
Changeux JP (2012) Allostery and the Monod-Wyman-Changeux model after 50 years. *Annu Rev Biophys* **41**:103–133.
Chen Y and Burnett JC (2018) Particulate guanylyl cyclase A/cGMP signaling pathway in the kidney: physiologic and therapeutic indications. *Int J Mol Sci* **19**:1006–1017.
Chen Y, Joe Y, Park J, Song HC, Kim UH, and Chung HT (2019a) Carbon monoxide induces the assembly of stress granule through the integrated stress response. *Biochem Biophys Res Commun* **512**:289–294.
Chen Y, Park HJ, Park J, Song HC, Ryter SW, Surh YJ, Kim UH, Joe Y, and Chung HT (2019b) Carbon monoxide ameliorates acetaminophen-induced liver injury by increasing hepatic HO-1 and Parkin expression. *FASEB J* **33**:13905–13919.
Cheng Y and Levy RJ (2014) Subclinical carbon monoxide limits apoptosis in the developing brain after isoflurane exposure. *Anesth Analg* **118**:1284–1292.
Chhikara M, Wang S, Kern SJ, Ferreyra GA, Barb JJ, Munson PJ, and Danner RL (2009) Carbon monoxide blocks lipopolysaccharide-induced gene expression by interfering with proximal TLR4 to NF-kappaB signal transduction in human monocytes. *PLoS One* **4**:e8139.
Cho CH, Chiu NC, Ho CS, and Peng CC (2008) Carbon monoxide poisoning in children. *Pediatr Neonatol* **49**:121–125.
Cho HS, Schotte F, Stadnytskyi V, DiChiara A, Henning R, and Anfinrud P (2018) Dynamics of quaternary structure transitions in R-state carbonmonoxyhemoglobin unveiled in time-resolved X-ray scattering patterns following a temperature jump. *J Phys Chem B* **122**:11488–11496.
Choi YK, Maki T, Mandeville ET, Koh SH, Hayakawa K, Arai K, Kim YM, Whalen MJ, Xing C, Wang X, et al. (2016) Dual effects of carbon monoxide on pericytes and neurogenesis in traumatic brain injury. *Nat Med* **22**:1335–1341.
Chong GW, Karbelkar AA, and El-Naggar MY (2018) Nature's conductors: what can microbial multi-heme cytochromes teach us about electron transport and biological energy conversion? *Curr Opin Chem Biol* **47**:7–17.
Chrzanowska-Lightowlers ZM, Turnbull DM, and Lightowlers RN (1993) A microtiter plate assay for cytochrome c oxidase in permeabilized whole cells. *Anal Biochem* **214**:45–49.
Chung Y, Huang SJ, Glabe A, and Jue T (2006) Implication of CO inactivation on myoglobin function. *Am J Physiol Cell Physiol* **290**:C1616–C1624.
Coburn RF (1970) The carbon monoxide body stores. *Ann N Y Acad Sci* **174**:11–22.
Coburn RF and Mayers LB (1971) Myoglobin O2 tension determined from measurement of carboxymyoglobin in skeletal muscle. *Am J Physiol* **220**:66–74.
Coburn RF, Williams WJ, and Kahn SB (1966) Endogenous carbon monoxide production in patients with hemolytic anemia. *J Clin Invest* **45**:460–468.
Cockayne DA, Dunn PM, Zhong Y, Rong W, Hamilton SG, Knight GE, Ruan H-Z, Ma B, Yip P, Nunn P, et al. (2005) P2X2 knockout mice and P2X2/P2X3 double knockout mice reveal a role for the P2X2 receptor subunit in mediating multiple sensory effects of ATP. *J Physiol* **567**:621–639.
Collman JP, Brauman JI, and Doxsee KM (1979) Carbon monoxide binding to iron porphyrins. *Proc Natl Acad Sci USA* **76**:6035–6039.
Collman JP, Brauman JI, Halbert TR, and Suslick KS (1976) Nature of O2 and CO binding to metalloporphyrins and heme proteins. *Proc Natl Acad Sci USA* **73**:3333–3337.
Cooper CE (1999) Nitric oxide and iron proteins. *Biochim Biophys Acta* **1411**:290–309.
Cooper CE, Mason MG, and Nicholls P (2008) A dynamic model of nitric oxide inhibition of mitochondrial cytochrome c oxidase. *Biochim Biophys Acta* **1777**:867–876.
Correa-Costa M, Gallo D, Csizmadia E, Gomperts E, Lieberum J-L, Hauser CJ, Ji X, Wang B, Câmara NOS, Robson SC, et al. (2018) Carbon monoxide protects the kidney through the central circadian clock and CD39. *Proc Natl Acad Sci USA* **115**:E2302–E2310.
Dai Y, Schlanger S, Haque MM, Misra S, and Stuehr DJ (2019) Heat shock protein 90 regulates soluble guanylyl cyclase maturation by a dual mechanism. *J Biol Chem* **294**:12880–12891.
Dallas ML, Yang Z, Boyle JP, Boycott HE, Scragg JL, Milligan CJ, Elies J, Duke A, Thireau J, Reboul C, et al. (2012) Carbon monoxide induces cardiac arrhythmia via induction of the late Na+ current. *Am J Respir Crit Care Med* **186**:648–656.
D'Amico G, Lam F, Hagen T, and Moncada S (2006) Inhibition of cellular respiration by endogenously produced carbon monoxide. *J Cell Sci* **119**:2291–2298.
Daniels HG, Fast OG, Shell SM, and Beckford FA (2019) Chemistry and biology of manganese carbon-releasing molecules containing thiosemicarbazone ligands. *J Photochem Photobiol A Chem* **374**:84–94 DOI: 10.1016/j.jphotochem.2019.01.037.
Davydov RM, Greshner Z, Stepanov SV, and Rukpaul' K (1980) Flash-photolysis study of the influence of substrates on the kinetics of the recombination of carbon monoxide with microsomal cytochrome P450. *Mol Biol (Mosk)* **14**:685–693.
Davydov RM, Khanina OIu, Iagofarov S, Uvarov VIu, and Archakov AI (1986) Effect of lipids and substrates on the kinetics of binding of ferrocytochrome P-450 to CO. *Biokhimiia* **51**:125–129.
De La Cruz LKC, Benoit SL, Pan Z, Yu B, Maier RJ, Ji X, and Wang B (2018) Click, release, and fluoresce: a chemical strategy for a cascade prodrug system for codelivery of carbon monoxide, a drug payload, and a fluorescent reporter. *Org Lett* **20**:897–900.
De La Cruz LK and Wang Bb (2022) Endogenous CO production in sickness and in health, in *Carbon Monoxide in Drug Discovery: Basics, Pharmacology, and Therapeutic Potential* (Wang B and Otterbein LE, eds). John Wiley and Sons, Hoboken, NJ.
De La Cruz LK, Yang X, Menshikh A, Brewer M, Lu W, Wang M, Wang S, Ji X, Cachuela A, Yang H, et al. (2021) Adapting decarbonylation chemistry for the development of prodrugs capable of *in vivo* delivery of carbon monoxide utilizing sweeteners as carrier molecules. *Chem Sci (Camb)* **12**:10649–10654.
Debey P, Balny C, and Douzou P (1973) Low temperature studies of microsomal cytochrome P450 flash photolysis experiments. *FEBS Lett* **35**:86–90.
Decaluwé K, Pauwels B, Boydens C, and Van de Voorde J (2012a) Divergent molecular mechanisms underlay CO- and CORM-2-induced relaxation of corpora cavernosa. *J Sex Med* **9**:2284–2292.
Decaluwé K, Pauwels B, Verpoest S, and Van de Voorde J (2012b) Divergent mechanisms involved in CO and CORM-2 induced vasorelaxation. *Eur J Pharmacol* **674**:370–377.
Denninger JW and Marletta MA (1999) Guanylate cyclase and the. NO/cGMP signaling pathway. *Biochim Biophys Acta* **1411**:334–350.
Derbyshire ER and Marletta MA (2012) Structure and regulation of soluble guanylate cyclase. *Annu Rev Biochem* **81**:533–559.
Dewilde S, Kiger L, Burmester T, Hankeln T, Baudin-Creuza V, Aerts T, Marden MC, Caubergs R, and Moens L (2001) Biochemical characterization and ligand binding properties of neuroglobin, a novel member of the globin family. *J Biol Chem* **276**:38949–38955.
Dickerson RE, ed (1983) *Hemoglobin: Structure, Function, Evolution, and Pathology*, Benjamin-Cummings Publishing Company, Redwood City, CA.
Dioum EM, Rutter J, Tuckerman JR, Gonzalez G, Gilles-Gonzalez M-A, and McKnight SL (2002) NPAS2: a gas-responsive transcription factor. *Science* **298**:2385–2387.
Dong DL, Chen C, Huang W, Chen Y, Zhang XL, Li Z, Li Y, and Yang BF (2008) Tricarbonyldichlororuthenium (II) dimer (CORM2) activates non-selective cation current in human endothelial cells independently of carbon monoxide releasing. *Eur J Pharmacol* **590**:99–104.
Dubey A and Dubey S (2019) Neuroglobins: a look into the future. *Eur Respir J* **5**:926–927 DOI: 10.18621/eurj.470361.
Dugbartey GJ, Alornyo KK, Luke PPW, and Sener A (2021) Application of carbon monoxide in kidney and heart transplantation: a novel pharmacological strategy for a broader use of suboptimal renal and cardiac grafts. *Pharmacol Res* **173**:105883.
Dunford HB (2010) *Peroxidases and Catalases: Biochemistry, Biophysics, Biotechnology and Physiology*, John Wiley and Sons, Hoboken, NJ.
Egan B and Zierath JR (2013) Exercise metabolism and the molecular regulation of skeletal muscle adaptation. *Cell Metab* **17**:162–184.
Eichhorn L, Michaelis D, Kemmerer M, Jüttner B, and Tetzlaff K (2018) Carbon monoxide poisoning from waterpipe smoking: a retrospective cohort study. *Clin Toxicol (Phila)* **56**:264–272.
Elies J, Dallas ML, Boyle JP, Scragg JL, Duke A, Steele DS, and Peers C (2014) Inhibition of the cardiac Na^+ channel Nav1.5 by carbon monoxide. *J Biol Chem* **289**:16421–16429.
Ellis Jr WR, Wang H, Blair DF, Gray HB, and Chan SI (1986) Spectroelectrochemical study of the cytochrome a site in carbon monoxide inhibited cytochrome c oxidase. *Biochemistry* **25**:161–167.
Elton L, Carpentier I, Verhelst K, Staal J, and Beyaert R (2015) The multifaceted role of the E3 ubiquitin ligase HOIL-1: beyond linear ubiquitination. *Immunol Rev* **266**:208–221.
Epstein SK and Singh N (2001) Respiratory acidosis. *Respir Care* **46**:366–383.
Fago A, Crumbliss AL, Hendrich MP, Pearce LL, Peterson J, Henkens R, and Bonaventura C (2013) Oxygen binding to partially nitrosylated hemoglobin. *Biochim Biophys Acta* **1834**:1894–1900.
Fago A, Mathews AJ, Moens L, Dewilde S, and Brittain T (2006) The reaction of neuroglobin with potential redox protein partners cytochrome b5 and cytochrome c. *FEBS Lett* **580**:4884–4888.

Faleo G, Neto JS, Kohmoto J, Tomiyama K, Shimizu H, Takahashi T, Wang Y, Sugimoto R, Choi AM, Stolz DB, et al. (2008) Carbon monoxide ameliorates renal cold ischemia-reperfusion injury with an upregulation of vascular endothelial growth factor by activation of hypoxia-inducible factor. *Transplantation* **85**:1833–1840.
Faller M, Matsunaga M, Yin S, Loo JA, and Guo F (2007) Heme is involved in microRNA processing. *Nat Struct Mol Biol* **14**:23–29.
Fan JS, Zheng Y, Choy WY, Simplaceanu V, Ho NT, Ho C, and Yang D (2013) Solution structure and dynamics of human hemoglobin in the carbonmonoxy form. *Biochemistry* **52**:5809–5820.
Farrugia G and Szurszewski JH (2014) Carbon monoxide, hydrogen sulfide, and nitric oxide as signaling molecules in the gastrointestinal tract. *Gastroenterology* **147**:303–313.
Fazekas AS, Wewalka M, Zauner C, and Funk GC (2012) Carboxyhemoglobin levels in medical intensive care patients: a retrospective, observational study. *Crit Care* **16**:R6.
Feil R and Kemp-Harper B (2006) cGMP signalling: from bench to bedside. Conference on cGMP generators, effectors and therapeutic implications. *EMBO Rep* **7**:149–153.
Fiocchetti M, Fernandez VS, Montalesi E, and Marino M (2019) Neuroglobin: a novel player in the oxidative stress response of cancer cells. *Oxid Med Cell Longev* **2019**:6315034.
Fleischhacker AS, Carter EL, and Ragsdale SW (2018) Redox regulation of heme oxygenase-2 and the transcription factor, Rev-erb, through heme regulatory motifs. *Antioxid Redox Signal* **29**:1841–1857.
Frauenfelder H, McMahon BH, Austin RH, Chu K, and Groves JT (2001) The role of structure, energy landscape, dynamics, and allostery in the enzymatic function of myoglobin. *Proc Natl Acad Sci USA* **98**:2370–2374.
Friebe A and Koesling D (1998) Mechanism of YC-1-induced activation of soluble guanylyl cyclase. *Mol Pharmacol* **53**:123–127.
Friebe A, Sandner P, and Schmidtko A (2020) cGMP: a unique 2nd messenger molecule - recent developments in cGMP research and development. *Naunyn Schmiedebergs Arch Pharmacol* **393**:287–302.
Friebe A, Schultz G, and Koesling D (1996) Sensitizing soluble guanylyl cyclase to become a highly CO-sensitive enzyme. *EMBO J* **15**:6863–6868.
Frumento G, Rotondo R, Tonetti M, Damonte G, Benatti U, and Ferrara GB (2002) Tryptophan-derived catabolites are responsible for inhibition of T and natural killer cell proliferation induced by indoleamine 2,3-dioxygenase. *J Exp Med* **196**:459–468.
Fujisaki N, Kohama K, Nishimura T, Yamashita H, Ishikawa M, Kanematsu A, Yamada T, Lee S, Yumoto T, Tsukahara K, et al. (2016) Donor pretreatment with carbon monoxide prevents ischemia/reperfusion injury following heart transplantation in rats. *Med Gas Res* **6**:122–129.
García-Gallego S and Bernardes GJL (2014) Carbon-monoxide-releasing molecules for the delivery of therapeutic CO in vivo. *Angew Chem Int Ed Engl* **53**:9712–9721.
Garry DJ and Mammen PP (2007) Molecular insights into the functional role of myoglobin. *Adv Exp Med Biol* **618**:181–193.
Gell DA (2018) Structure and function of haemoglobins. *Blood Cells Mol Dis* **70**:13–42.
Gessner G, Sahoo N, Swain SM, Hirth G, Schönherr R, Mede R, Westerhausen M, Brewitz HH, Heimer P, Imhof D, et al. (2017) CO-independent modification of K^+ channels by tricarbonyldichlororuthenium(II) dimer (CORM-2). *Eur J Pharmacol* **815**:33–41.
Gibson QH and Greenwood C (1963) Reactions of cytochrome oxidase with oxygen and carbon monoxide. *Biochem J* **86**:541–554.
Gibson QH, Olson JS, McKinnie RE, and Rohlfs RJ (1986) A kinetic description of ligand binding to sperm whale myoglobin. *J Biol Chem* **261**:10228–10239.
Gilles-Gonzalez MA and Gonzalez G (2005) Heme-based sensors: defining characteristics, recent developments, and regulatory hypotheses. *J Inorg Biochem* **99**:1–22.
Gilun P, Stefanczyk-Krzymowska S, Romerowicz-Misielak M, Tabecka-Lonczynska A, Przekop F, and Koziorowski M (2013) Carbon monoxide-mediated humoral pathway for the transmission of light signal to the hypothalamus. *J Physiol Pharmacol* **64**:761–772.
Goebel U, Siepe M, Schwer CI, Schibilsky D, Foerster K, Neumann J, Wiech T, Priebe HJ, Schlensak C, and Loop T (2010) Inhaled carbon monoxide prevents acute kidney injury in pigs after cardiopulmonary bypass by inducing a heat shock response. *Anesth Analg* **111**:29–37.
Goldbaum LR, Ramirez RG, and Absalon KB (1975) What is the mechanism of carbon monoxide toxicity? *Aviat Space Environ Med* **46**:1289–1291.
Goldman AL (1977) Carboxyhemoglobin levels in primary and secondary cigar and pipe smokers. *Chest* **72**:33–35.
Gong Q, Simplaceanu V, Lukin JA, Giovannelli JL, Ho NT, and Ho C (2006) Quaternary structure of carbonmonoxyhemoglobins in solution: structural changes induced by the allosteric effector inositol hexaphosphate. *Biochemistry* **45**:5140–5148.
Graham IM, Daly LE, Refsum HM, Robinson K, Brattström LE, Ueland PM, Palma-Reis RJ, Boers GHJ, Sheahan RG, Israelsson B, et al. (1997) Plasma homocysteine as a risk factor for vascular disease. The European Concerted Action Project. *JAMA* **277**:1775–1781.
Gray RD (1982) Kinetics and mechanism of carbon monoxide binding to purified liver microsomal cytochrome P-450 isozymes. *J Biol Chem* **257**:1086–1094.
Guengerich FP, Waterman MR, and Egli M (2016) Recent structural insights into cytochrome P450 function. *Trends Pharmacol Sci* **37**:625–640.
Hada H, Shiraki T, Watanabe-Matsui M, and Igarashi K (2014) Hemopexin-dependent heme uptake via endocytosis regulates the Bach1 transcription repressor and heme oxygenase gene activation. *Biochim Biophys Acta* **1840**:2351–2360.
Hampson NB (2018) Carboxyhemoglobin: a primer for clinicians. *Undersea Hyperb Med* **45**:165–171.
Hart CL, Smith GD, Hole DJ, and Hawthorne VM (2006) Carboxyhaemoglobin concentration, smoking habit, and mortality in 25 years in the Renfrew/Paisley prospective cohort study. *Heart* **92**:321–324.
Hegazi RA, Rao KN, Mayle A, Sepulveda AR, Otterbein LE, and Plevy SE (2005) Carbon monoxide ameliorates chronic murine colitis through a heme oxygenase 1-dependent pathway. *J Exp Med* **202**:1703–1713.
Heinemann SH, Hoshi T, Westerhausen M, and Schiller A (2014) Carbon monoxide–physiology, detection and controlled release. *Chem Commun (Camb)* **50**:3644–3660.
Hilser VJ, Wrabl JO, and Motlagh HN (2012) Structural and energetic basis of allostery. *Annu Rev Biophys* **41**:585–609.
Hines JP, Smith AT, Jacob JP, Lukat-Rodgers GS, Barr I, Rodgers KR, Guo F, and Burstyn JN (2016) CO and NO bind to Fe(II) DiGeorge critical region 8 heme but do not restore primary microRNA processing activity. *Eur J Biochem* **21**:1021–1035.
Hishiki T, Yamamoto T, Morikawa T, Kubo A, Kajimura M, and Suematsu M (2012) Carbon monoxide: impact on remethylation/transsulfuration metabolism and its pathophysiologic implications. *J Mol Med (Berl)* **90**:245–254.
Hlastala MP, McKenna HP, Franada RL, and Detter JC (1976) Influence of carbon monoxide on hemoglobin-oxygen binding. *J Appl Physiol* **41**:893–899.
Hoffmann LS, Kretschmer A, Lawrenz B, Hocher B, and Stasch JP (2015) Chronic activation of heme free guanylate cyclase leads to renal protection in Dahl salt-sensitive rats. *PLoS One* **10**:e0145048.
Hoogewijs D, Ebner B, Germani F, Hoffmann FG, Fabrizius A, Moens L, Burmester T, Dewilde S, Storz JF, Vinogradov SN, et al. (2012) Androglobin: a chimeric globin in metazoans that is preferentially expressed in mammalian testes. *Mol Biol Evol* **29**:1105–1114.
Hopper CP, De La Cruz LK, Lyles KV, Wareham LK, Gilbert JA, Eichenbaum Z, Magierowski M, Poole RK, Wollborn J, and Wang B (2020) Role of carbon monoxide in host-gut microbiome communication. *Chem Rev* **120**:13273–13311.
Hou S, Xu R, Heinemann SH, and Hoshi T (2008) The RCK1 high-affinity Ca2+ sensor confers carbon monoxide sensitivity to Slo1 BK channels. *Proc Natl Acad Sci USA* **105**:4039–4043.
Hourihan JM, Kenna JG, and Hayes JD (2013) The gasotransmitter hydrogen sulfide induces nrf2-target genes by inactivating the keap1 ubiquitin ligase substrate adaptor through formation of a disulfide bond between cys-226 and cys-613. *Antioxid Redox Signal* **19**:465–481.
Huang LE, Willmore WG, Gu J, Goldberg MA, and Bunn HF (1999) Inhibition of hypoxia-inducible factor 1 activation by carbon monoxide and nitric oxide. Implications for oxygen sensing and signaling. *J Biol Chem* **274**:9038–9044.
Huysal K, Ustundag Budak Y, Aydin U, Demirci H, Turk T, and Karadag M (2016) COHb level and high-sensitivity cardiac troponin T in 2012 in Bursa, Turkey: a retrospective single-center study. *Iran Red Crescent Med J* **18**:e27061.
Ikeda A, Ueki S, Nakao A, Tomiyama K, Ross MA, Stolz DB, Geller DA, and Murase N (2009) Liver graft exposure to carbon monoxide during cold storage protects sinusoidal endothelial cells and ameliorates reperfusion injury in rats. *Liver Transpl* **15**:1458–1468.
Ingi T, Cheng J, and Ronnett GV (1996) Carbon monoxide: an endogenous modulator of the nitric oxide-cyclic GMP signaling system. *Neuron* **16**:835–842.
Ingi T and Ronnett GV (1995) Direct demonstration of a physiological role for carbon monoxide in olfactory receptor neurons. *J Neurosci* **15**:8214–8222.
Ishigami I, Zatsepin NA, Hikita M, Conrad CE, Nelson G, Coe JD, Basu S, Grant TD, Seaberg MH, Sierra RG, et al. (2017) Crystal structure of CO-bound cytochrome *c* oxidase determined by serial femtosecond X-ray crystallography at room temperature. *Proc Natl Acad Sci USA* **114**:8011–8016.
Ishikawa H, Kato M, Hori H, Ishimori K, Kirisako T, Tokunaga F, and Iwai K (2005a) Involvement of heme regulatory motif in heme-mediated ubiquitination and degradation of IRP2. *Mol Cell* **19**:171–181.
Ishikawa M, Kajimura M, Adachi T, Maruyama K, Makino N, Goda N, Yamaguchi T, Sekizuka E, and Suematsu M (2005b) Carbon monoxide from heme oxygenase-2 Is a tonic regulator against NO-dependent vasodilatation in the adult rat cerebral microcirculation. *Circ Res* **97**:e104–e114.
Jackson CS, Schmitt S, Dou QP, and Kodanko JJ (2011) Synthesis, characterization, and reactivity of the stable iron carbonyl complex [Fe(CO)(N4Py)](ClO4)2: photoactivated carbon monoxide release, growth inhibitory activity, and peptide ligation. *Inorg Chem* **50**:5336–5338.
Jaggar JH, Li A, Parfenova H, Liu J, Umstot ES, Dopico AM, and Leffler CW (2005) Heme is a carbon monoxide receptor for large-conductance Ca2+-activated K+ channels. *Circ Res* **97**:805–812.
Jara-Oseguera A, Ishida IG, Rangel-Yescas GE, Espinosa-Jalapa N, Pérez-Guzmán JA, Elías-Viñas D, Le Lagadec R, Rosenbaum T, and Islas LD (2011) Uncoupling charge movement from channel opening in voltage-gated potassium channels by ruthenium complexes. *J Biol Chem* **286**:16414–16425.
Ji X, Aghoghovbia RE, De La Cruz LKC, Pan Z, Yang X, Yu B, and Wang B (2019a) Click and release: a high-content bioorthogonal prodrug with multiple outputs. *Org Lett* **21**:3649–3652.
Ji X, De La Cruz LKC, Pan Z, Chittavong V, and Wang B (2017a) pH-Sensitive metal-free carbon monoxide prodrugs with tunable and predictable release rates. *Chem Commun (Camb)* **53**:9628–9631.
Ji X, Ji K, Chittavong V, Aghoghovbia RE, Zhu M, and Wang B (2017b) Click and fluoresce: a bioorthogonally activated smart probe for wash-free fluorescent labeling of biomolecules. *J Org Chem* **82**:1471–1476.
Ji X, Ji K, Chittavong V, Yu B, Pan Z, and Wang B (2017c) An esterase-activated click and release approach to metal-free CO-prodrugs. *Chem Commun (Camb)* **53**:8296–8299.
Ji X, Pan Z, Li C, Kang T, De La Cruz LKC, Yang L, Yuan Z, Ke B, and Wang B (2019b) Esterase-sensitive and pH-controlled carbon monoxide prodrugs for treating systemic inflammation. *J Med Chem* **62**:3163–3168.
Ji X and Wang B (2018) Strategies toward organic carbon monoxide prodrugs. *Acc Chem Res* **51**:1377–1385.

Ji X, Zhou C, Ji K, Aghoghovbia RE, Pan Z, Chittavong V, Ke B, and Wang B (2016) Click and release: a chemical strategy toward developing gasotransmitter prodrugs by using an intramolecular Diels-Alder reaction. *Angew Chem Int Ed Engl* **55**:15846–15851.
Jimenez J, Chakraborty I, Carrington SJ, and Mascharak PK (2016) Light-triggered CO delivery by a water-soluble and biocompatible manganese photoCORM. *Dalton Trans* **45**:13204–13213.
Joe Y, Kim S, Kim HJ, Park J, Chen Y, Park HJ, Jekal SJ, Ryter SW, Kim UH, and Chung HT (2018) FGF21 induced by carbon monoxide mediates metabolic homeostasis via the PERK/ATF4 pathway. *FASEB J* **32**:2630–2643.
Joe Y, Uddin MJ, Zheng M, Kim HJ, Chen Y, Yoon NA, Cho GJ, Park JW, and Chung HT (2014) Tristetraprolin mediates anti-inflammatory effect of carbon monoxide against DSS-induced colitis. *PLoS One* **9**:e88776.
Joffe AR, Brin G, and Farrow S (2020) Unreliable early neuroprognostication after severe carbon monoxide poisoning is likely due to cytopathic hypoxia: a case report and discussion. *J Child Neurol* **35**:111–115.
Jue T and Chung Y (2003) Role of myoglobin in regulating respiration. *Adv Exp Med Biol* **530**:671–680.
Juszczak M, Kluska M, Wysokiński D, and Woźniak K (2020) DNA damage and antioxidant properties of CORM-2 in normal and cancer cells. *Sci Rep* **10**:12200–12211.
Kaasik K and Lee CC (2004) Reciprocal regulation of haem biosynthesis and the circadian clock in mammals. *Nature* **430**:467–471.
Kabil O, Weeks CL, Carballal S, Gherasim C, Alvarez B, Spiro TG, and Banerjee R (2011) Reversible heme-dependent regulation of human cystathionine β-synthase by a flavoprotein oxidoreductase. *Biochemistry* **50**:8261–8263.
Kaczara P, Przyborowski K, Mohaissen T, and Chlopicki S (2021) Distinct pharmacological properties of gaseous CO and CO-releasing molecule in human platelets. *Int J Mol Sci* **22**:3584–3594.
Kagan VE, Chu CT, Tyurina YY, Cheikhi A, and Bayir H (2014) Cardiolipin asymmetry, oxidation and signaling. *Chem Phys Lipids* **179**:64–69.
Kaizu T, Nakao A, Tsung A, Toyokawa H, Sahai R, Geller DA, and Murase N (2005) Carbon monoxide inhalation ameliorates cold ischemia/reperfusion injury after rat liver transplantation. *Surgery* **138**:229–235.
Kanaori K, Tajiri Y, Tsuneshige A, Ishigami I, Ogura T, Tajima K, Neya S, and Yonetani T (2011) T-quaternary structure of oxy human adult hemoglobin in the presence of two allosteric effectors, L35 and IHP. *Biochim Biophys Acta* **1807**:1253–1261.
Kang Y, Liu R, Wu JX, and Chen L (2019) Structural insights into the mechanism of human soluble guanylate cyclase. *Nature* **574**:206–210.
Kao LW and Nañagas KA (2005) Carbon monoxide poisoning. *Med Clin North Am* **89**:1161–1194.
Kapetanaki SM, Burton MJ, Basran J, Uragami C, Moody PCE, Mitcheson JS, Schmid R, Davies NW, Dorlet P, Vos MH, et al. (2018) A mechanism for CO regulation of ion channels. *Nat Commun* **9**:907–916.
Kapetanaki SM, Silkstone G, Husu I, Liebl U, Wilson MT, and Vos MH (2009) Interaction of carbon monoxide with the apoptosis-inducing cytochrome c-cardiolipin complex. *Biochemistry* **48**:1613–1619.
Kawahara B, Gao L, Cohn W, Whitelegge JP, Sen S, Janzen C, and Mascharak PK (2019a) Diminished viability of human ovarian cancer cells by antigen-specific delivery of carbon monoxide with a family of photoactivatable antibody-photoCORM conjugates. *Chem Sci (Camb)* **11**:467–473.
Kawahara B, Moller T, Hu-Moore K, Carrington S, Faull KF, Sen S, and Mascharak PK (2017) Attenuation of antioxidant capacity in human breast cancer cells by carbon monoxide through inhibition of cystathionine β-synthase activity: implications in chemotherapeutic drug sensitivity. *J Med Chem* **60**:8000–8010.
Kawahara B, Ramadoss S, Chaudhuri G, Janzen C, Sen S, and Mascharak PK (2019b) Carbon monoxide sensitizes cisplatin-resistant ovarian cancer cell lines toward cisplatin via attenuation of levels of glutathione and nuclear metallothionein. *J Inorg Biochem* **191**:29–39.
Kery V, Bukovska G, and Kraus JP (1994) Transsulfuration depends on heme in addition to pyridoxal 5′-phosphate. Cystathionine beta-synthase is a heme protein. *J Biol Chem* **269**:25283–25288.
Khakh BS and North RA (2006) P2X receptors as cell-surface ATP sensors in health and disease. *Nature* **442**:527–532.
Khanina OIu, Uvarov VIu, and Davydov RM (1987) Effect of lipids on CO recombination with ferrocytochrome P-450. *Biofizika* **32**:686–688.
Kim HJ, Joe Y, Kim SK, Park SU, Park J, Chen Y, Kim J, Ryu J, Cho GJ, Surh YJ, et al. (2017) Carbon monoxide protects against hepatic steatosis in mice by inducing sestrin-2 via the PERK-eIF2α-ATF4 pathway. *Free Radic Biol Med* **110**:81–91.
Kim HJ, Joe Y, Kong JS, Jeong SO, Cho GJ, Ryter SW, and Chung HT (2013) Carbon monoxide protects against hepatic ischemia/reperfusion injury via ROS-dependent Akt signaling and inhibition of glycogen synthase kinase 3β. *Oxid Med Cell Longev* **2013**:306421.
Kishimoto Y, Kondo K, and Momiyama Y (2019) The protective role of heme oxygenase-1 in atherosclerotic diseases. *Int J Mol Sci* **20**:3628–3642.
Kitagishi H and Minegishi S (2017) Iron(II)porphyrin-cyclodextrin supramolecular complex as a carbon monoxide-depleting agent in living organisms. *Chem Pharm Bull (Tokyo)* **65**:336–340.
Kitagishi H, Minegishi S, Yumura A, Negi S, Taketani S, Amagase Y, Mizukawa Y, Urushidani T, Sugiura Y, and Kano K (2016) Feedback response to selective depletion of endogenous carbon monoxide in the blood. *J Am Chem Soc* **138**:5417–5425.
Klemz R, Reischl S, Wallach T, Witte N, Jürchott K, Klemz S, Lang V, Lorenzen S, Knauer M, Heidenreich S, et al. (2017) Reciprocal regulation of carbon monoxide metabolism and the circadian clock. *Nat Struct Mol Biol* **24**:15–22.
Koglin M, Vehse K, Budaeus L, Scholz H, and Behrends S (2001) Nitric oxide activates the beta 2 subunit of soluble guanylyl cyclase in the absence of a second subunit. *J Biol Chem* **276**:30737–30743.
Kohmoto J, Nakao A, Kaizu T, Tsung A, Ikeda A, Tomiyama K, Billiar TR, Choi AM, Murase N, and McCurry KR (2006) Low-dose carbon monoxide inhalation prevents ischemia/reperfusion injury of transplanted rat lung grafts. *Surgery* **140**:179–185.
Kohmoto J, Nakao A, Sugimoto R, Wang Y, Zhan J, Ueda H, and McCurry KR (2008) Carbon monoxide-saturated preservation solution protects lung grafts from ischemia-reperfusion injury. *J Thorac Cardiovasc Surg* **136**:1067–1075.
Kolawole AO, Hixon BP, Dameron LS, Chrisman IM, and Smirnov VV (2015) Catalytic activity of human indoleamine 2,3-dioxygenase (hIDO1) at low oxygen. *Arch Biochem Biophys* **570**:47–57.
Kollau A, Gesslbauer B, Russwurm M, Koesling D, Gorren ACF, Schrammel A, and Mayer B (2018) Modulation of nitric oxide-stimulated soluble guanylyl cyclase activity by cytoskeleton-associated proteins in vascular smooth muscle. *Biochem Pharmacol* **156**:168–176.
Kraus DW, Wittenberg JB, Lu JF, and Peisach J (1990) Hemoglobins of the Lucina pectinata/bacteria symbiosis. II. An electron paramagnetic resonance and optical spectral study of the ferric proteins. *J Biol Chem* **265**:16054–16059.
Krikun G and Cederbaum AI (1985) Evaluation of microsomal pathways of oxidation of alcohols and hydroxyl radical scavenging agents with carbon monoxide and cobalt protoporphyrin IX. *Biochem Pharmacol* **34**:2929–2935.
Kueh JTB, Seifert-Simpson JM, Thwaite SH, Rodgers GD, Harrison JC, Sammut IA, and Larsen DS (2020) Studies towards non-toxic, water soluble, vasoactive norbornene organic carbon monoxide releasing molecules. *Asian J Org Chem* **9**:2127–2135 DOI: 10.1002/ajoc.202000546.
Kueh JTB, Stanley NJ, Hewitt RJ, Woods LM, Larsen L, Harrison JC, Rennison D, Brimble MA, Sammut IA, and Larsen DS (2017) Norborn-2-en-7-ones as physiologically-triggered carbon monoxide-releasing prodrugs. *Chem Sci (Camb)* **8**:5454–5459.
Kuniavsky M, Bechor Y, Leitman M, and Efrati S (2018) Carbon monoxide poisoning in a young, healthy patient: a case study of heart failure recovery after hyperbaric oxygenation treatment. *Intensive Crit Care Nurs* **47**:85–88.
Kuthan H and Ullrich V (1982) Oxidase and oxygenase function of the microsomal cytochrome P450 monooxygenase system. *Eur J Biochem* **126**:583–588.
Lal J, Maccarini M, Fouquet P, Ho NT, Ho C, and Makowski L (2017) Modulation of hemoglobin dynamics by an allosteric effector. *Protein Sci* **26**:505–514.
Lamon BD, Zhang FF, Puri N, Brodsky SV, Goligorsky MS, and Nasjletti A (2009) Dual pathways of carbon monoxide-mediated vasoregulation: modulation by redox mechanisms. *Circ Res* **105**:775–783.
Lazarus LS, Dederich CT, Anderson SN, Benninghoff AD, and Berreau LM (2022) Flavonol-based carbon monoxide delivery molecule with endoplasmic reticulum, mitochondria, and lysosome localization. *ACS Med Chem Lett* **13**:236–242.
Leclerc-L'Hostis E, Franzen S, Lambry JC, Martin JL, Leclerc L, Poyart C, and Marden MC (1996) Picosecond geminate recombination of CO to the complexes calmodulin*heme-CO and calmodulin*heme-CO*melittin. *Biochim Biophys Acta* **1293**:140–146.
Leemann T, Bonnabry P, and Dayer P (1994) Selective inhibition of major drug metabolizing cytochrome P450 isozymes in human liver microsomes by carbon monoxide. *Life Sci* **54**:951–956.
Levitt DG and Levitt MD (2015) Carbon monoxide: a critical quantitative analysis and review of the extent and limitations of its second messenger function. *Clin Pharmacol* **7**:37–56.
Li T, Bonkovsky HL, and Guo JT (2011) Structural analysis of heme proteins: implications for design and prediction. *BMC Struct Biol* **11**:13–25.
Lim I, Gibbons SJ, Lyford GL, Miller SM, Strege PR, Sarr MG, Chatterjee S, Szurszewski JH, Shah VH, and Farrugia G (2005) Carbon monoxide activates human intestinal smooth muscle L-type Ca2+ channels through a nitric oxide-dependent mechanism. *Am J Physiol Gastrointest Liver Physiol* **288**:G7–G14.
Lin YW (2015) The broad diversity of heme-protein cross-links: an overview. *Biochim Biophys Acta* **1854**:844–859.
Lin YW (2018) Structure and function of heme proteins regulated by diverse post-translational modifications. *Arch Biochem Biophys* **641**:1–30.
Liu X, Miller MJ, Joshi MS, Thomas DD, and Lancaster Jr JR (1998a) Accelerated reaction of nitric oxide with O2 within the hydrophobic interior of biological membranes. *Proc Natl Acad Sci USA* **95**:2175–2179.
Liu Y, Christou H, Morita T, Laughner E, Semenza GL, and Kourembanas S (1998b) Carbon monoxide and nitric oxide suppress the hypoxic induction of vascular endothelial growth factor gene via the 5′ enhancer. *J Biol Chem* **273**:15257–15262.
Lo Iacono L, Boczkowski J, Zini R, Salouage I, Berdeaux A, Motterlini R, and Morin D (2011) A carbon monoxide-releasing molecule (CORM-3) uncouples mitochondrial respiration and modulates the production of reactive oxygen species. *Free Radic Biol Med* **50**:1556–1564.
Lodemann P, Schorer G, and Frey BM (2010) Wrong molar hemoglobin reference values-a longstanding error that should be corrected. *Ann Hematol* **89**:209.
Lukat-Rodgers GS, Correia C, Botuyan MV, Mer G, and Rodgers KR (2010) Heme-based sensing by the mammalian circadian protein CLOCK. *Inorg Chem* **49**:6349–6365.
Ma X, Sayed N, Beuve A, and van den Akker F (2007) NO and CO differentially activate soluble guanylyl cyclase via a heme pivot-bend mechanism. *EMBO J* **26**:578–588.
Magierowska K, Korbut E, Hubalewska-Mazgaj M, Surmiak M, Chmura A, Bakalarz D, Buszewicz G, Wójcik D, Śliwowski Z, Ginter G, et al. (2019) Oxidative gastric mucosal damage induced by ischemia/reperfusion and the mechanisms of its prevention by carbon monoxide-releasing tricarbonyldichlororuthenium (II) dimer. *Free Radic Biol Med* **145**:198–208.
Makino M, Sawai H, Shiro Y, and Sugimoto H (2011) Crystal structure of the carbon monoxide complex of human cytoglobin. *Proteins* **79**:1143–1153.
Manikandan P and Nagini S (2018) Cytochrome P450 structure, function and clinical significance: a review. *Curr Drug Targets* **19**:38–54.

Mann BE (2012) CO-releasing molecules: a personal view. *Organometallics* **31**:5728–5735 DOI: 10.1021/om300364a.
Mao Q, Kawaguchi AT, Mizobata S, Motterlini R, Foresti R, and Kitagishi H (2021) Sensitive quantification of carbon monoxide in vivo reveals a protective role of circulating hemoglobin in CO intoxication. *Commun Biol* **4**:425–439.
Marden MC, Dufour E, Christova P, Huang Y, Leclerc-L'Hostis E, and Haertlé T (1994) Binding of heme-CO to bovine and porcine beta-lactoglobulins. *Arch Biochem Biophys* **311**:258–262.
Martin E, Berka V, Bogatenkova E, Murad F, and Tsai A-L (2006) Ligand selectivity of soluble guanylyl cyclase: effect of the hydrogen-bonding tyrosine in the distal heme pocket on binding of oxygen, nitric oxide, and carbon monoxide. *J Biol Chem* **281**:27836–27845.
Mathai C, Jourd'heuil FL, Lopez-Soler RI, and Jourd'heuil D (2020) Emerging perspectives on cytoglobin, beyond NO dioxygenase and peroxidase. *Redox Biol* **32**:101468.
Meier M, Janosik M, Kery V, Kraus JP, and Burkhard P (2001) Structure of human cystathionine beta-synthase: a unique pyridoxal 5′-phosphate-dependent heme protein. *EMBO J* **20**:3910–3916.
Mense SM and Zhang L (2006) Heme: a versatile signaling molecule controlling the activities of diverse regulators ranging from transcription factors to MAP kinases. *Cell Res* **16**:681–692.
Meuli M, Yue AJ, Swerdloff M, Feustel PJ, Hanakova M, and Ehlers MA (2020) Influence of the cigarette smoking trend on carboxyhemoglobin levels in banked blood – an update fourteen years later. *J Clin Anesth* **61**:109677.
Michel H (1999) Cytochrome c oxidase: catalytic cycle and mechanisms of proton pumping–a discussion. *Biochemistry* **38**:15129–15140.
Mihailescu MR and Russu IM (2001) A signature of the T —> R transition in human hemoglobin. *Proc Natl Acad Sci USA* **98**:3773–3777.
Minegishi S, Sagami I, Negi S, Kano K, and Kitagishi H (2018) Circadian clock disruption by selective removal of endogenous carbon monoxide. *Sci Rep* **8**:11996.
Miró O, Casademont J, Barrientos A, Urbano-Márquez A, and Cardellach F (1998) Mitochondrial cytochrome c oxidase inhibition during acute carbon monoxide poisoning. *Pharmacol Toxicol* **82**:199–202.
Mishra S, Fujita T, Lama VN, Nam D, Liao H, Okada M, Minamoto K, Yoshikawa Y, Harada H, and Pinsky DJ (2006) Carbon monoxide rescues ischemic lungs by interrupting MAPK-driven expression of early growth response 1 gene and its downstream target genes. *Proc Natl Acad Sci USA* **103**:5191–5196.
Mitani F, Iizuka T, Shimada H, Ueno R, and Ishimura Y (1985) Flash photolysis studies on the CO complexes of ferrous cytochrome P-450scc and cytochrome P-45011 beta. Effects of steroid binding on the photochemical and ligand binding properties. *J Biol Chem* **260**:12042–12048.
Mitchell MK (1979) Smoking, carboxyhemoglobin, and oxygen therapy. *Chest* **75**:407–408.
Moffet DA, Case MA, House JC, Vogel K, Williams RD, Spiro TG, McLendon GL, and Hecht MH (2001) Carbon monoxide binding by de novo heme proteins derived from designed combinatorial libraries. *J Am Chem Soc* **123**:2109–2115.
Moon YW, Hajjar J, Hwu P, and Naing A (2015) Targeting the indoleamine 2,3-dioxygenase pathway in cancer. *J Immunother Cancer* **3**:51–60.
Morikawa T, Kajimura M, Nakamura T, Hishiki T, Nakanishi T, Yukutake Y, Nagahata Y, Ishikawa M, Hattori K, Takenouchi T, et al. (2012) Hypoxic regulation of the cerebral microcirculation is mediated by a carbon monoxide-sensitive hydrogen sulfide pathway. *Proc Natl Acad Sci USA* **109**:1293–1298.
Morse D, Sethi J, and Choi AM (2002) Carbon monoxide-dependent signaling. *Crit Care Med* **30** (Suppl 1):S12–S17.
Motterlini R, Clark JE, Foresti R, Sarathchandra P, Mann BE, and Green CJ (2002) Carbon monoxide-releasing molecules: characterization of biochemical and vascular activities. *Circ Res* **90**:E17–E24.
Motterlini R, Foresti R, Bassi R, Calabrese V, Clark JE, and Green CJ (2000) Endothelial heme oxygenase-1 induction by hypoxia. Modulation by inducible nitric-oxide synthase and S-nitrosothiols. *J Biol Chem* **275**:13613–13620.
Motterlini R and Otterbein LE (2010) The therapeutic potential of carbon monoxide. *Nat Rev Drug Discov* **9**:728–743.
Murokawa T, Sahara H, Sekijima M, Pomposelli T, Iwanaga T, Ichinari Y, Shimizu A, and Yamada K (2020) The protective effects of carbon monoxide against hepatic warm ischemia-reperfusion injury in MHC-inbred miniature swine. *J Gastrointest Surg* **24**:974–982.
Murphy EJ, Maréchal A, Segal AW, and Rich PR (2010) CO binding and ligand discrimination in human myeloperoxidase. *Biochemistry* **49**:2150–2158.
Musiek ES and Holtzman DM (2016) Mechanisms linking circadian clocks, sleep, and neurodegeneration. *Science* **354**:1004–1008.
Nagao S, Taguchi K, Miyazaki Y, Wakayama T, Chuang VT, Yamasaki K, Watanabe H, Sakai H, Otagiri M, and Maruyama T (2016) Evaluation of a new type of nano-sized carbon monoxide donor on treating mice with experimentally induced colitis. *J Control Release* **234**:49–58.
Nagarajan V, Fonarow GC, Ju C, Pencina M, Laskey WK, Maddox TM, Hernandez A, and Bhatt DL (2017) Seasonal and circadian variations of acute myocardial infarction: findings from the Get With The Guidelines-Coronary Artery Disease (GWTG-CAD) program. *Am Heart J* **189**:85–93.
Naito Y, Uchiyama K, Takagi T, and Yoshikawa T (2012) Therapeutic potential of carbon monoxide (CO) for intestinal inflammation. *Curr Med Chem* **19**:70–76.
Nakahira K and Choi AM (2015) Carbon monoxide in the treatment of sepsis. *Am J Physiol Lung Cell Mol Physiol* **309**:L1387–L1393.
Nakao A, Faleo G, Shimizu H, Nakahira K, Kohmoto J, Sugimoto R, Choi AM, McCurry KR, Takahashi T, and Murase N (2008) Ex vivo carbon monoxide prevents cytochrome P450 degradation and ischemia/reperfusion injury of kidney grafts. *Kidney Int* **74**:1009–1016.
Natella F, Nardini M, Ursini F, and Scaccini C (1998) Oxidative modification of human low-density lipoprotein by horseradish peroxidase in the absence of hydrogen peroxide. *Free Radic Res* **29**:427–434.
Nielsen VG (2020a) The anticoagulant effect of Apis mellifera phospholipase A_2 is inhibited by CORM-2 via a carbon monoxide-independent mechanism. *J Thromb Thrombolysis* **49**:100–107.
Nielsen VG (2020b) Ruthenium, not carbon monoxide, inhibits the procoagulant activity of *Atheris*, *Echis*, and *Pseudonaja* venoms. *Int J Mol Sci* **21**:2970–2981.
Nielsen VG and Garza JI (2014) Comparison of the effects of CORM-2, CORM-3 and CORM-A1 on coagulation in human plasma. *Blood Coagul Fibrinolysis* **25**:801–805.
Nielsen VG, Wagner MT, and Frank N (2020) Mechanisms responsible for the anticoagulant properties of neurotoxic *Dendroaspis* venoms: a viscoelastic analysis. *Int J Mol Sci* **21**:2082–2093.
Niesel J, Pinto A, Peindy N'Dongo HW, Merz K, Ott I, Gust R, and Schatzschneider U (2008) Photoinduced CO release, cellular uptake and cytotoxicity of a tris(pyrazolyl)methane (tpm) manganese tricarbonyl complex. *Chem Commun (Camb)* (15):1798–1800.
Nishitani Y, Okutani H, Takeda Y, Uchida T, Iwai K, and Ishimori K (2019) Specific heme binding to heme regulatory motifs in iron regulatory proteins and its functional significance. *J Inorg Biochem* **198**:110726.
Nobre LS, Jeremias H, Romão CC, and Saraiva LM (2016) Examining the antimicrobial activity and toxicity to animal cells of different types of CO-releasing molecules. *Dalton Trans* **45**:1455–1466.
North RA (2002) Molecular physiology of P2X receptors. *Physiol Rev* **82**:1013–1067.
O'Brien T and Dolan L (2022) Immune checkpoint inhibitors and timing of administration. *Lancet Oncol* **23**:e55.
Oertle M, Richter C, Winterhalter KH, and Di Iorio EE (1985) Kinetics of carbon monoxide binding to phenobarbital-induced cytochrome P-450 from rat liver microsomes: a simple bimolecular process. *Proc Natl Acad Sci USA* **82**:4900–4904.
Ojha S, Wu J, LoBrutto R, and Banerjee R (2002) Effects of heme ligand mutations including a pathogenic variant, H65R, on the properties of human cystathionine β-synthase. *Biochemistry* **41**:4649–4654.
Olson KR and Donald JA (2009) Nervous control of circulation–the role of gasotransmitters, NO, CO, and H2S. *Acta Histochem* **111**:244–256.
Omar SA and Webb AJ (2014) Nitrite reduction and cardiovascular protection. *J Mol Cell Cardiol* **73**:57–69.
Omura T, Sadano H, Hasegawa T, Yoshida Y, and Kominami S (1984) Hemoprotein H-450 identified as a form of cytochrome P-450 having an endogenous ligand at the 6th coordination position of the heme. *J Biochem* **96**:1491–1500.
Oren DA, Sit DK, Goudarzi SH, and Wisner KL (2020) Carbon monoxide: a critical physiological regulator sensitive to light. *Transl Psychiatry* **10**:87–93.
Ortiz de Montellano PR and Correia MA (2005) Inhibition of cytochrome P450 enzymes, in *Cytochrome P450: Structure, Mechanism, and Biochemistry* (Ortiz de Montellano PR, ed) pp 247–322, Kluwer Academic/Plenum Publishers, New York.
Otterbein LE, Soares MP, Yamashita K, and Bach FH (2003) Heme oxygenase-1: unleashing the protective properties of heme. *Trends Immunol* **24**:449–455.
Palao E, Slanina T, Muchová L, Šolomek T, Vítek L, and Klán P (2016) Transition-metal-free CO-releasing BODIPY derivatives activatable by visible to NIR light as promising bioactive molecules. *J Am Chem Soc* **138**:126–133.
Pan Z, Chittavong V, Li W, Zhang J, Ji K, Zhu M, Ji X, and Wang B (2017) Organic CO prodrugs: structure-CO-release rate relationship studies. *Chemistry* **23**:9838–9845.
Pan Z, Zhang J, Ji K, Chittavong V, Ji X, and Wang B (2018) Organic CO prodrugs activated by endogenous ROS. *Org Lett* **20**:8–11.
Park J, Zeng JS, Sahasrabudhe A, Jin K, Fink Y, Manthiram K, and Anikeeva P (2021) Electrochemical modulation of carbon monoxide-mediated cell signaling. *Angew Chem Int Ed Engl* **60**:20325–20330.
Peng P, Wang C, Shi Z, Johns VK, Ma L, Oyer J, Copik A, Igarashi R, and Liao Y (2013) Visible-light activatable organic CO-releasing molecules (PhotoCORMs) that simultaneously generate fluorophores. *Org Biomol Chem* **11**:6671–6674.
Petersen LC (1977) The effect of inhibitors on the oxygen kinetics of cytochrome c oxidase. *Biochim Biophys Acta* **460**:299–307.
Piantadosi CA (2008) Carbon monoxide, reactive oxygen signaling, and oxidative stress. *Free Radic Biol Med* **45**:562–569.
Poloukhtine A and Popik VV (2006) Mechanism of the cyclopropenone decarbonylation reaction. A density functional theory and transient spectroscopy study. *J Phys Chem A* **110**:1749–1757.
Popova M, Lazarus LS, Ayad S, Benninghoff AD, and Berreau LM (2018) Visible-light-activated quinolone carbon-monoxide-releasing molecule: prodrug and albumin-assisted delivery enables anticancer and potent anti-inflammatory effects. *J Am Chem Soc* **140**:9721–9729.
Postnikova GB and Shekhovtsova EA (2018) Myoglobin: oxygen depot or oxygen transporter to mitochondria? A novel mechanism of myoglobin deoxygenation in cells (review). *Biochemistry (Mosc)* **83**:168–183.
Poulos TL (2014) Heme enzyme structure and function. *Chem Rev* **114**:3919–3962.
Priviero FB and Webb RC (2010) Heme-dependent and independent soluble guanylate cyclase activators and vasodilation. *J Cardiovasc Pharmacol* **56**:229–233.
Prockop LD and Chichkova RI (2007) Carbon monoxide intoxication: an updated review. *J Neurol Sci* **262**:122–130.
Puranik M, Weeks CL, Lahaye D, Kabil Ö, Taoka S, Nielsen SB, Groves JT, Banerjee R, and Spiro TG (2006) Dynamics of carbon monoxide binding to cystathionine β-synthase. *J Biol Chem* **281**:13433–13438.
Purohit R, Fritz BG, The J, Issaian A, Weichsel A, David CL, Campbell E, Hausrath AC, Rassouli-Taylor L, Garcin ED, et al. (2014) YC-1 binding to the β subunit of soluble guanylyl cyclase overcomes allosteric inhibition by the α subunit. *Biochemistry* **53**:101–114.
Qian DC, Kleber T, Brammer B, Xu KM, Switchenko JM, Janopaul-Naylor JR, Zhong J, Yushak ML, Harvey RD, Paulos CM, et al. (2021) Effect of immunotherapy time-of-day infusion on overall survival among patients with advanced melanoma in the USA (MEMOIR): a propensity score-matched analysis of a single-centre, longitudinal study. *Lancet Oncol* **22**:1777–1786.

Qiu XY and Chen XQ (2014) Neuroglobin - recent developments. *Biomol Concepts* **5**:195–208.
Queiroga CS, Almeida AS, Alves PM, Brenner C, and Vieira HL (2011) Carbon monoxide prevents hepatic mitochondrial membrane permeabilization. *BMC Cell Biol* **12**:10–17.
Rahman FU, Park DR, Joe Y, Jang KY, Chung HT, and Kim UH (2019) Critical roles of carbon monoxide and nitric oxide in Ca^{2+} signaling for insulin secretion in pancreatic islets. *Antioxid Redox Signal* **30**:560–576.
Raub JA and Benignus VA (2002) Carbon monoxide and the nervous system. *Neurosci Biobehav Rev* **26**:925–940.
Reedy CJ, Elvekrog MM, and Gibney BR (2008) Development of a heme protein structure-electrochemical function database. *Nucleic Acids Res* **36**:D307–D313.
Ren Y, D'Ambrosio MA, Wang H, Falck JR, Peterson EL, Garvin JL, and Carretero OA (2012) Mechanisms of carbon monoxide attenuation of tubuloglomerular feedback. *Hypertension* **59**:1139–1144.
Ren Y, D'Ambrosio MA, Wang H, Liu R, Garvin JL, and Carretero OA (2008) Heme oxygenase metabolites inhibit tubuloglomerular feedback (TGF). *Am J Physiol Renal Physiol* **295**:F1207–F1212.
Richards MP (2013) Redox reactions of myoglobin. *Antioxid Redox Signal* **18**:2342–2351.
Robergs RA, Ghiasvand F, and Parker D (2004) Biochemistry of exercise-induced metabolic acidosis. *Am J Physiol Regul Integr Comp Physiol* **287**:R502–R516.
Romanski S, Kraus B, Schatzschneider U, Neudörfl JM, Amslinger S, and Schmalz HG (2011) Acyloxybutadiene iron tricarbonyl complexes as enzyme-triggered CO-releasing molecules (ET-CORMs). *Angew Chem Int Ed Engl* **50**:2392–2396.
Romão CC, Blättler WA, Seixas JD, and Bernardes GJ (2012) Developing drug molecules for therapy with carbon monoxide. *Chem Soc Rev* **41**:3571–3583.
Rose JJ, Bocian KA, Xu Q, Wang L, DeMartino AW, Chen X, Corey CG, Guimarães DA, Azarov I, Huang XN, et al. (2020) A neuroglobin-based high-affinity ligand trap reverses carbon monoxide-induced mitochondrial poisoning. *J Biol Chem* **295**:6357–6371.
Rose JJ, Wang L, Xu Q, McTiernan CF, Shiva S, Tejero J, and Gladwin MT (2017) Carbon monoxide poisoning: pathogenesis, management, and future directions of therapy. *Am J Respir Crit Care Med* **195**:596–606.
Rösen P and Stier A (1973) Kinetics of CO and O 2 complexes of rabbit liver microsomal cytochrome P 450. *Biochem Biophys Res Commun* **51**:603–611.
Rossier J, Delasoie J, Haeni L, Hauser D, Rothen-Rutishauser B, and Zobi F (2020) Cytotoxicity of Mn-based photoCORMs of ethynyl-α-diimine ligands against different cancer cell lines: the key role of CO-depleted metal fragments. *J Inorg Biochem* **209**:111122.
Rotko D, Bednarczyk P, Koprowski P, Kunz WS, Szewczyk A, and Kulawiak B (2020) Heme is required for carbon monoxide activation of mitochondrial BKCa channel. *Eur J Pharmacol* **881**:173191.
Rouzbahani M, Azimivghar J, Moghadam RH, Montazeri N, Janjani P, Rai A, Rad EJ, Naderipour A, and Salehi N (2021) Acute myocardial infarction: circadian, daily, monthly and seasonal patterns of occurrence in diabetics. *J Diabetes Metab Disord* **20**:765–770.
Ruetz M, Kumutima J, Lewis BE, Filipovic MR, Lehnert N, Stemmler TL, and Banerjee R (2017) A distal ligand mutes the interaction of hydrogen sulfide with human neuroglobin. *J Biol Chem* **292**:6512–6528.
Rumi JAD and Whinfield EH (2004) *Rumi: Selections from the "Masnavi"*, Axiom Publishing, Adelaide, Australia.
Ryan MJ, Jernigan NL, Drummond HA, McLemore Jr GR, Rimoldi JM, Poreddy SR, Gadepalli RSV, and Stec DE (2006) Renal vascular responses to CORM-A1 in the mouse. *Pharmacol Res* **54**:24–29.
Ryter SW, Otterbein LE, Morse D, and Choi AM (2002) Heme oxygenase/carbon monoxide signaling pathways: regulation and functional significance. *Mol Cell Biochem* **234-235**:249–263.
Rytömaa M and Kinnunen PKJ (1995) Reversibility of the binding of cytochrome c to liposomes. Implications for lipid-protein interactions. *J Biol Chem* **270**:3197–3202.
Saffran WA and Gibson QH (1978) The effect of pH on carbon monoxide binding to menhaden hemoglobin. Allosteric transitions in a root effect hemoglobin. *J Biol Chem* **253**:3171–3179.
Sahara H, Shimizu A, Setoyama K, Okumi M, Oku M, Samelson-Jones E, and Yamada K (2010) Carbon monoxide reduces pulmonary ischemia-reperfusion injury in miniature swine. *J Thorac Cardiovasc Surg* **139**:1594–1601.
Santos-Silva T, Mukhopadhyay A, Seixas JD, Bernardes GJ, Romão CC, and Romão MJ (2011a) CORM-3 reactivity toward proteins: the crystal structure of a Ru(II) dicarbonyl-lysozyme complex. *J Am Chem Soc* **133**:1192–1195.
Santos-Silva T, Mukhopadhyay A, Seixas JD, Bernardes GJ, Romão CC, and Romão MJ (2011b) Towards improved therapeutic CORMs: understanding the reactivity of CORM-3 with proteins. *Curr Med Chem* **18**:3361–3366.
Sarewicz M and Osyczka A (2015) Electronic connection between the quinone and cytochrome C redox pools and its role in regulation of mitochondrial electron transport and redox signaling. *Physiol Rev* **95**:219–243.
Sato H, Nomura S, Sagami I, Ito O, Daff S, and Shimizu T (1998) CO binding studies of nitric oxide synthase: effects of the substrate, inhibitors and tetrahydrobiopterin. *FEBS Lett* **430**:377–380.
Sawicki CA and Gibson QH (1978) The relation between carbon monoxide binding and the conformational change of hemoglobin. *Biophys J* **24**:21–33.
Schallner N, Lieberum J-L, Gallo D, LeBlanc 3rd RH, Fuller PM, Hanafy KA, and Otterbein LE (2017) Carbon monoxide preserves circadian rhythm to reduce the severity of subarachnoid hemorrhage in mice. *Stroke* **48**:2565–2573.
Schmidt M, Gerlach F, Avivi A, Laufs T, Wystub S, Simpson JC, Nevo E, Saaler-Reinhardt S, Reuss S, Hankeln T, et al. (2004) Cytoglobin is a respiratory protein in connective tissue and neurons, which is up-regulated by hypoxia. *J Biol Chem* **279**:8063–8069.
Scragg JL, Dallas ML, Wilkinson JA, Varadi G, and Peers C (2008) Carbon monoxide inhibits L-type Ca2+ channels via redox modulation of key cysteine residues by mitochondrial reactive oxygen species. *J Biol Chem* **283**:24412–24419.
Seixas JD, Santos MF, Mukhopadhyay A, Coelho AC, Reis PM, Veiros LF, Marques AR, Penacho N, Gonçalves AM, Romão MJ, et al. (2015) A contribution to the rational design of Ru(CO)3Cl2L complexes for in vivo delivery of CO. *Dalton Trans* **44**:5058–5075.
Sen S, Kawahara B, Gupta D, Tsai R, Khachatryan M, Roy-Chowdhuri S, Bose S, Yoon A, Faull K, Farias-Eisner R, et al. (2015) Role of cystathionine β-synthase in human breast cancer. *Free Radic Biol Med* **86**:228–238.
Shaklai N, Sharma VS, Muller-Eberhard U, and Morgan WT (1981) The interaction of heme-hemopexin with CO. *J Biol Chem* **256**:1544–1548.
Sharma VS, Geibel JF, and Ranney HM (1978) "Tension" on heme by the proximal base and ligand reactivity: conclusions drawn from model compounds for the reaction of hemoglobin. *Proc Natl Acad Sci USA* **75**:3747–3750.
Sharma VS, Schmidt MR, and Ranney HM (1976) Dissociation of CO from carboxyhemoglobin. *J Biol Chem* **251**:4267–4272.
Sheps DS, Herbst MC, Hinderliter AL, Adams KF, Ekelund LG, O'Neil JJ, Goldstein GM, Bromberg PA, Ballenger M, Davis SM, et al. (1991) Effects of 4 percent and 6 percent carboxyhemoglobin on arrhythmia production in patients with coronary artery disease. *Res Rep Health Eff Inst* **41**:1–46, discussion 47–58.
Sher EA, Shaklai M, and Shaklai N (2012) Carbon monoxide promotes respiratory hemoproteins iron reduction using peroxides as electron donors. *PLoS One* **7**:e33039.
Sher EA, Sholto AY, Shaklai M, and Shaklai N (2014) Can gas replace protein function? CO abrogates the oxidative toxicity of myoglobin. *PLoS One* **9**:e104075.
Shimizu T, Lengalova A, Martínek V, and Martínková M (2019) Heme: emergent roles of heme in signal transduction, functional regulation and as catalytic centres. *Chem Soc Rev* **48**:5624–5657.
Shintani T, Iwabuchi T, Soga T, Kato Y, Yamamoto T, Takano N, Hishiki T, Ueno Y, Ikeda S, Sakuragawa T, et al. (2009) Cystathionine β-synthase as a carbon monoxide-sensitive regulator of bile excretion. *Hepatology* **49**:141–150.
Shykoff BE and Lee RL (2019) Risks from breathing elevated oxygen. *Aerosp Med Hum Perform* **90**:1041–1049.
Silkstone G, Kapetanaki SM, Husu I, Vos MH, and Wilson MT (2010) Nitric oxide binds to the proximal heme coordination site of the ferrocytochrome c/cardiolipin complex: formation mechanism and dynamics. *J Biol Chem* **285**:19785–19792.
Singh S, Madzelan P, Stasser J, Weeks CL, Becker D, Spiro TG, Penner-Hahn J, and Banerjee R (2009) Modulation of the heme electronic structure and cystathionine β-synthase activity by second coordination sphere ligands: the role of heme ligand switching in redox regulation. *J Inorg Biochem* **103**:689–697.
Sinibaldi F, Fiorucci L, Patriarca A, Lauceri R, Ferri T, Coletta M, and Santucci R (2008) Insights into cytochrome c-cardiolipin interaction. Role played by ionic strength. *Biochemistry* **47**:6928–6935.
Siow RC, Sato H, and Mann GE (1999) Heme oxygenase-carbon monoxide signalling pathway in atherosclerosis: anti-atherogenic actions of bilirubin and carbon monoxide? *Cardiovasc Res* **41**:385–394.
Sitnikov NS, Li Y, Zhang D, Yard B, and Schmalz HG (2015) Design, synthesis, and functional evaluation of CO-releasing molecules triggered by penicillin G amidase as a model protease. *Angew Chem Int Ed Engl* **54**:12314–12318.
Smith LJ, Kahraman A, and Thornton JM (2010) Heme proteins–diversity in structural characteristics, function, and folding. *Proteins* **78**:2349–2368.
Soboleva T and Berreau LM (2019) 3-Hydroxyflavones and 3-hydroxy-4-oxoquinolines as carbon monoxide-releasing molecules. *Molecules* **24**:1252–1277.
Song XJ, Simplaceanu V, Ho NT, and Ho C (2008) Effector-induced structural fluctuation regulates the ligand affinity of an allosteric protein: binding of inositol hexaphosphate has distinct dynamic consequences for the T and R states of hemoglobin. *Biochemistry* **47**:4907–4915.
Southam HM, Smith TW, Lyon RL, Liao C, Trevitt CR, Middlemiss LA, Cox FL, Chapman JA, El-Khamisy SF, Hippler M, et al. (2018) A thiol-reactive Ru(II) ion, not CO release, underlies the potent antimicrobial and cytotoxic properties of CO-releasing molecule-3. *Redox Biol* **18**:114–123.
Southam HM, Williamson MP, Chapman JA, Lyon RL, Trevitt CR, Henderson PJF, and Poole RK (2021) 'Carbon-monoxide-releasing molecule-2 (CORM-2)' is a misnomer: ruthenium toxicity, not CO release, accounts for its antimicrobial effects. *Antioxidants* **10**:915–936.
Steiger C, Hermann C, and Meinel L (2017) Localized delivery of carbon monoxide. *Eur J Pharm Biopharm* **118**:3–12.
Steiger C, Uchiyama K, Takagi T, Mizushima K, Higashimura Y, Gutmann M, Hermann C, Botov S, Schmalz HG, Naito Y, et al. (2016) Prevention of colitis by controlled oral drug delivery of carbon monoxide. *J Control Release* **239**:128–136.
Stone JR and Marletta MA (1994) Soluble guanylate cyclase from bovine lung: activation with nitric oxide and carbon monoxide and spectral characterization of the ferrous and ferric states. *Biochemistry* **33**:5636–5640.
Stone JR and Marletta MA (1998) Synergistic activation of soluble guanylate cyclase by YC-1 and carbon monoxide: implications for the role of cleavage of the iron-histidine bond during activation by nitric oxide. *Chem Biol* **5**:255–261.
Stucki D, Krahl H, Walter M, Steinhausen J, Hommel K, Brenneisen P, and Stahl W (2020a) Effects of frequently applied carbon monoxide releasing molecules (CORMs) in typical CO-sensitive model systems - a comparative in vitro study. *Arch Biochem Biophys* **687**:108383.
Stucki D, Steinhausen J, Westhoff P, Krahl H, Brilhaus D, Massenberg A, Weber APM, Reichert AS, Brenneisen P, and Stahl W (2020b) Endogenous carbon monoxide signaling modulates mitochondrial function and intracellular glucose utilization: impact of the heme oxygenase substrate hemin. *Antioxidants* **9**:652–670.
Suematsu M, Nakamura T, Tokumoto Y, Yamamoto T, Kajimura M, and Kabe Y (2016) CO-CBS-H2 S axis: from vascular mediator to cancer regulator. *Microcirculation* **23**:183–190.

Suliman HB, Carraway MS, Ali AS, Reynolds CM, Welty-Wolf KE, and Piantadosi CA (2007) The CO/HO system reverses inhibition of mitochondrial biogenesis and prevents murine doxorubicin cardiomyopathy. *J Clin Invest* **117**:3730–3741.
Supervía A, De Paz Picornell R, Córdoba F, Gallardo P, Pallàs O, and Cirera I (2021) Carbon monoxide poisoning in hookah users. *Emergencias (Madr)* **33**:320–321.
Surprenant A and North RA (2009) Signaling at purinergic P2X receptors. *Annu Rev Physiol* **71**:333–359.
Swenson ER (2016) Hypoxia and its acid-base consequences: from mountains to malignancy. *Adv Exp Med Biol* **903**:301–323.
Szabo C (2017) Hydrogen sulfide, an enhancer of vascular nitric oxide signaling: mechanisms and implications. *Am J Physiol Cell Physiol* **312**:C3–C15.
Szabo C, Coletta C, Chao C, Módis K, Szczesny B, Papapetropoulos A, and Hellmich MR (2013) Tumor-derived hydrogen sulfide, produced by cystathionine-β-synthase, stimulates bioenergetics, cell proliferation, and angiogenesis in colon cancer. *Proc Natl Acad Sci USA* **110**:12474–12479.
Taguchi K, Ogaki S, Nagasaki T, Yanagisawa H, Nishida K, Maeda H, Enoki Y, Matsumoto K, Sekijima H, Ooi K, et al. (2020) Carbon monoxide rescues the developmental lethality of experimental rat models of rhabdomyolysis-induced acute kidney injury. *J Pharmacol Exp Ther* **372**:355–365.
Takagi T, Naito Y, Tanaka M, Mizushima K, Ushiroda C, Toyokawa Y, Uchiyama K, Hamaguchi M, Handa O, and Itoh Y (2018) Carbon monoxide ameliorates murine T-cell-dependent colitis through the inhibition of Th17 differentiation. *Free Radic Res* **52**:1328–1335.
Tang XD, Xu R, Reynolds MF, Garcia ML, Heinemann SH, and Hoshi T (2003) Haem can bind to and inhibit mammalian calcium-dependent Slo1 BK channels. *Nature* **425**:531–535.
Taoka S and Banerjee R (2001) Characterization of NO binding to human cystathionine β-synthase: possible implications of the effects of CO and NO binding to the human enzyme. *J Inorg Biochem* **87**:245–251.
Taoka S, West M, and Banerjee R (1999) Characterization of the heme and pyridoxal phosphate cofactors of human cystathionine β-synthase reveals nonequivalent active sites. *Biochemistry* **38**:2738–2744.
Tiso M, Tejero J, Basu S, Azarov I, Wang X, Simplaceanu V, Frizzell S, Jayaraman T, Geary L, Shapiro C, et al. (2011) Human neuroglobin functions as a redox-regulated nitrite reductase. *J Biol Chem* **286**:18277–18289.
Tiwari PB, Astudillo L, Pham K, Wang X, He J, Bernad S, Derrien V, Sebban P, Miksovska J, and Darici Y (2015) Characterization of molecular mechanism of neuroglobin binding to cytochrome c: a surface plasmon resonance and isothermal titration calorimetry study. *Inorg Chem Commun* **62**:37–41 DOI: 10.1016/j.inoche.2015.10.010.
Tomita T, Gonzalez G, Chang AL, Ikeda-Saito M, and Gilles-Gonzalez M-A (2002) A comparative resonance Raman analysis of heme-binding PAS domains: heme iron coordination structures of the BjFixL, AxPDEA1, EcDos, and MtDos proteins. *Biochemistry* **41**:4819–4826.
Tornio A and Backman JT (2018) Cytochrome P450 in pharmacogenetics: an update. *Adv Pharmacol* **83**:3–32.
Trashin S, de Jong M, Luyckx E, Dewilde S, and De Wael K (2016) Electrochemical evidence for neuroglobin activity on NO at physiological concentrations. *J Biol Chem* **291**:18959–18966.
Tripathi R, Yang X, Ryter SW, and Wang B (2021) Carbon monoxide as a therapeutic for airway diseases: contrast and comparison of various CO delivery modalities. *Curr Top Med Chem* **21**:2890–2908.
Tsai AL, Berka V, Martin E, and Olson JS (2012) A "sliding scale rule" for selectivity among NO, CO, and O_2, by heme protein sensors. *Biochemistry* **51**:172–186.
Tsujino H, Yamashita T, Nose A, Kukino K, Sawai H, Shiro Y, and Uno T (2014) Disulfide bonds regulate binding of exogenous ligand to human cytoglobin. *J Inorg Biochem* **135**:20–27.
Tsukihara T, Aoyama H, Yamashita E, Tomizaki T, Yamaguchi H, Shinzawa-Itoh K, Nakashima R, Yaono R, and Yoshikawa S (1995) Structures of metal sites of oxidized bovine heart cytochrome c oxidase at 2.8 A. *Science* **269**:1069–1074.
Tsukihara T, Shimokata K, Katayama Y, Shimada H, Muramoto K, Aoyama H, Mochizuki M, Shinzawa-Itoh K, Yamashita E, Yao M, et al. (2003) The low-spin heme of cytochrome c oxidase as the driving element of the proton-pumping process. *Proc Natl Acad Sci USA* **100**:15304–15309.
Tu BP and McKnight SL (2009) Evidence of carbon monoxide-mediated phase advancement of the yeast metabolic cycle. *Proc Natl Acad Sci USA* **106**:14293–14296.
Tuckey RC and Kamin H (1983) Kinetics of O2 and CO Binding to adrenal cytochrome P-450scc. Effect of cholesterol, intermediates, and phosphatidylcholine vesicles. *J Biol Chem* **258**:4232–4237.
Unzai S, Eich R, Shibayama N, Olson JS, and Morimoto H (1998) Rate constants for O2 and CO binding to the alpha and beta subunits within the R and T states of human hemoglobin. *J Biol Chem* **273**:23150–23159.
US-EPA (2000) Pharmacokinetics and mechanisms of action of carbon monoxide, in *Air Quality Criteria for Carbon Monoxide*, pp 5–1–5-30, Office of Research and Development, Washington, DC.
Vandegriff KD, Le Tellier YC, Winslow RM, Rohlfs RJ, and Olson JS (1991) Determination of the rate and equilibrium constants for oxygen and carbon monoxide binding to R-state human hemoglobin cross-linked between the alpha subunits at lysine 99. *J Biol Chem* **266**:17049–17059.
Vicente JB, Colaço HG, Malagrinò F, Santo PE, Gutierres A, Bandeiras TM, Sarti P, Leandro P, Brito JA, and Giuffrè A (2018) P-376 - Crosstalk between gasotransmitters at the H2S-synthesizing human cystathionine β-synthase: heme-based regulation by CO and NO. *Free Radic Biol Med* **120** (Suppl 1):S159 DOI: 10.1016/j.freeradbiomed.2018.04.523.
Vicente JB, Colaço HG, Mendes MIS, Sarti P, Leandro P, and Giuffrè A (2014) NO* binds human cystathionine β-synthase quickly and tightly. *J Biol Chem* **289**:8579–8587.
Vicente JB, Colaço HG, Sarti P, Leandro P, and Giuffrè A (2016) S-adenosyl-l-methionine modulates CO and NO• binding to the human H2S-generating enzyme cystathionine β-synthase. *J Biol Chem* **291**:572–581.
Vincent SR, Das S, and Maines MD (1994) Brain heme oxygenase isoenzymes and nitric oxide synthase are co-localized in select neurons. *Neuroscience* **63**:223–231.
Vítek L (2020) Bilirubin as a signaling molecule. *Med Res Rev* **40**:1335–1351.
Vogel KM, Hu S, Spiro TG, Dierks EA, Yu AE, and Burstyn JN (1999) Variable forms of soluble guanylyl cyclase: protein-ligand interactions and the issue of activation by carbon monoxide. *J Biol Inorg Chem* **4**:804–813.
Wakasugi K, Nakano T, and Morishima I (2003) Oxidized human neuroglobin acts as a heterotrimeric Galpha protein guanine nucleotide dissociation inhibitor. *J Biol Chem* **278**:36505–36512.
Walewska A, Szewczyk A, and Koprowski P (2018) Gas signaling molecules and mitochondrial potassium channels. *Int J Mol Sci* **19**:3227–3246.
Wang B and Otterbein LE, eds (2022) *Carbon Monoxide in Drug Discovery: Basics, Pharmacology, and Therapeutic Potential*, John Wiley and Sons, Hoboken, NJ.
Wang D, Viennois E, Ji K, Damera K, Draganov A, Zheng Y, Dai C, Merlin D, and Wang B (2014) A click-and-release approach to CO prodrugs. *Chem Commun (Camb)* **50**:15890–15893.
Wang G (2017) Mechanistic insight into the heme-independent interplay between iron and carbon monoxide in CFTR and Slo1 BK_{Ca} channels. *Metallomics* **9**:634–645.
Wang M, Yang X, Pan Z, Wang Y, De La Cruz LK, Wang B, and Tan C (2020) Towards "CO in a pill": pharmacokinetic studies of carbon monoxide prodrugs in mice. *J Control Release* **327**:174–185.
Wang R (1998) Resurgence of carbon monoxide: an endogenous gaseous vasorelaxing factor. *Can J Physiol Pharmacol* **76**:1–15.
Wang R, ed (2001) *Carbon Monoxide and Cardiovascular Functions*, CRC Press, Boca Raton, FL.
Wang XL and Li L (2021) Circadian clock regulates inflammation and the development of neurodegeneration. *Front Cell Infect Microbiol* **11**:696554.
Wang XM, Kim HP, Nakahira K, Ryter SW, and Choi AM (2009) The heme oxygenase-1/carbon monoxide pathway suppresses TLR4 signaling by regulating the interaction of TLR4 with caveolin-1. *J Immunol* **182**:3809–3818.
Wang Y, Gao L, Chen J, Li Q, Huo L, Wang Y, Wang H, and Du J (2021) Pharmacological modulation of Nrf2/HO-1 signaling pathway as a therapeutic target of Parkinson's disease. *Front Pharmacol* **12**:757161.
Wareham LK, Poole RK, and Tinajero-Trejo M (2015) CO-releasing metal carbonyl compounds as antimicrobial agents in the post-antibiotic era. *J Biol Chem* **290**:18999–19007.
Weeks CL, Singh S, Madzelan P, Banerjee R, and Spiro TG (2009) Heme regulation of human cystathionine β-synthase activity: insights from fluorescence and Raman spectroscopy. *J Am Chem Soc* **131**:12809–12816.
Wegiel B, Gallo D, Csizmadia E, Harris C, Belcher J, Vercellotti GM, Penacho N, Seth P, Sukhatme V, Ahmed A, et al. (2013) Carbon monoxide expedites metabolic exhaustion to inhibit tumor growth. *Cancer Res* **73**:7009–7021.
Wegiel B, Larsen R, Gallo D, Chin BY, Harris C, Mannam P, Kaczmarek E, Lee PJ, Zuckerbraun BS, Flavell R,, et al. (2014) Macrophages sense and kill bacteria through carbon monoxide-dependent inflammasome activation. *J Clin Invest* **124**:4926–4940.
Weitz SH, Gong M, Barr I, Weiss S, and Guo F (2014) Processing of microRNA primary transcripts requires heme in mammalian cells. *Proc Natl Acad Sci USA* **111**:1861–1866.
Wharton DC and Tzagoloff A (1967) Cytochrome oxidase from beef heart mitochondria, in *Methods in Enzymology*, **vol 10**, pp 245–250, Academic Press, Cambridge, MA.
White KA and Marletta MA (1992) Nitric oxide synthase is a cytochrome P-450 type hemoprotein. *Biochemistry* **31**:6627–6631.
Wilkinson WJ, Gadeberg HC, Harrison AWJ, Allen ND, Riccardi D, and Kemp PJ (2009) Carbon monoxide is a rapid modulator of recombinant and native P2X(2) ligand-gated ion channels. *Br J Pharmacol* **158**:862–871.
Wollborn J, Hermann C, Goebel U, Merget B, Wunder C, Maier S, Schäfer T, Heuler D, Müller-Buschbaum K, Buerkle H, et al. (2018) Overcoming safety challenges in CO therapy - extracorporeal CO delivery under precise feedback control of systemic carboxyhemoglobin levels. *J Control Release* **279**:336–344.
Wollborn J, Steiger C, Doostkam S, Schallner N, Schroeter N, Kari FA, Meinel L, Buerkle H, Schick MA, and Goebel U (2020) Carbon monoxide exerts functional neuroprotection after cardiac arrest using extracorporeal resuscitation in pigs. *Crit Care Med* **48**:e299–e307.
Wood H (2016) Traumatic brain injury: carbon monoxide - a potential therapy for traumatic brain injury? *Nat Rev Neurol* **12**:615.
Xiao S, Li Q, Hu L, Yu Z, Yang J, Chang Q, Chen Z, and Hu G (2019) Soluble guanylate cyclase stimulators and activators: where are we and where to go? *Mini Rev Med Chem* **19**:1544–1557.
Xing L, Wang B, Li J, Guo X, Lu X, Chen X, Sun H, Sun Z, Luo X, Qi S, et al. (2022) A fluorogenic $ONOO^-$-triggered carbon monoxide donor for mitigating brain ischemic damage. *J Am Chem Soc* **144**:2114–2119.
Yamamoto T, Takano N, Ishiwata K, Ohmura M, Nagahata Y, Matsuura T, Kamata A, Sakamoto K, Nakanishi T, Kubo A, et al. (2014) Reduced methylation of PFKFB3 in cancer cells shunts glucose towards the pentose phosphate pathway. *Nat Commun* **5**:3480.
Yamamoto T, Takano N, Ishiwata K, and Suematsu M (2011) Carbon monoxide stimulates global protein methylation via its inhibitory action on cystathionine β-synthase. *J Clin Biochem Nutr* **48**:96–100.
Yanagisawa S, Sugimoto H, Shiro Y, and Ogura T (2010) A specific interaction of L-tryptophan with CO of CO-bound indoleamine 2,3-dioxygenase identified by resonance Raman spectroscopy. *Biochemistry* **49**:10081–10088.
Yang PM, Cheng KC, Yuan SH, and Wung BS (2020a) Carbon monoxide-releasing molecules protect against blue light exposure and inflammation in retinal pigment epithelial cells. *Int J Mol Med* **46**:1096–1106.

Yang X, de Caestecker M, Otterbein LE, and Wang B (2020b) Carbon monoxide: an emerging therapy for acute kidney injury. *Med Res Rev* **40**:1147–1177.
Yang XX, Ke BW, Lu W, and Wang BH (2020c) CO as a therapeutic agent: discovery and delivery forms. *Chin J Nat Med* **18**:284–295.
Yang X, Lu W, Hopper CP, Ke B, and Wang B (2021a) Nature's marvels endowed in gaseous molecules I: carbon monoxide and its physiological and therapeutic roles. *Acta Pharm Sin B* **11**:1434–1445.
Yang X, Lu W, Wang M, Tan C, and Wang B (2021b) "CO in a pill": towards oral delivery of carbon monoxide for therapeutic applications. *J Control Release* **338**:593–609.
Yang X, Wang M, Tan C, Lu W, and Wang B (2022a) Pharmacokinetic characteristics of carbon monoxide, in *Carbon Monoxide in Drug Discovery: Basics, Pharmacology, and Therapeutic Potential* (Wang B and Otterbein LE, eds) John Wiley and Sons, Hoboken, NJ.
Yang X, Lu W, Wang M, De La Cruz LKC, Tan C, and Wang B (2022b) Activated charcoal dispersion of carbon monoxide prodrugs for oral delivery of CO in a pill. *Int J Pharm* **618**:121650–121660.
Yeh P-Y, Li C-Y, Hsieh C-W, Yang Y-C, Yang P-M, and Wung B-S (2014) CO-releasing molecules and increased heme oxygenase-1 induce protein S-glutathionylation to modulate NF-κB activity in endothelial cells. *Free Radic Biol Med* **70**:1–13.
Yi L, Morgan JT, and Ragsdale SW (2010) Identification of a thiol/disulfide redox switch in the human BK channel that controls its affinity for heme and CO. *J Biol Chem* **285**:20117–20127.
Yonetani T (1960) Studies on cytochrome oxidase. I. Absolute and difference absorption spectra. *J Biol Chem* **235**:845–852.
Yonetani T (1961) Studies on cytochrome oxidase. III. Improved preparation and some properties. *J Biol Chem* **236**:1680–1688.
Yonetani T and Laberge M (2008) Protein dynamics explain the allosteric behaviors of hemoglobin. *Biochim Biophys Acta* **1784**:1146–1158.
Yonetani T, Park SI, Tsuneshige A, Imai K, and Kanaori K (2002) Global allostery model of hemoglobin. Modulation of O(2) affinity, cooperativity, and Bohr effect by heterotropic allosteric effectors. *J Biol Chem* **277**:34508–34520.
Yoshii K, Tajima F, Ishijima S, and Sagami I (2015) Changes in pH and NADPH regulate the DNA binding activity of neuronal PAS domain protein 2, a mammalian circadian transcription factor. *Biochemistry* **54**:250–259.
Yuan Y, Tam MF, Simplaceanu V, and Ho C (2015) New look at hemoglobin allostery. *Chem Rev* **115**:1702–1724.
Yuan Z, Yang X, De La Cruz LKC, and Wang B (2020) Nitro reduction-based fluorescent probes for carbon monoxide require reactivity involving a ruthenium carbonyl moiety. *Chem Commun (Camb)* **56**:2190–2193.
Yuan Z, Yang X, and Wang B (2021a) Redox and catalase-like activities of four widely used carbon monoxide releasing molecules (CO-RMs). *Chem Sci (Camb)* **12**:13013–13020.
Yuan Z, Yang X, Ye Y, Tripathi R, and Wang B (2021b) Chemical reactivities of two widely used ruthenium-based CO-releasing molecules with a range of biologically important reagents and molecules. *Anal Chem* **93**:5317–5326.
Zaidi S, Hassan MI, Islam A, and Ahmad F (2014) The role of key residues in structure, function, and stability of cytochrome-c. *Cell Mol Life Sci* **71**: 229–255.
Zenke-Kawasaki Y, Dohi Y, Katoh Y, Ikura T, Ikura M, Asahara T, Tokunaga F, Iwai K, and Igarashi K (2007) Heme induces ubiquitination and degradation of the transcription factor Bach1. *Mol Cell Biol* **27**:6962–6971.
Zhang D, Lin Z, Zheng Y, Song J, Li J, Zeng Y, and Liu X (2020) Ultrasound-driven biomimetic nanosystem suppresses tumor growth and metastasis through sonodynamic therapy, CO therapy, and indoleamine 2,3-dioxygenase inhibition. *ACS Nano* **14**:8985–8999.
Zhang LM, Zhang DX, Fu L, Li Y, Wang XP, Qi MM, Li CC, Song PP, Wang XD, and Kong XJ (2019) Carbon monoxide-releasing molecule-3 protects against cortical pyroptosis induced by hemorrhagic shock and resuscitation via mitochondrial regulation. *Free Radic Biol Med* **141**:299–309.
Zhang X, Shan P, Alam J, Fu XY, and Lee PJ (2005) Carbon monoxide differentially modulates STAT1 and STAT3 and inhibits apoptosis via a phosphatidylinositol 3-kinase/Akt and p38 kinase-dependent STAT3 pathway during anoxia-reoxygenation injury. *J Biol Chem* **280**:8714–8721.
Zheng Y, Ji X, Yu B, Ji K, Gallo D, Csizmadia E, Zhu M, Choudhury MR, De La Cruz LKC, Chittavong V, et al. (2018) Enrichment-triggered prodrug activation demonstrated through mitochondria-targeted delivery of doxorubicin and carbon monoxide. *Nat Chem* **10**:787–794.
Zhou Y, Wu H, Zhao M, Chang C, and Lu Q (2016) The Bach family of transcription factors: a comprehensive review. *Clin Rev Allergy Immunol* **50**:345–356.
Zhou YD, Barnard M, Tian H, Li X, Ring HZ, Francke U, Shelton J, Richardson J, Russell DW, and McKnight SL (1997) Molecular characterization of two mammalian bHLH-PAS domain proteins selectively expressed in the central nervous system. *Proc Natl Acad Sci USA* **94**:713–718.
Zock JP (1990) Carbon monoxide binding in a model of hemoglobin differs between the T and the R conformation. *Adv Exp Med Biol* **277**:199–207.
Zuckerbraun BS, Chin BY, Bilban M, d'Avila JC, Rao J, Billiar TR, and Otterbein LE (2007) Carbon monoxide signals via inhibition of cytochrome c oxidase and generation of mitochondrial reactive oxygen species. *FASEB J* **21**:1099–1106.